Effect of Cu addition on microstructure and impact toughness in the simulated coarse-grained heat-affected zone of high-strength low-alloy steels

Journal Item

Materials Science and Technology

Effectof Cuaddition on microstructure and impact toughness inthe simulated CGHAZ of HSLAsteels

--Manuscript Draft--

Manuscript Number:	MST12200R1
Full Title:	Effectof Cuaddition on microstructure and impact toughness inthe simulated CGHAZ of HSLAsteels
Article Type:	Research Paper
Keywords:	CGHAZ, impact toughness, acicular ferrite, M-A constituent, Cu precipitation.
Corresponding Author:	K. M. Wu, Ph.D. Wuhan University of Science and Technology CHINA
Corresponding Author Secondary Information:	
Corresponding Author's Institution:	Wuhan University of Science and Technology
Corresponding Author's Secondary Institution:	
First Author:	G. Huang, Master
First Author Secondary Information:	
Order of Authors:	G. Huang, Master
	X.L. Wan, Ph. D
	K. M. Wu, Ph.D.
	O. Isayev, Ph.D
	O. Hress, Ph. D
	Irina Rodionova, Ph.D
	A. A. Shirzadi, Ph. D
Order of Authors Secondary Information:	
Abstract:	The effects of Cu content on microstructure and impact toughness in the simulated coarse-grained heat-affected zone (CGHAZ) of high-strength low-alloy steels were investigated. It has been observed that the microstructure in the simulated CGHAZ of Cu-free steel is dominated by a small proportion of acicular ferrite and predominantly bainite with martensite-austenite constituent. Whereas, in the 0.45% and 1.01% Cu-containing steels, the acicular ferrite increased significantly due to the effective nucleation on intragranular inclusions with outer layer of MnS and CuS. The formation of acicular ferrite is attributed to superior high heat-affected zone impact toughness in the 0.45% Cu-containing steel. Furthermore, the increasing martensite-austenite constituent and ε-Cu precipitates in the simulated CGHAZ of 1.01% Cu-containing steel caused degradation in impact toughness.
Additional Information:	
Question	**Response**
Is your article an invited article for a special issue? If yes, please select the issue from the drop down list	
Please state the novelty of your submission by providing (at least) four aspects of originality or uniqueness in your article. Please keep each point to a maximum of 12 words.	1. The effect of Cu content on the microstructure and impact toughness in the simulated coarse-grained heat-affected zone of high-strength low-alloy steels were investigated under high heat input welding thermal cycles. 2. High intensity of acicular ferrite formed due to the effective nucleation on intragranular inclusions with outer layer of MnS and CuS in the 0.45% and 1.01% Cu-

	containing steels. 3. The superior impact toughness of the CGHAZ of 0.45% Cu-containing steel is mainly attributed to the formation of high intensity of acicular ferrite. 4.The degradation of impact toughness in the simulated CGHAZ of 1.01% Cu-containing steel was caused by the big area fraction of massive M-A constituents and coarse ε-Cu precipitates.
Funding Information:	China Postdoctoral Science Foundation (2014M550414) — X.L. Wan International Science and Technology Corporation Program of Hubei Province (2015BHE008) — Prof. K. M. Wu International Science and Technology Corporation Program of Central Government (2011DFR51040) — Prof. K. M. Wu

Effect of Cu addition on microstructure and impact toughness in the simulated coarse-grained heat-affected zone of high-strength low-alloy steels

G. Huang[1], X.L. Wan[1], K.M. Wu[1,*], O. Isayev[1], O. Hress[1], Irina Rodionova[2], A. A. Shirzadi[1,3,4]

[1]The State Key Laboratory of Refractories and Metallurgy, Hubei Province Key Laboratory of Systems Science in Metallurgical Process, International Research Institute for Steel Technology, Wuhan University of Science and Technology, Wuhan 430081, China

[2]Center of physical chemistry, materials science, bimetals and special forms of corrosion (CPMC), I. P. Bardin Central Research Institute for Ferrous Metallurgy, Moscow, 105005, Russian Federation

[3]Department of Engineering and Innovation, The Open University, Walton Hall, Milton Keynes, MK7 6AA, UK

[4]Department of Materials Science and Metallurgy, University of Cambridge, 27 Charles Babbage Road, Cambridge CB3 0FS, UK

* Corresponding author: K.M. Wu

Tel.: +86 27 68862772; fax: +86 27 68862606

E-mail address: wukaiming@wust.edu.cn, 1052516931@qq.com

Abstract:

The effects of Cu content on microstructure and impact toughness in the simulated coarse-grained heat-affected zone (CGHAZ) of high-strength low-alloy steels were investigated. It has been observed that the microstructure in the simulated CGHAZ of Cu-free steel is dominated by a small proportion of acicular ferrite and predominantly bainite with martensite-austenite constituent. Whereas, in the 0.45% and 1.01% Cu-containing steels, the acicular ferrite increased significantly due to the effective nucleation on intragranular inclusions with outer layer of MnS and CuS. The formation of acicular ferrite is attributed to superior high heat-affected zone impact toughness in the 0.45% Cu-containing steel. Furthermore, the increasing martensite-austenite constituent and ε-Cu precipitates in the simulated CGHAZ of 1.01% Cu-containing steel caused degradation in impact toughness.

Key words: CGHAZ, impact toughness, acicular ferrite, M-A constituent, Cu precipitation.

1. Introduction

High-strength low-alloy (HSLA) steels are important structural materials, such as pipeline, pressure vessel, ship, bridge and building. They have good mechanical properties, including high strength, resistance to brittle fracture, cold formability and good weldability. Recently, there has been an increasing tendency to apply high heat input welding technique to reduce cost and increase productivity of HSLA steels. It is known that the high heat input welding thermal cycle induces coarse austenite grain and poor microstructure in the coarse-grained heat-affected zone (CGHAZ), leads degradation in toughness. Therefore, improving the toughness of the CGHAZ is an important consideration to fulfill the requirements of high heat input welding technology.

It is generally accepted that the toughness of CGHAZ is strongly influenced by their microstructural feature, which is greatly dependent on chemical compositions of the steel [1-8]. Microalloying elements, such as Nb, V, Ti, Ca, Mg, Zr and rare earth elements played an important role in pinning austenite grain boundary by particle during welding thermal cycle and to provide beneficial sites for the nucleation of intragranular acicular ferrite at intermediate temperatures, which led to refined CGHAZ grains. Some alloy elements, like Al and Si modified the morphology of martensite-austenite (M-A) constituent [6-8].

Cu is usually seen as an excellent aging hardening alloying element, and the adding of Cu content can effectively strengthen the weld metal [9-10]. Many investigations have also been made on the role of Cu content on microstructure evolution and mechanical properties of HSLA steels [11-14]. However, the influence of Cu on microstructural transformation and impact toughness in CGHAZ of Cu-containing HSLA steel is relatively scarce, especially when subjected to high-heat input weld thermal cycles. The objective of present work is to understand the underlying effect of Cu content on the microstructural transformation and accompanying impact toughness in the simulated CGHAZ of HSLA steels subjected to high heat input welding thermal cycle.

2. Experimental procedures

Three tested steels, microalloyed with 0.0%, 0.45% and 1.01% Cu contents, were prepared in a 10 kg vacuum melt induction furnace. The chemical compositions are listed in Table 1. The ingots were forged and then machined to make samples with the dimensions of 10 mm×10 mm×55 mm. The simulation of the CGHAZ was carried out using a Gleeble 3800. The peak temperature for thermal cycle simulation was 1350°C, with a heating rate of 300°C/s, and a holding time of 3 s. The cooling time from 800°C to 500°C ($t_{8/5}$) was 52.8 s, which was approximately equivalent to submerged arc welding at the heat input of 100 kJ/cm [6].

After CGHAZ simulation, the specimens were then impact-tested at -20 ^{o}C. Microstructural observations were done by means of optical microscope (Olympus BM51) and a Nova 400 Nano field scanning electron microscope (FE-SEM). The acicular ferrite and martensite-austenite (M-A) constituents in the digital images of the simulated CGHAZ were selected and painted black using Adobe Photoshop, as shown in Fig. 1. The density and area fraction of acicular ferrite grains and M-A constituents were estimated by using a commercial image processing software, which had provision for quantitative analysis. 20 digital images were analyzed to arrive at an average value of the above parameters. The characteristics of particles in the simulated CGHAZ were also revealed in a TEM (JEM-2100) operated at 200 kV. The orientation relationship and crystallographic grain size of microstructure was examined using electron backscattered diffraction (EBSD) by means of a Philips XL30W/TMP scanning electron microscope (SEM).

In order to characterize the inclusion, samples (80 mm × Φ10 mm) taken from the investigated steels were electrolyzed in a nonaqueous solution, having pH value 8. The inclusions separated from the steels were not destroyed, which was verified by the isotope tracer method [15]. The inclusions were then observed by SEM and energy-dispersive spectroscopy (EDS) analysis.

3. Results

3.1 Microstructure characteristics in the simulated CGHAZ

Fig. 2 shows optical micrographs in the CGHAZ of specimens with different Cu contents. The microstructure in the simulated CGHAZ of Cu-free steel mainly consists of small proportion of acicular ferrite and predominant bainite, which were composed of paralleled bainitic ferrite and M-A constituents, as shown in Figs. 2a and 2b. A few of acicular ferrite grains were scattered in the prior austenite grain (indicated by red arrow in Fig. 2b). Most of intragranular inclusions in Cu-free steels were observed as ineffective nucleation sites for acicular ferrite formation (indicated by white arrow in Fig. 2b). The bainite nucleated on grain boundary and grew into grain interior (indicated by yellow arrow in Fig. 2b). These bainitic ferrite sheaves grew in the form of packets and acicular ferrite grain embedded in the packets. However, the predominant microstructure has been changed in Cu-containing steels. The microstructures in the 0.45% and 1.01% Cu-containing steels mainly consist of high intensity of acicular ferrite grains at the vicinity of intragranular inclusions, as represented in Figs. 2c-f. The typical high magnification image, as shown in Figs. 2d and 2f, indicated that some acicular ferrite grains nucleated on an inclusion, grew at different directions, impinged and intersected with neighboring acicular ferrite and formed interlocked microstructure [15].

The prior austenite grain size is important to investigate the microstructural

evolution [16]. The size of prior austenite grains was measured by the method based on averaging the long and short axes of the grains in about 20 optical micrographs for each sample. The mean diameters of prior austenite grains of all samples increased visibly from 62 to 79 μm when the Cu content increased from 0% to 0.45%, as shown the measured results in Fig. 3a. Furthermore, when Cu content continues increasing to 1.01%, the mean austenite grain diameter for the sample was increased slightly from 79 to 81 μm.

The formation of acicular ferrite is one of the most important factors for improving toughness in the CGHAZ of HSLA steels [17]. The area fraction of acicular ferrite grains in the simulated CGHAZ of all samples were measured and revealed in Fig. 4b. The minimum area fraction of acicular ferrite is 8% in the simulated CGHAZ of the Cu-free steel. The area fraction of acicular ferrite increased to 38% with Cu content increased to 0.45%. Furthermore, when the Cu content increased to 1.01%, the variation of frequency of acicular ferrite in the simulated CGHAZ is minor and unobvious.

Figs. 4a-c shows the typical color metallographic images in the simulated CGHAZ of three investigated steels. The M-A constituents were observed in between the bainite packets and acicular ferrite with shape of block-like and rod-like (indicated by black and white arrows, respectively). It reveals that the fraction and density of M-A

constituents vary with increasing Cu content. The quantitative analysis in Figs. 4d-f shows that the parameters of M-A constituents change obviously as a function of Cu content. The addition of Cu has a different influence on area fraction and density of M-A constituents, as shown in Figs. 4d and 4e, respectively. The area fraction of M-A constituents increased obviously with increasing Cu content. However, the density of M-A constituents in the simulated CGHAZ of each specimen is found between $3\sim4\times10^4$ pieces/mm^2 and the difference of each other is relative small. It was previously reported that the M-A constituents with large length (length > 2μm) and small length/width ratio (length/width < 4) are regarded as massive M-A constituents, which is usually considered as a harmful factor for impact toughness [18]. It is clear from Fig. 4f that the fraction of massive M-A increased visibly with increasing Cu content. The fraction of massive M-A constituents in the specimen of 1.01% Cu is more than three times of that in the specimen with 0.45% Cu.

3.2 Particle analysis in the simulated CGHAZ

Inclusion analysis was carried out by using SEM equipped with EDS. SEM micrographs and the respective elemental intensity of particles in the simulated CGHAZ of samples with different Cu contents are presented in Fig. 5. Many inclusions with spherical shape were observed in samples (Fig. 5a, c, e). The inclusion in the simulated CGHAZ of Cu-free steel represented in Fig. 5a was 2.3 μm in

diameter, which was similar to that in the 0.45% and 1.01% Cu-containing steels (Figs. 5c and 5e). The corresponding intensities of the aforementioned elements in the EDS spectra are represented in Figs. 5b, d and f. It was indicated that the inclusion in Cu-free steel mainly consisted of Al, Ti, Mn, S, and O elements. The element composition of inclusions in the 0.45% and 1.01% Cu-containing steels show that it consisted of Al, Ti, Mn, Cu, S and O elements. From these results, it is clear that the differences associated with the acicular ferrite formation in steels are attributed to the differences observed in EDS analysis, in particular to Cu-element.

In order to avoid the influence of the steel matrix on the analysis of the inclusions in steels, those inclusions were separated in a nonaqueous solution from the Cu-free and 0.45% Cu-containing steels. Figs. 6 and 7 show the exterior shape and the respective EDS mapping images of inclusions, respectively. The inclusion separated from the Cu-free steel is spherical in shape with 6 μm in diameter (Fig. 6a). The elemental mapping of the inclusions was conducted - see Figs. 6b-f. It is indicated that the inclusion was composite oxide, which mainly consisted of Al, Ti, Si, Mn and O elements. The S is observed in the top-left corner part of the inclusion, which was usually seen as Al-Ti oxides covered with an outer layer of MnS [19]. However, the element composition of inclusion in the simulated CGHAZ of 0.45% Cu-containing steel shows that it consisted of Al, Ti, Mn, Cu, S and O elements (Figs. 7b-f), which

was usually seen as Al-Ti oxides covered with an outer layer of MnS and CuS [20]. The Cu and S elements are observed in the upper part of the inclusion and are overlapped (Figs. 7e and 7f), indicating the presence of CuS.

TEM micrograph and the respective EDS analysis of inclusion in the 0.45% Cu-containing steel were conducted to reveal the location of Cu and S in details -see Fig. 8. The EDS analysis in center (spectrum 1) and corner (spectrum 2) in Figs. 8a and b indicates that the CuS is on the outer layer of inclusion.

Furthermore, the observation by TEM and EDS indicated that not only oxides but also a large number of (Ti,Nb)(N,C) and ε-Cu were precipitated in the specimens. Fig.9 shows typical TEM images in the simulated CGHAZ of three steels, and the black and white arrows were used to indicate the typical (Ti,Nb)(N,C) and ε-Cu precipitates, respectively. With the increasing of Cu content, the number of ε-Cu precipitates increased and coarsened obviously, as shown in Figs. 9d and 9f. The diameter distribution of ε-Cu precipitates was revealed in Fig. 10. Approximately all of ε-Cu precipitates are smaller than 20 nm in 0.45% Cu-containing steel whereas only about 81% of them are in the same range in 1.01% Cu-containing steel. The mean diameters of ε-Cu precipitates in 0.45% and 1.01% Cu-containing steels are 8.3 nm and 16 nm, respectively. It is indicated that the fine ε-Cu precipitates existed in 0.45% Cu-containing steel are more than that in 1.01% Cu-containing steel.

3.3 EBSD analysis and grain size determination

Figs. 11 shows EBSD analysis in the simulated CGHAZ of three samples. Figs. 11a-c are the corresponding EBSD orientation image maps of normal direction of CGHAZ in the steel with 0%, 0.45% and 1.01% Cu content, respectively. The final microstructure of bainite packets in the Cu-free steel nucleated on different sites of grain boundaries, and different bainite packets are represented by different color and characterized with high angle grain boundaries between the packets with large misorientations (50° - 60°). The bainitic ferrite laths/plates in the same bainite packets represented by similar color, indicate that the bainitic ferrite plates occur in bundles or packets and are characterized with low angle grain boundaries (<3°) among those plates [12]. However, Figs. 11b and 11c represented that the acicular ferrite grains in 0.45% and 1.01% Cu-containing steels grew radially in the interior of prior austenite grain and have different orientations with neighboring ferrite plates. The misorientation through those acicular ferrite grains shows that the boundary of ferrite plates have high misorientation of 50° - 60°. Different bainite packets are represented by different color and characterized with high angle grain boundary between the packets with large misorientations (50° - 60°) [16].

Figs. 12a and b shows the distribution of the grain boundary misorientation angles between adjacent grains. It is clear that the frequency of low angle grain boundaries

(3° - 15°) in the simulated CGHAZ of Cu-free steel is larger than that in the 0.45% and 1.01% Cu-containing steels (Fig. 12a). In contrast, more number of high angle grain boundaries (45° - 62°) was observed in 0.45% and 1.01% Cu-containing steels (Fig. 12b). In the present work, the large angle grain boundary threshold is estimated to be 15°. It means that the grain boundary with a misorientation larger than 15° can be regarded as the boundary of two grains. The grains were assumed to be spherical to facilitate grain size measurement. Fig. 12c shows the statistical distribution of crystallographic grain size, in which the crystallographic grain sizes in the simulated CGHAZ of three steels are 9.4 μm, 4.7 and 4.3 μm, (Fig. 12d). These grains are much smaller than that of prior austenite grains (62 μm, 79 μm and 81 μm for Cu-free and Cu-0.45%and Cu-1.01% steels, respectively). The crystallographic grain size is smaller and more uniform in the Cu-containing steel. The percentage of grain refinement from prior austenite grain size is more in the 0.45%and 1.01% Cu-containing steels due to the formation of acicular ferrite i.e. ~94% (16.8 times finer in 0.45% Cu-containing steel) and ~95% (18.8 times finer in 1.01% Cu-containing steel). In case of Cu-free steel the percentage of grain refinement is ~85% (8.6 times finer).

3.4 Impact toughness and impact fractured surface

The Charpy-V notch absorbed energy data of the simulated CGHAZ in specimens with different Cu addition at -20 ^{o}C is obtained and presented in Fig. 13. It is revealed

that the average absorbed energy of the samples increase obviously with increasing Cu content from 0% to 0.45%. The average absorbed energy in the simulated CGHAZ of Cu-free and 0.45% Cu-containing steels are 78 J and 299 J, respectively. Superior high HAZ toughness in the 0.45% Cu-containing steel is obtained. However, with the Cu content increased to 1.01%, it is obvious that the mean impact energy of simulated CGHAZ decreased abruptly to 41 J.

Fracture surfaces of all samples are consisting with the corresponding toughness values [21]. Fig. 14 shows the impact fracture feature for the samples with different Cu contents. There was striking difference in the nature of fracture associated with specimens with different impact energy. It is revealed in Fig. 14b that the impact fracture surface of CGHAZ in the 0.45% Cu-containing steel consists of dimples. The presence of dimples indicates typical ductile fracture. On the other hand, the fracture surface of the CGHAZ in Fig. 14a and 14c with a river pattern exhibits a quasi-cleavage fracture mechanism. The difference observed in the impact toughness values and nature of fracture mechanisms was attributed to the microstructure in each samples.

4. Discussion

4.1 Effect of Cu on superior HAZ toughness in the 0.45% Cu-containing steel

The nucleation of acicular ferrite is usually considered to be stimulated by (a) the

solute depletion in the vicinity of non-metallic inclusions [22], (b) the reduced interfacial energy between austenite and ferrite [23], (c) the thermal strain energy due to the differential thermal contraction [23], and (d) the provision of an inert surface [24]. The predominant mechanisms contributing to the acicular ferrite nucleation can be one, or combination of the above four mechanisms. The inclusions formed during steelmaking process may consist of oxides, sulfides, and nitrides [20, 25]. Sulfides and nitrides usually cover on the surface of oxides and form complex inclusions. Due to this complex nature of inclusions, it is difficult to determine the predominant nucleation mechanism for acicular ferrite. Several studies reported on the theoretical and experimental analysis concluded that there may be a combination of nucleation mechanisms involved in the formation of acicular ferrite [20, 25]. However, the dominant mechanism for the nucleation of acicular ferrite is the formation of an element depletion zone around inclusions [26].

In Cu-free steel, few acicular ferrite grains were nucleated on certain inclusions. These inclusions consist of Al, Ti, Mn, O and S elements. It has been observed that the inclusions were Al and Ti complex oxides covered with MnS, which usually induces the formation of Mn depleted zones due to the MnS precipitation [22]. The formation of Mn depleted zones increased the phase transformation temperature and driving energy for nucleation, thereby promoting the nucleation of acicular ferrite

grains. In contrast to Cu-free steel, the inclusion in the 0.45% Cu-containing steel was characterized with Al and Ti complex oxides covered with MnS and CuS. The presence of CuS in the vicinity of complex inclusions has contributed to the formation of high density of acicular ferrite grains [26]. This difference is also explained in terms of lattice constant and the percentage mismatch with ferrite. The lattice constant of CuS has lower mismatched with ferrite (~3%) than MnS with ferrite (~9%) [20, 25, 27]. Hence the presence of CuS can effectively reduce interfacial energy between austenite and ferrite and thus promote the acicular ferrite formation [20]. So, the inclusion with MnS and CuS layer in Cu-containing steel is one of the most effective nucleation sites for acicular ferrite, due to the complex nucleation mechanism of the solute depletion in the vicinity of inclusion and the reduced interfacial energy between austenite and ferrite combination [20]. Furthermore, it is also known that prior austenite grain size has an important influence on acicular ferrite nucleation. The minimum austenite grain size for acicular ferrite nucleation is 50-60 μm in the CGHAZ, where the highest nucleation potential was achieved with austenite grain sizes of 180-190 μm [13, 16, 28]. The larger austenite grain size in simulated CGHAZ of Cu-containing steels also has an important influence on the formation of high intensity of acicular ferrite.

Acicular ferrite is considered to be a desirable microstructure in CGHAZ of HSLA steels as it contributes to higher toughness [17]. In the present study, the

frequency of acicular ferrite grains in 0.45% Cu-containing steel is nearly four times higher than that in Cu-free steel. The formation of high density of acicular ferrite grains contributed to the higher percentage of grain refinement [29]. Therefore, the average diameter of crystallographic grains was lower in the 0.45% Cu-containing steel. Because of the high density of fine-grained acicular ferrite, the cracks are less mobile and can change the route of propagation during Charpy V-notch impact test [21]. It absorbs more energy and forms a fracture surface with dimples in the simulated CGHAZ of 0.45% Cu-containing steel.

4.2 Effect of Cu on degradation of HAZ toughness in 1.01% Cu-containing steel

It is generally accepted that acicular ferrite microstructure in CGHAZ of HSLA steels provides excellent toughness by virtue of grain refinement. When the Cu content increased to 1.01%, higher intensity of fine-grained acicular ferrite in the simulated CGHAZ was obtained, as shown in Figs. 2f. However, the impact toughness in the simulated CGHAZ of 1.01% Cu-containing steel degenerates slightly to 41 J, and the fracture mechanism in the simulated CGHAZ changed to quasi-cleavage fracture in the 1.01% Cu-containing steel. The variation of impact toughness and fracture surface were affected by M-A constituents [18]. It has been found that M-A constituents can influence the impact toughness of HAZ [18]. The M-A constituent acts as an initiation site for a crack and also promotes its propagation, especially for

massive M-A constituent [18]. It induces the fracture and leads to the surface of CGHAZ in steel with a river pattern. Formation mechanism of M-A constituent is thought to be that carbon is diffused from acicular ferrite/bainitic ferrite into austenite, and the austenite with carbon concentration decreases temperature of $\gamma \rightarrow \alpha$ transformation [30]. Then a part of austenite will be transformed into martensite in lower temperature, and some untransformed austenite is retained. Cu is the element of stable austenite, which could promote the formation of more low temperature transformation product, such as retained austenite or M-A constituents, through decreasing the transformation start temperatures in the continuous cooling transformation (CCT) diagram [31]. In the present work, the A_{r3} temperature of the steels was calculated by JMatPro software. It reveals that the A_{r3} temperature decreases 9.8 °C and 22.8 °C when Cu content increased from 0 to 0.45% and 1.01%. the carbon atoms have a lower diffusion rate in Cu-containing steel when the austenite starts to transform to bainitic ferrite. Therefore the retained austenite with lower carbon content in Cu-containing steel will be larger than that in Cu-free steel. This phenomenon induces increasing size and fraction of M-A constituents, especially for massive M-A constituents (Fig. 4). Previous works revealed that the massive M-A constituents are dramatically detrimental to the toughness of CGHAZ [18]. Fig. 4f reveals that the area fraction of massive M-A constituents in the 1.01% Cu-containing steel is more than three times of that in the

0.45% Cu-containing steel, which thus resulted in the degradation in impact toughness of the latter.

Furthermore, the solubility of Cu is approximately 3 wt.% in γ phase and 0.1 wt.% in α phase in low carbon steels, respectively [32, 33]. The Cu in the simulated CGHAZ in 1.01% Cu-containing steel will be precipitated in form of not only CuS but also ε-Cu during cooling process in welding thermal cycle. A large number of ε-Cu precipitates in the matrix in the simulated CGHAZ of HSLA steels will increase the strength, and thus decrease the toughness [34, 35]. In the present work, a large amount of coarse ε-Cu particles existed in the ferrite in the simulated CGHAZ in 1.01% Cu-containing steel, which is another reason for the degradation in impact toughness.

5. Conclusions

(1) When the steel contains 0.45% Cu, the superior impact toughness of the CGHAZ of HSLA steels was obtained, which is mainly attributed to the formation of high intensity of acicular ferrite.

(2) The degradation of impact toughness in the simulated CGHAZ of 1.01% Cu-containing steel was mainly caused by the big area fraction of massive M-A constituents. The coarse ε-Cu precipitates during thermal cycles also have an important influence on degradation in impact toughness.

Acknowledgements

Authors gratefully acknowledge the support from the China Postdoctoral Science Foundation (No. 2014M550414) and from International Science and Technology Corporation Program of Hubei Province (No. 2015BHE008) and Central Government (No. 2011DFR51040).

References:

[1] W. Yan, Y.Y. Shan, K. Yang: *Metall. Mater. Trans. A*, 2007, **38**, 1211-1222.

[2] B.K. Show, R. Veerababu, R. Balamuralikrishnan, G. Malakondaiah: *Mater. Sci. Eng. A*, 2010, **527,** 1595-1604.

[3] G. Xu, X.L. Gan, G.J. Ma, F. Luo, H. Zou: *Mater. Des.*, 2010, **31**, 2891-2896.

[4] T. Funakoshi, T. Tanaka, S. Ueda, M. Ishikawa, N. Koshizuka, K. Kobayashi: *Trans. ISIJ.*, 1977, **17**, 419-427.

[5] S. Kanazawa, A. Nakashima, K. Okamoto, K. Knaya: *Trans. ISIJ*, 1976, **16**, 486-495.

[6] L. Yu, H.H. Wang, X.L. Wang, G. Huang, T.P. Hou, K.M. Wu: *Mater. Sci. Technol.*, 2014, **30(15)**, 1951-1958.

[7] E. Bonnevie, G. Ferriere, A. Ikhlef, D. Kaplan, J. M. Orain: *Mater. Sci. Eng. A*, 2004, **385**, 352-358.

[8] Y.Q. Zhang, H.Q. Zhang, W.M. Liu, H. Hou: *Mater. Sci. Eng. A,* 2009, **499**, 182-186.

[9] D.J. Widgery: *Met. Constr.,* 1978, **10**, 480-483.

[10] S.B.Li, J.X. Zhang, B.K. Zhu: *Weld. Joi.*, 2005, **11**, 27-30. (In Chinese)

[11] I. Madariaga, J.L. Romero, I. Gutiérres: *Metall. Mater. Trans. A,* 1998, **29A,** 1003-1015.

[12] M. Díaz-Fuentes, I. Madariaga, I. Gutiérres: *Mater. Sci. Forum,* 1998, **284-286,** 245-252.

[13] R. Laitinen: Improvement of weld HAZ toughness at low heat input by controlling the distribution of M-A constituents, University of Oulu, **2006,** Finland.

[14] X. Shi, W. Yan, W. Wang, Y. Shan, K. Yang: *Mater. Des.*, 2016, **92,** 300-305.

[15] X.L. Wan, H.H. Wang, L. Cheng, K.M. Wu: *Mater. Charact.*, 2012, **67**, 41-51.

[16] X.L. Wan, K.M. Wu, K.C. Nune, Y. Li, L. Cheng: *Sci. Technol Weld Joi.,* 2015, **20(3)**, 254-263.

[17] A.M. Guo, S.R. Li, J. Guo, P.H. Li, Q.F. Ding, K.M. Wu, X. L. He: *Mater. Charact.*, 2008, **59(1)**, 134-139.

[18] F. Matsuda, Z. Li, P. Bernazovsky, K. Ishihara, H. Okada: *Weld World*, 1991, **29(9/10),** 307-313.

[19] H. Mabuchi, R. Uemori, M. Fujioka: *ISIJ Int.,* 1996, **36**, 1406-1412.

[20] I. Madariaga, I. Gutiérres: *Scripta Mater.,* 1997, **37**, 1185-1192.

[21] M. Shi, P. Zhang, F. Zhu: *ISIJ Int.*, 2014, **54**, 188-192.

[22] H. Mabuchi, R. Uemori, M. Fujioka: *ISIJ Int.,* 1996, **36**, 1406-1412.

[23] S. Zhang, N. Hattori, M. Enomoto, T. Tarui: *ISIJ Int.*, 1996, **36**, 1301-1309.

[24] R.A. Ricks, P.R. Howell, G.S. Barritte: *J. Mater. Sci.*, 1982, **17**, 732-740.

[25] T Furuhara: *ISIJ Int.,* 2003, **43**, 2028-2037.

[26] J.H. Shim, J.S. Byun, Y.W. Cho, Y.J. Oh, J.D. Shim, D.N. Lee: *Scripta Mater.*, 2001, **44**, 49-54.

[27] Z. Liu, M. Kuwabara: *Steelmaking,* 2007, **23(3)**, 7-13. (In Chinese)

[28] J.L. Lee, Y.T. Pan: *Mater. Sci. Eng. A*, 1991, **136,** 109-119.

[29] X.L. Wan, R. Wei, K.M. Wu: *Mater .Charact.*, 2010, **61**, 726-731.

[30] E. Mazancová, K. Mazanec: *J. Mater. Process. Tech.*, 1997, **64(1)**, 287-292.

[31] L. Meyer, F. Heisterkamp, W. Mueschenborn: Proceedings of Microalloying 75, Washington, DC, 1975, 153-167.

[32] M. Morita, K. Sato, Y. Hosoya: *ISIJ Int.*, 1994,**34(1)**, 92-98.

[33] F. Soisson, A. Barbu, G. Martin: *Acta Mater*, 1996, **44 (9)**, 3789-3800.

[34] D. Dunne: Weldable Copper Strengthened Low Carbon Steels, Proceedings of HSLA steel, Beijing, 1995, **10**, 79-84.

[35] D.T. Liewllyn: *Ironmak. Steelmak.*, 1995, **22(1)**, 25-50.

Table caption:

Table 1 Chemical composition of the investigated steels (wt. %).

Samples	C	Si	Mn	Cu	Nb	V	Ti	Al	S	Fe
1#	0.055	0.21	1.61	-	0.040	0.022	0.012	0.022	0.0020	Bal.
2#	0.058	0.20	1.60	0.45	0.038	0.025	0.010	0.024	0.0018	Bal.
3#	0.054	0.23	1.63	1.01	0.041	0.020	0.013	0.020	0.0018	Bal.

Figure captions:

Fig. 1. The (a) gray and (c) color images showing microstructures in the simulated CGHAZ. (b) and (d) processed images of (a) and (c) using Adobe Photoshop, respectively.

Fig. 2. Optical micrographs of the simulated CGHAZ for (a,b) Cu-free, (c,d) 0.45% Cu, and (e,f) 1.01% Cu steels, respectively. The inclusion, acicular ferrite, bainite and M-A constituent were indicated by white, red, yellow and black arrows, respectively.

Fig. 3. The relationship of (a) prior austenite grain size and (b) area fraction of AF with copper content.

Fig. 4. The color metallographic images of the simulated CGHAZ in the specimens of (a) Cu-free, (c) Cu-0.45% and (d) Cu-1.01%; the relationship of (d) area fraction and (e) density M-A constituents with Cu content; and (f) the relation of fraction of massive M-A constituents with heat inputs. The block-like and rod-like M-A constituents were indicated by white and black arrows, respectively.

Fig. 5. SEM micrograph and corresponding EDS analysis of the simulated CGHAZ in (a, b) Cu-free steel, (c, d) Cu-0.45% and (e, f) Cu-1.01%, respectively.

Fig. 6. (a) SEM micrograph and corresponding (b-f) EDS mapping images of the inclusion in Cu-free steel.

Fig. 7. (a) SEM micrograph and corresponding (b-f) EDS mapping images of the

inclusion in the 0.45% Cu-containing steel.

Fig. 8. (a) TEM image and corresponding (b) EDS analysis of the inclusion in the 0.45% Cu-containing steel.

Fig. 9. TEM images of the simulated CGHAZ in (a, b) Cu-free, (c, d) Cu-0.45%, and (e, f) Cu-1.01% steels subjected to 100 kJ/cm heat input welding thermal cycle. The black and white arrows indicate the (Ti,Nb)(N,C) and ε-Cu precipitates, respectively.

Fig. 10. The diameter distributions of ε-Cu precipitates in (a) 0.45% and (b) 1.01% Cu-containing steels.

Fig.11. Orientation maps of bcc phases for the samples with (a) Cu-free, (b) Cu-0.45% and (c) Cu-1.01%, and (d) orientation color key.

Fig. 12. Statistical distribution of (a, b) grain angles between adjacent grains and (c) crystallographic grain size, and (d) mean crystallographic grain size of the simulated CGHAZ in investigated steels.

Fig. 13. The effect of copper content on impact toughness with the simulated heat input of 100 kJ/cm.

Fig. 14. SEM images showing fracture surfaces in the simulated CGHAZ in (a) Cu-free, (b) Cu-0.45% and (c) Cu-1.01% steels, respectively.

Fig.1a

Click here to download Colour figure (online version only) Fig.1a.tif

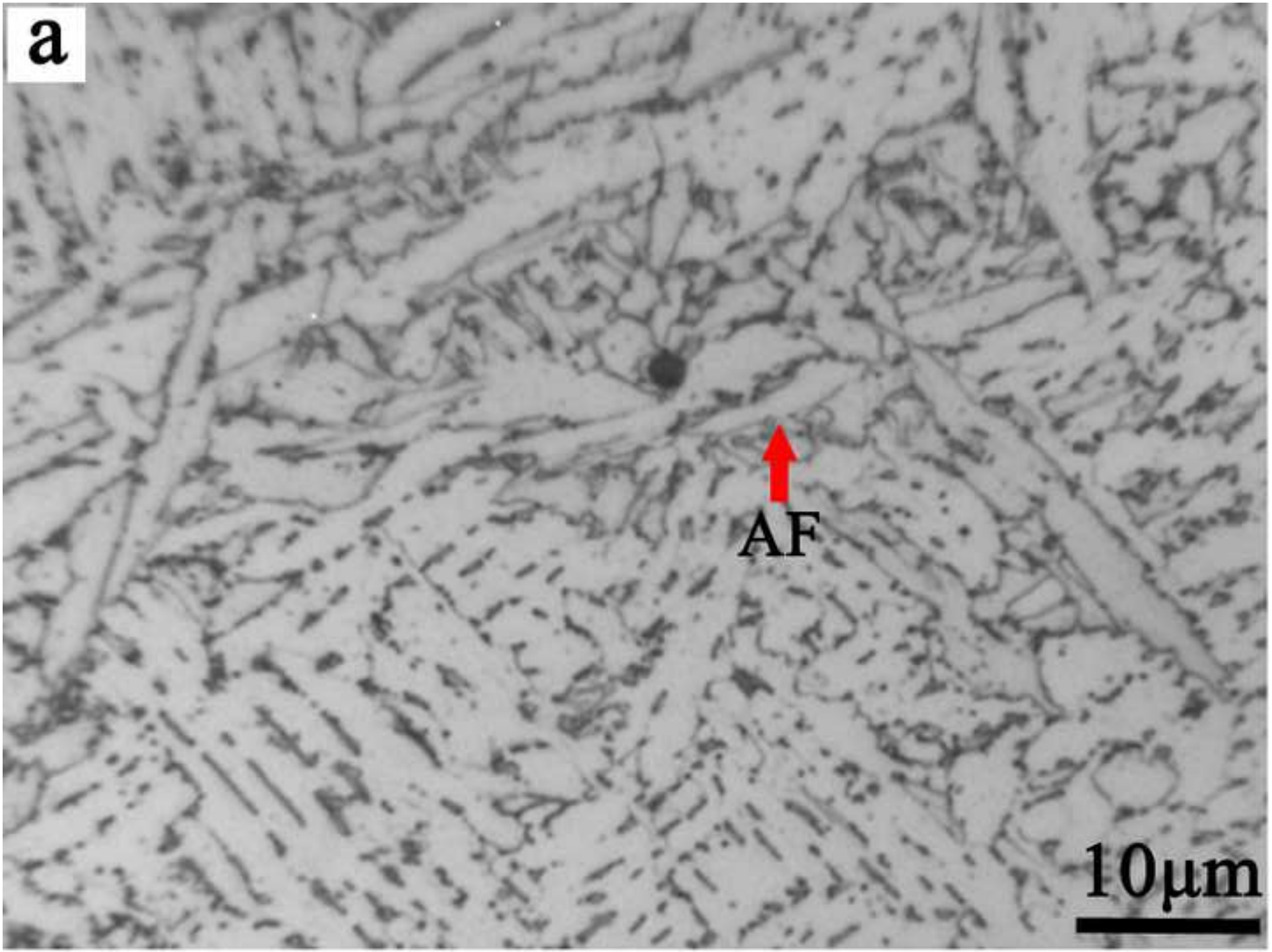

Fig.1b

Click here to download Colour figure (online version only) Fig.1b.tif

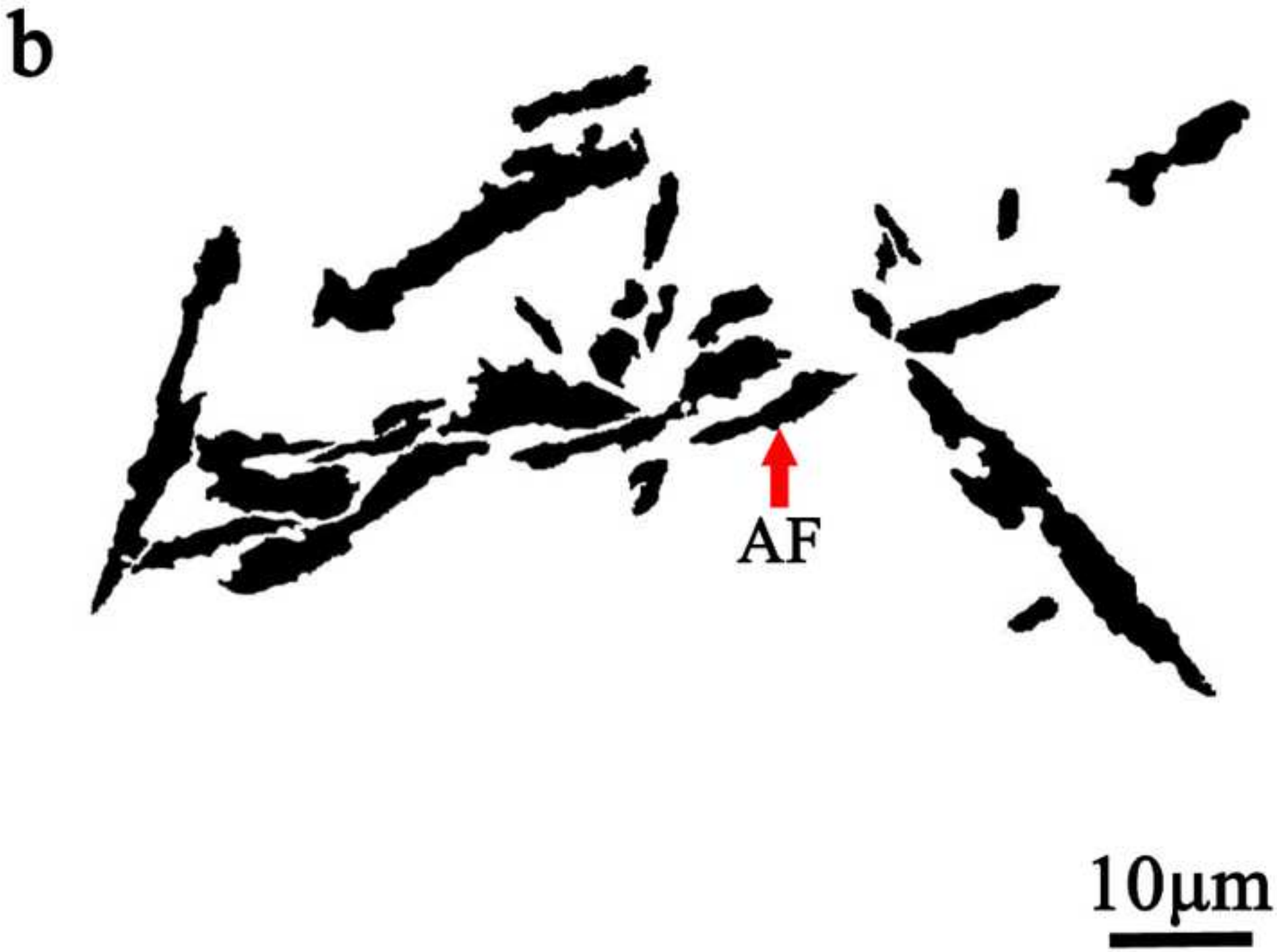

Fig.1c

Click here to download Colour figure (online version only) Fig.1c.tif

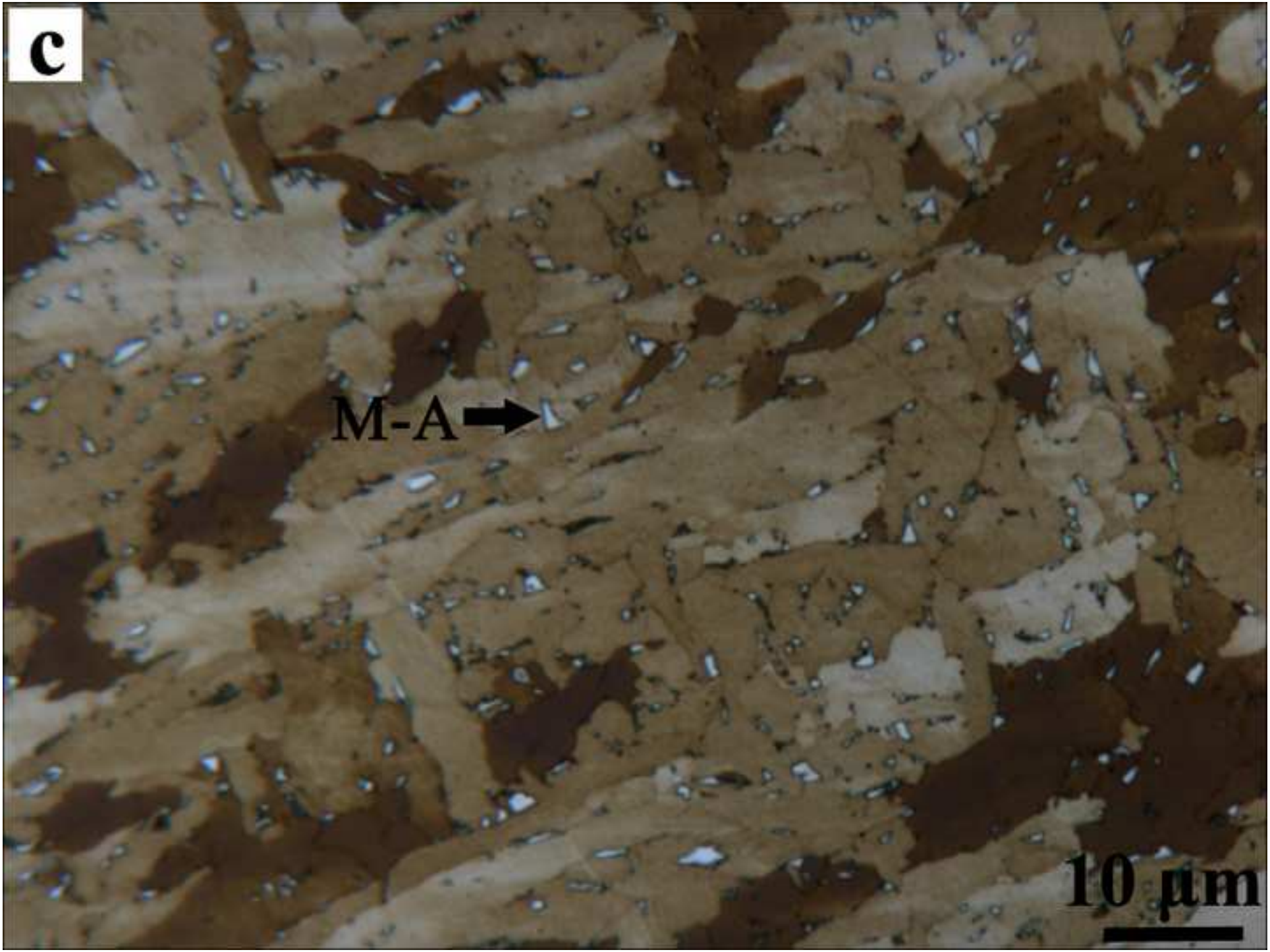

Fig.1d

Click here to download Colour figure (online version only) Fig.1d.tif

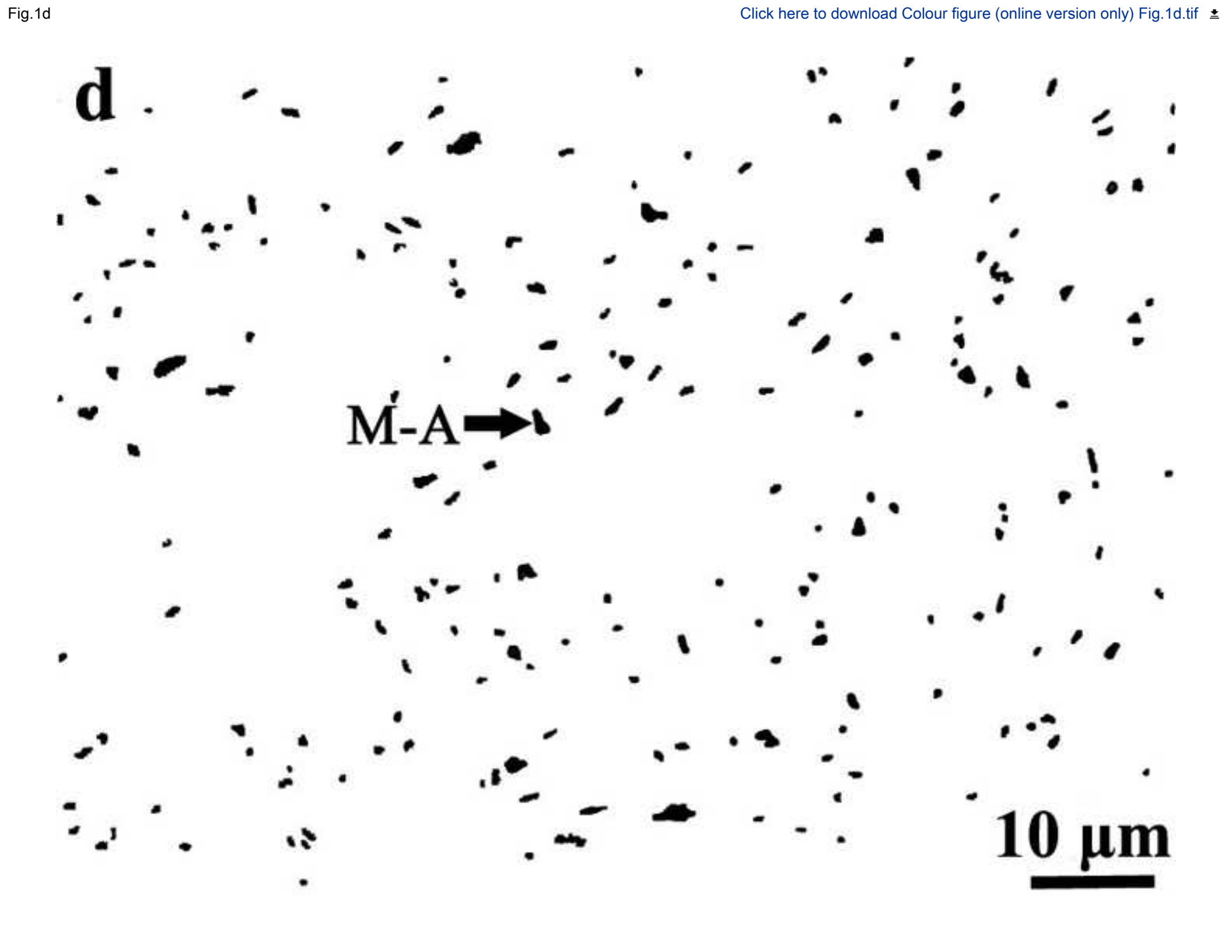

Fig.2a

Click here to download Non-colour figure Fig.2a.tif

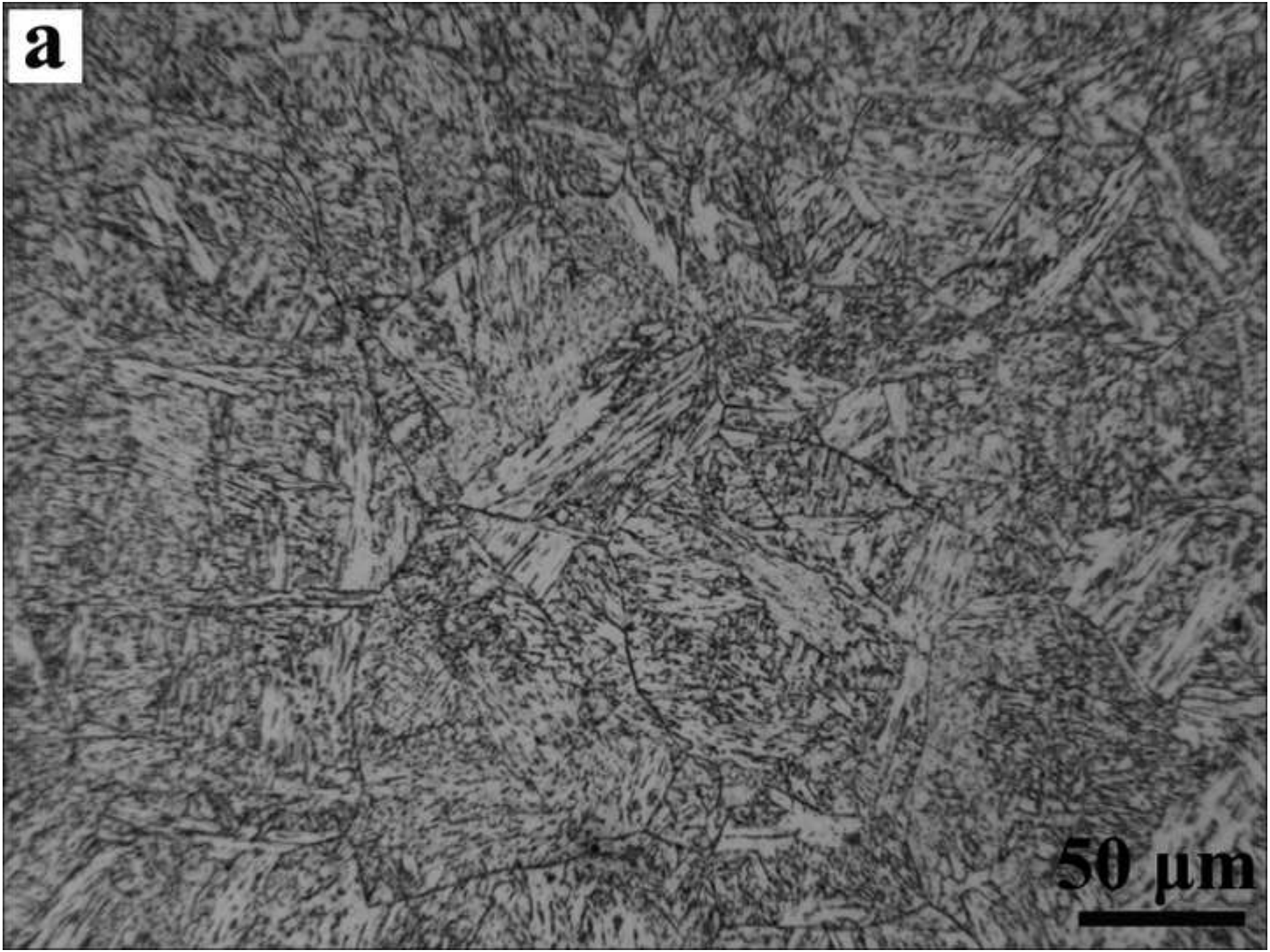

Fig.2b

Click here to download Colour figure (online version only) Fig.2b.tif

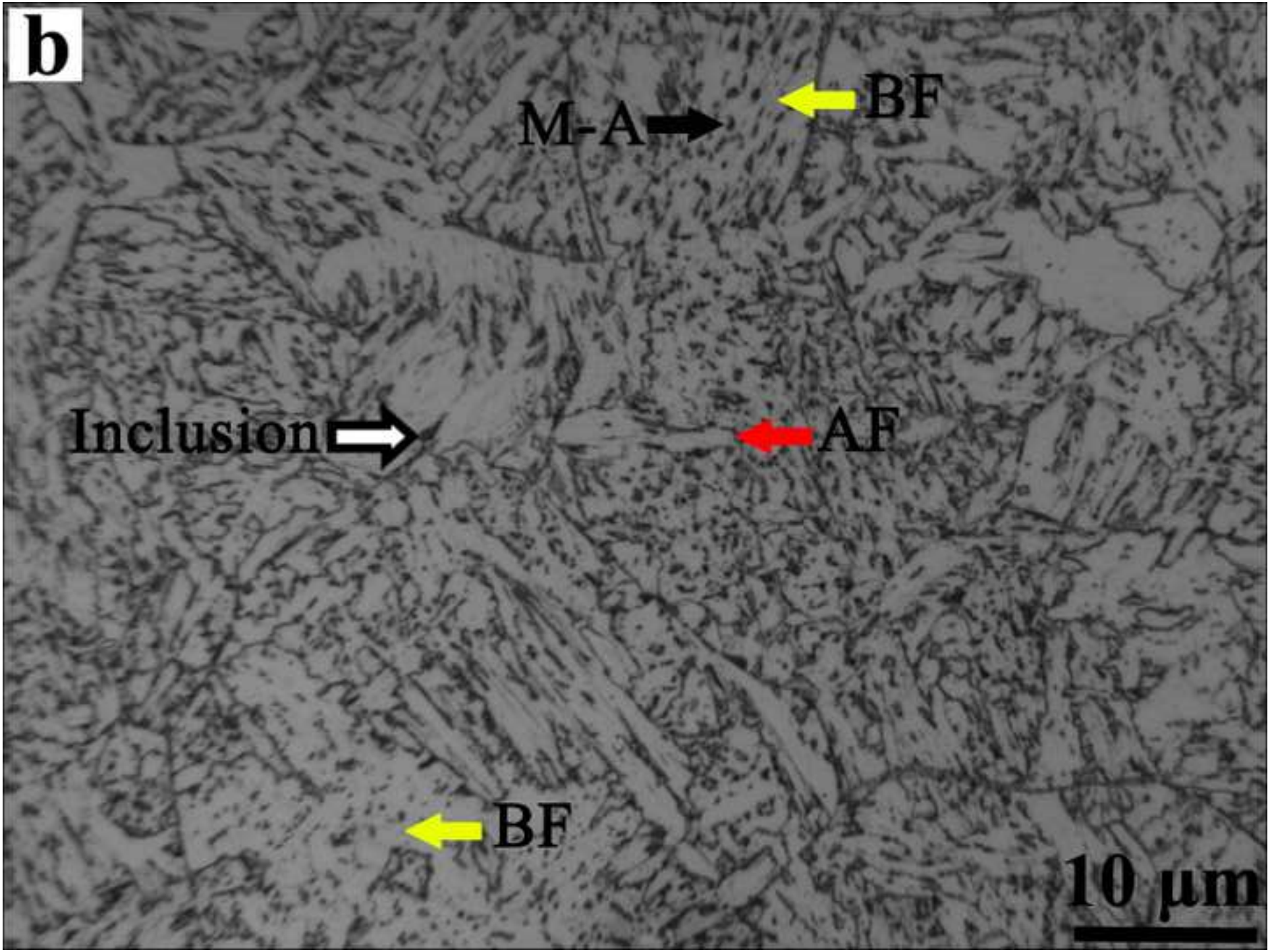

Fig.2c

Click here to download Non-colour figure Fig.2c.tif

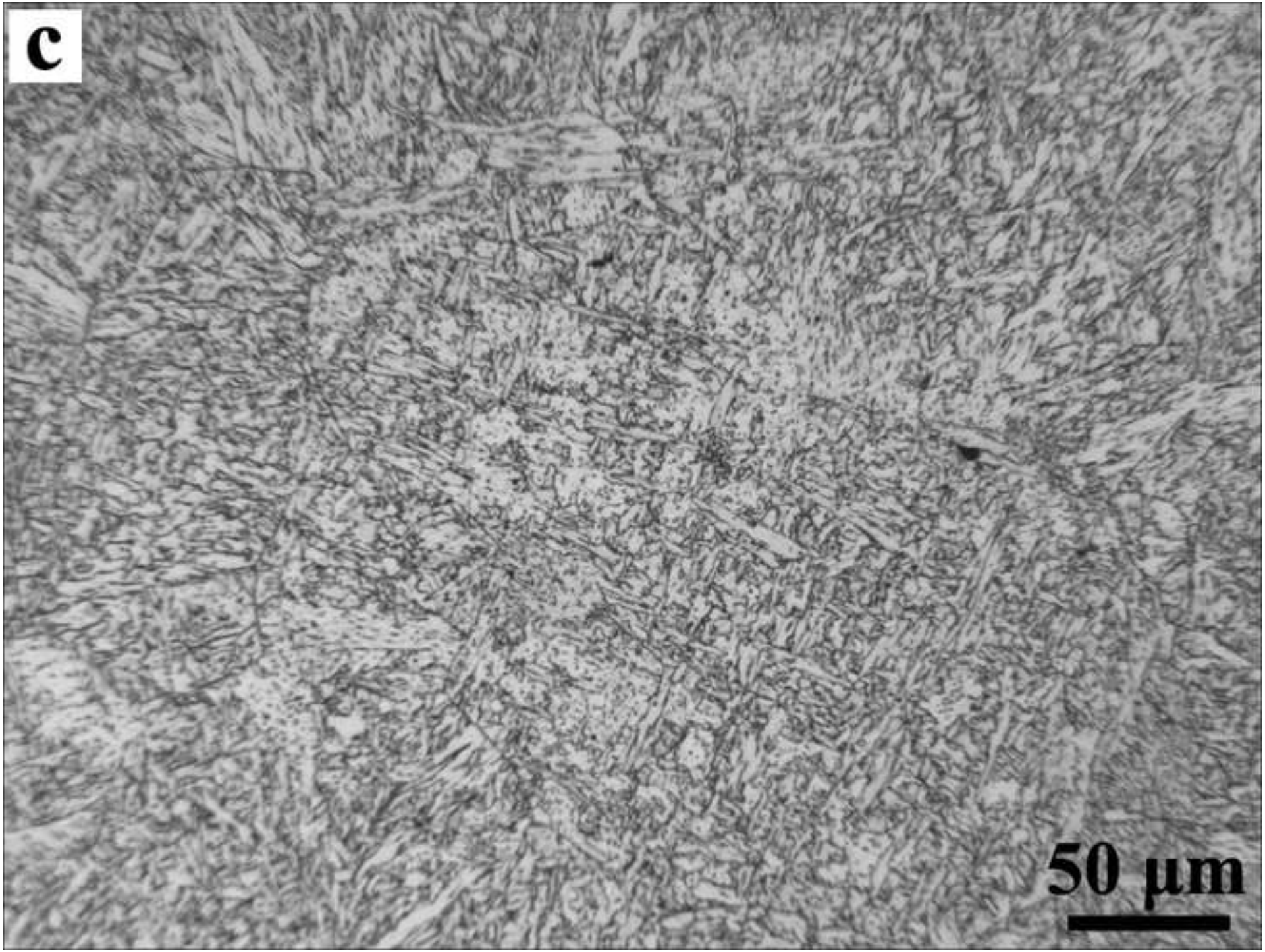

Fig.2d

Click here to download Colour figure (online version only) Fig.2d.tif

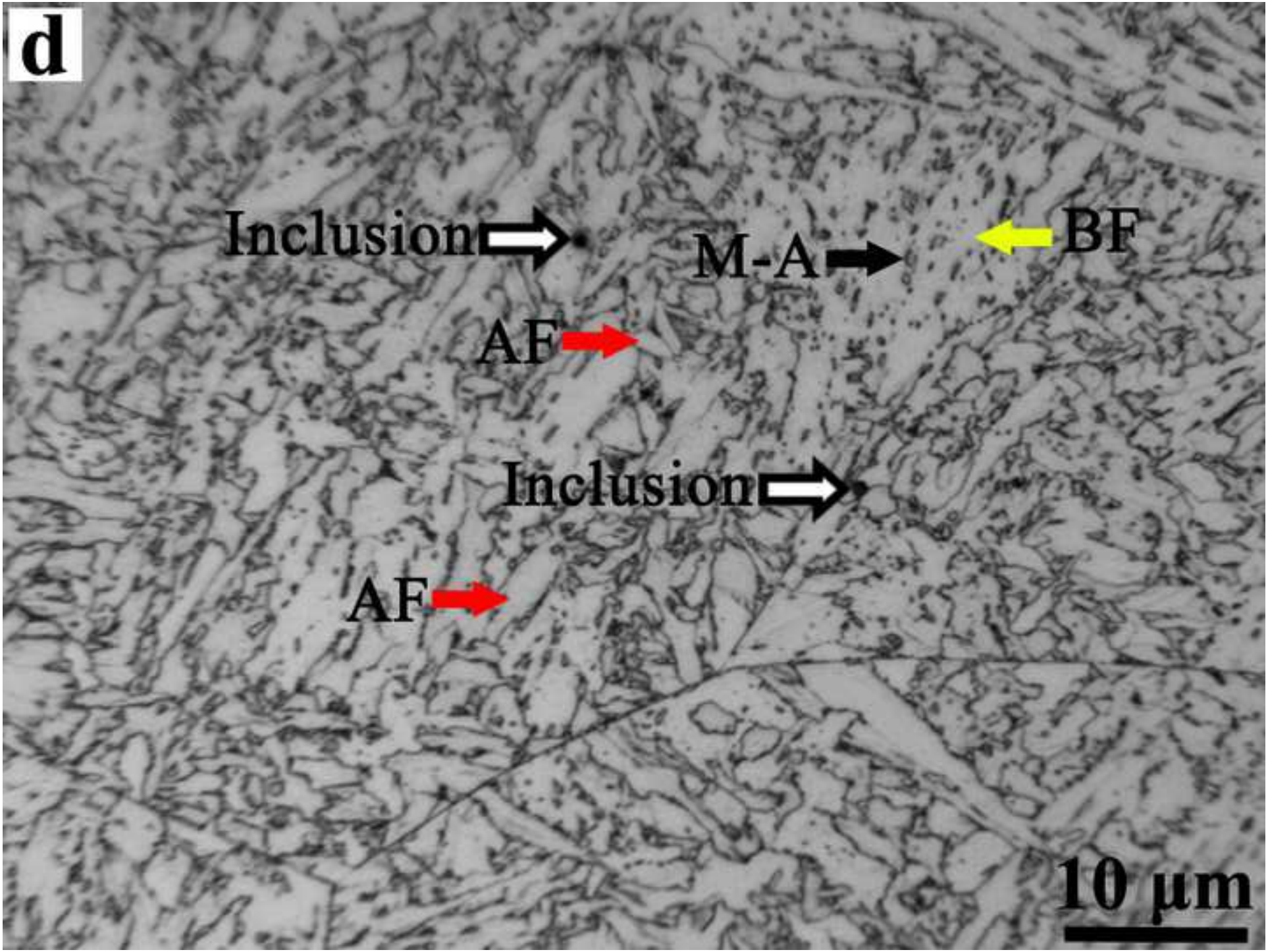

Fig.2e

Click here to download Non-colour figure Fig.2e.tif

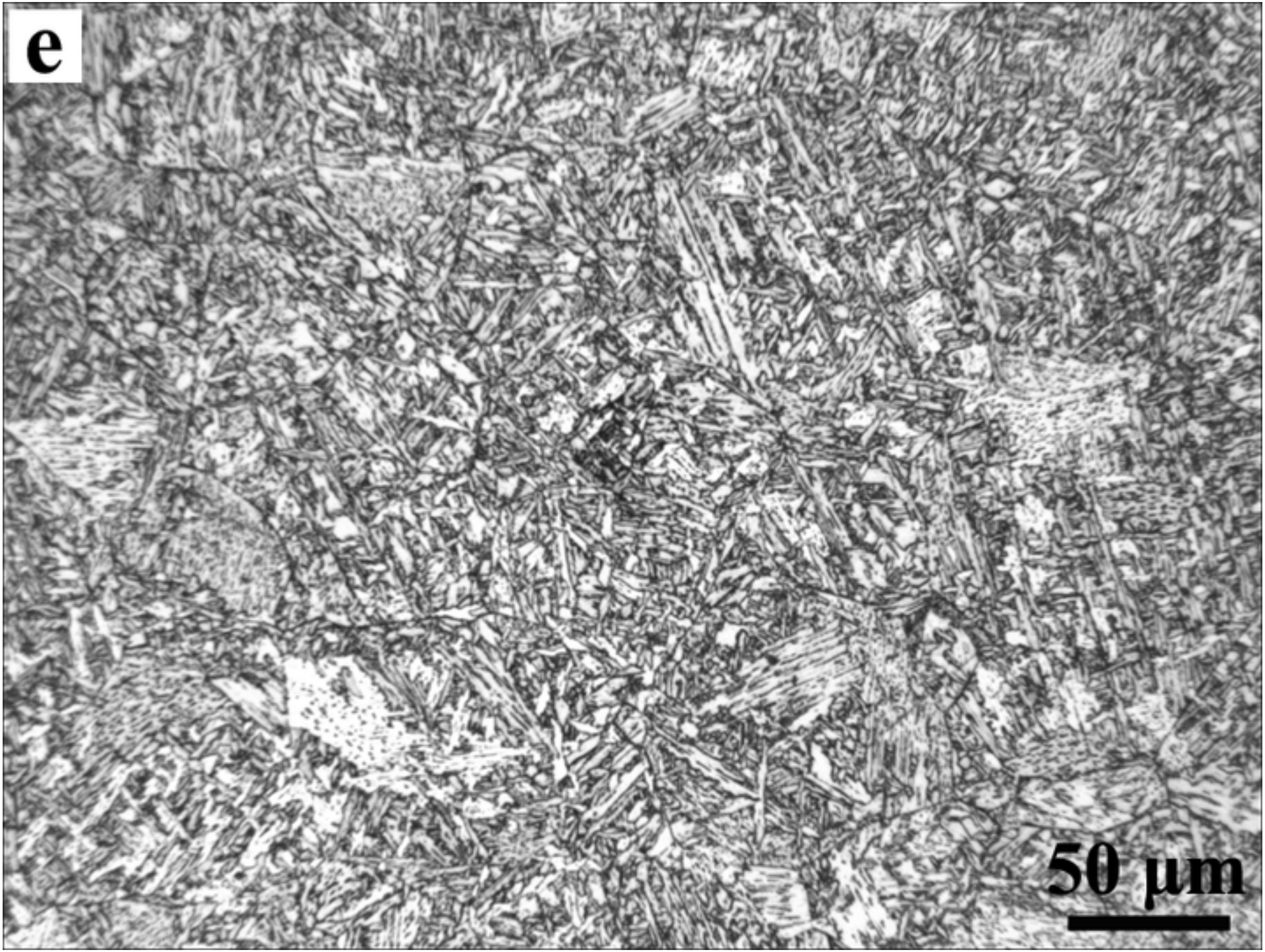

Fig.2f

Click here to download Colour figure (online version only) Fig.2f.tif

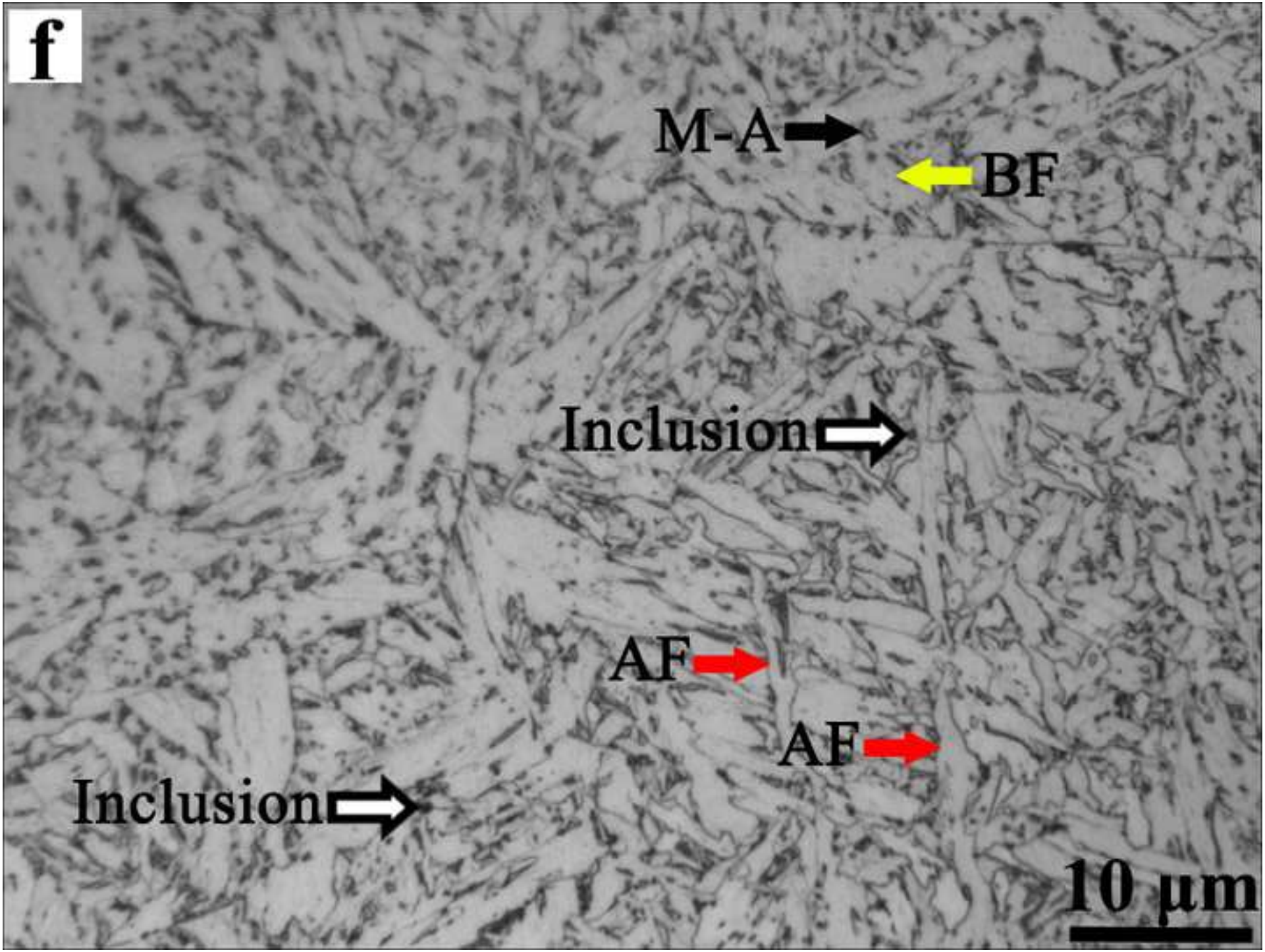

Fig.3a

Click here to download Non-colour figure Fig.3a.tif

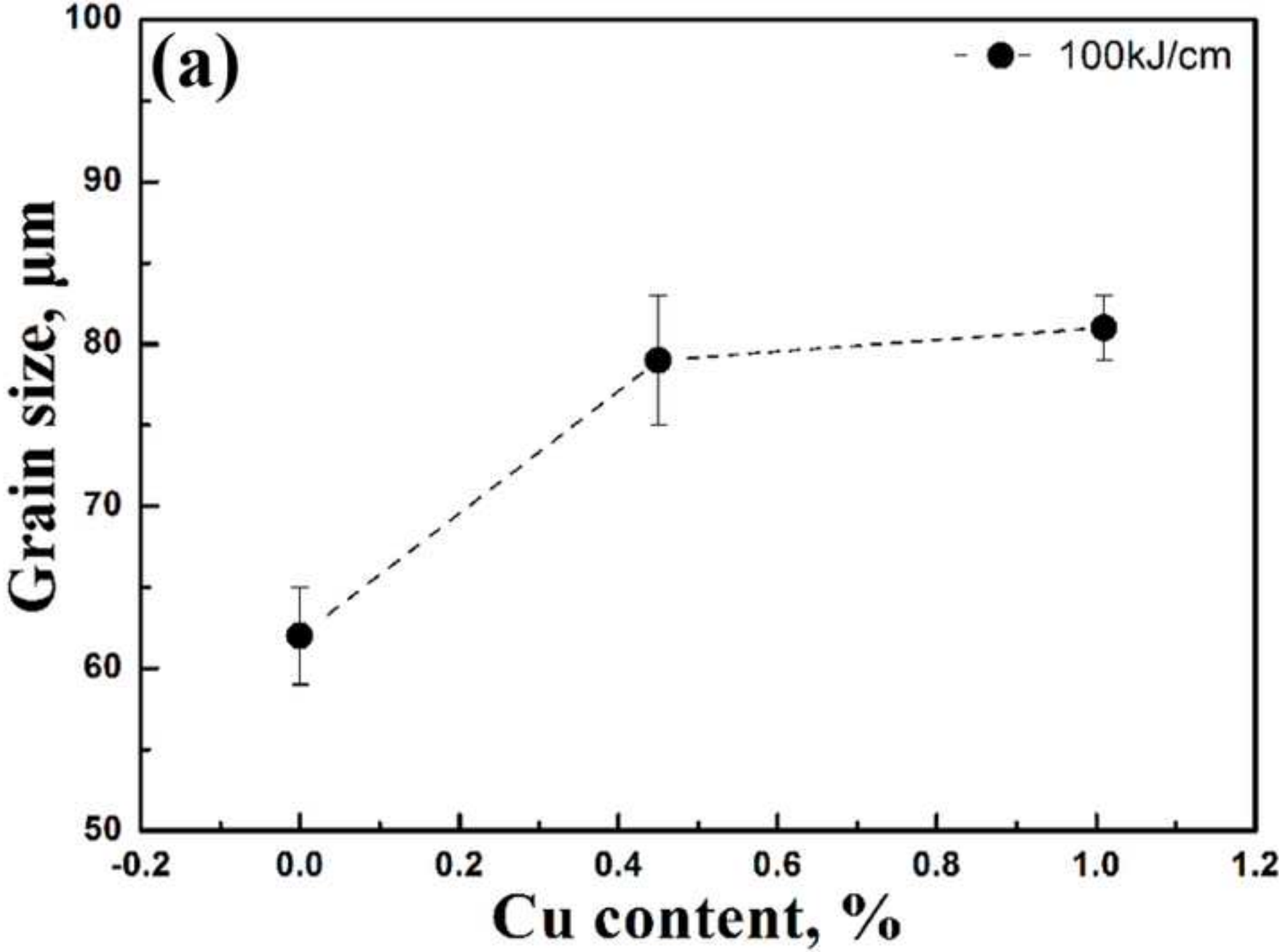

Fig.3b

Click here to download Non-colour figure Fig.3b.tif

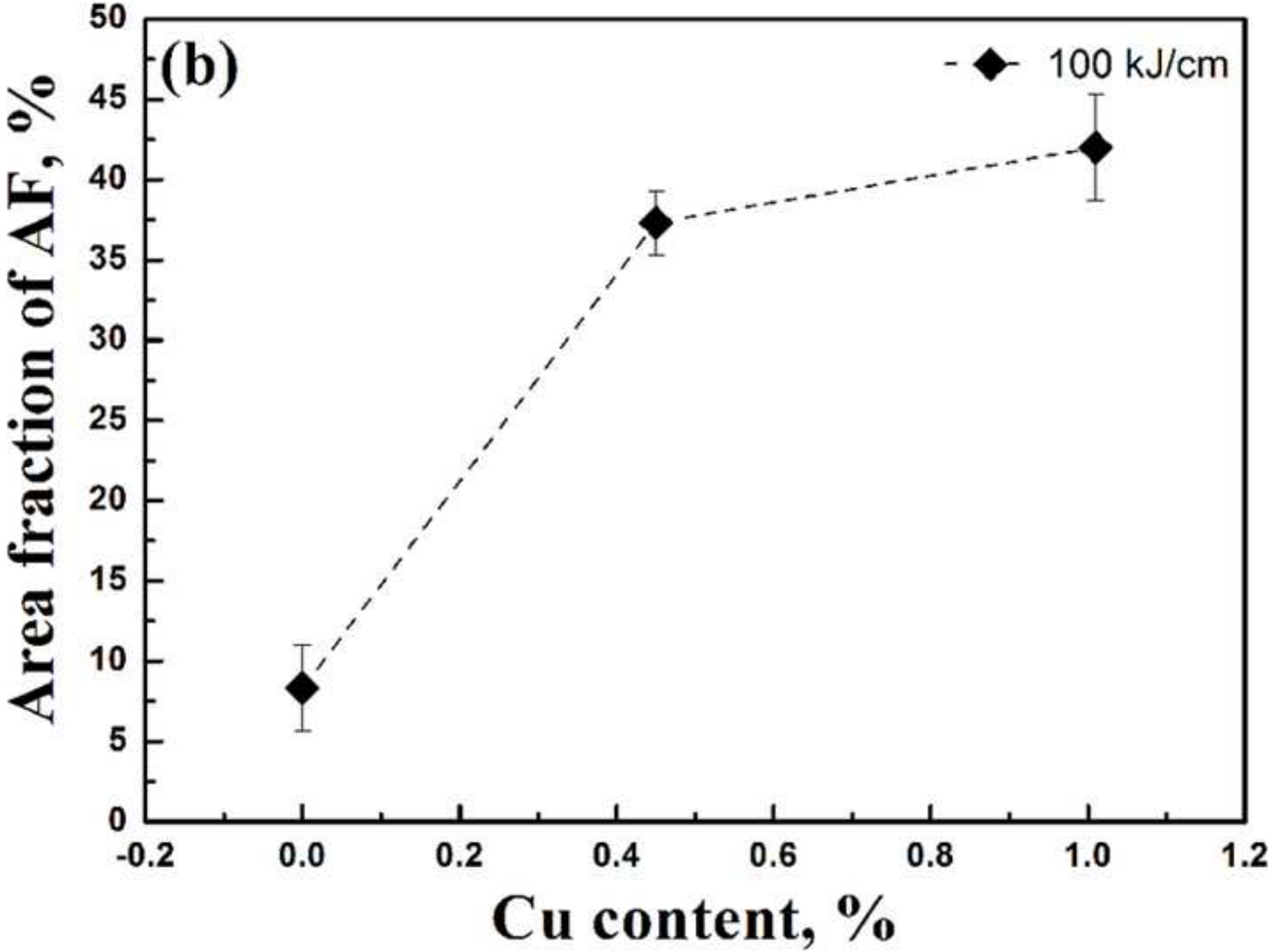

Fig.4a

Click here to download Colour figure (online version only) Fig.4a.tif

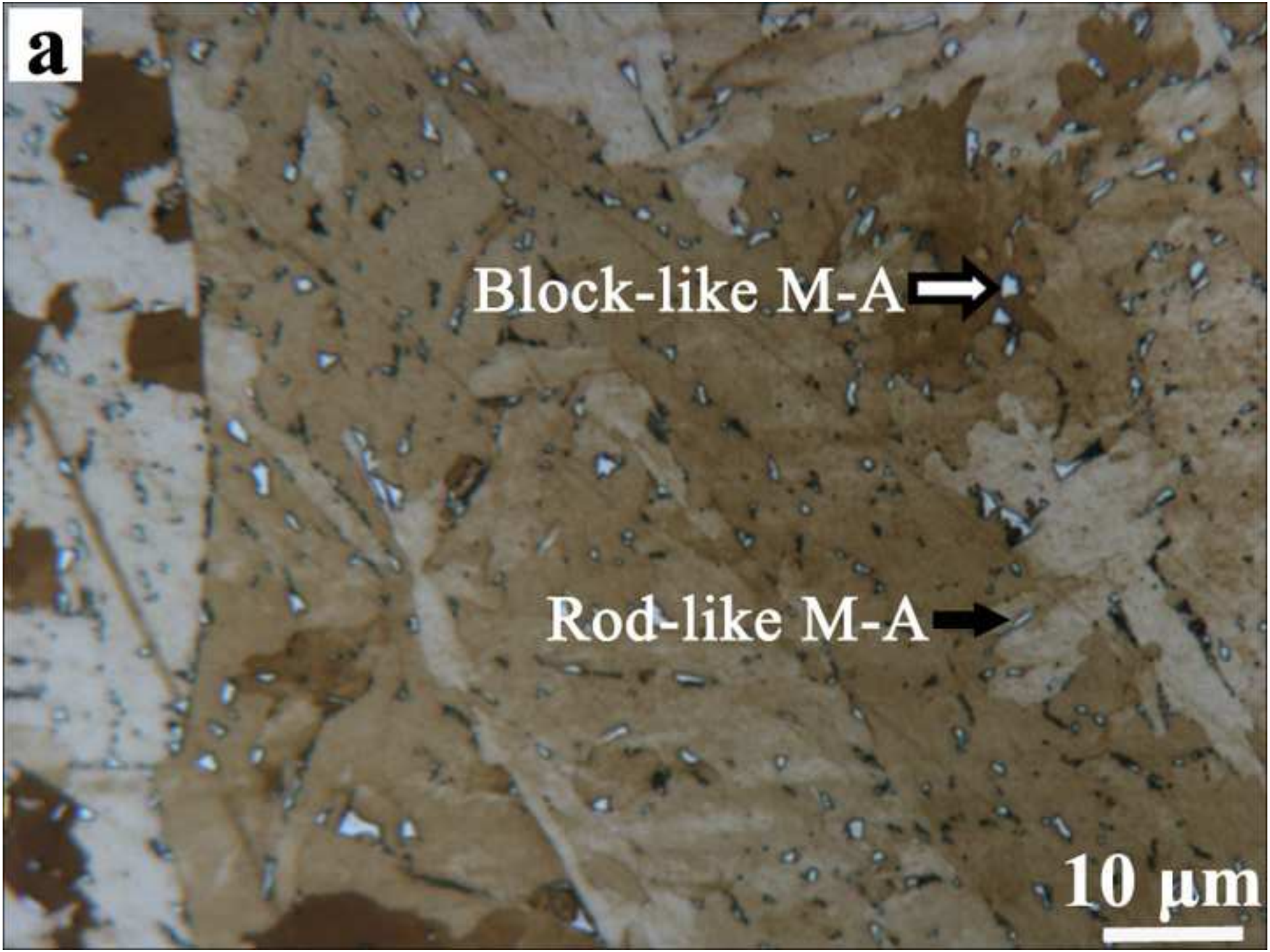

Fig.4b

Click here to download Colour figure (online version only) Fig.4b.tif

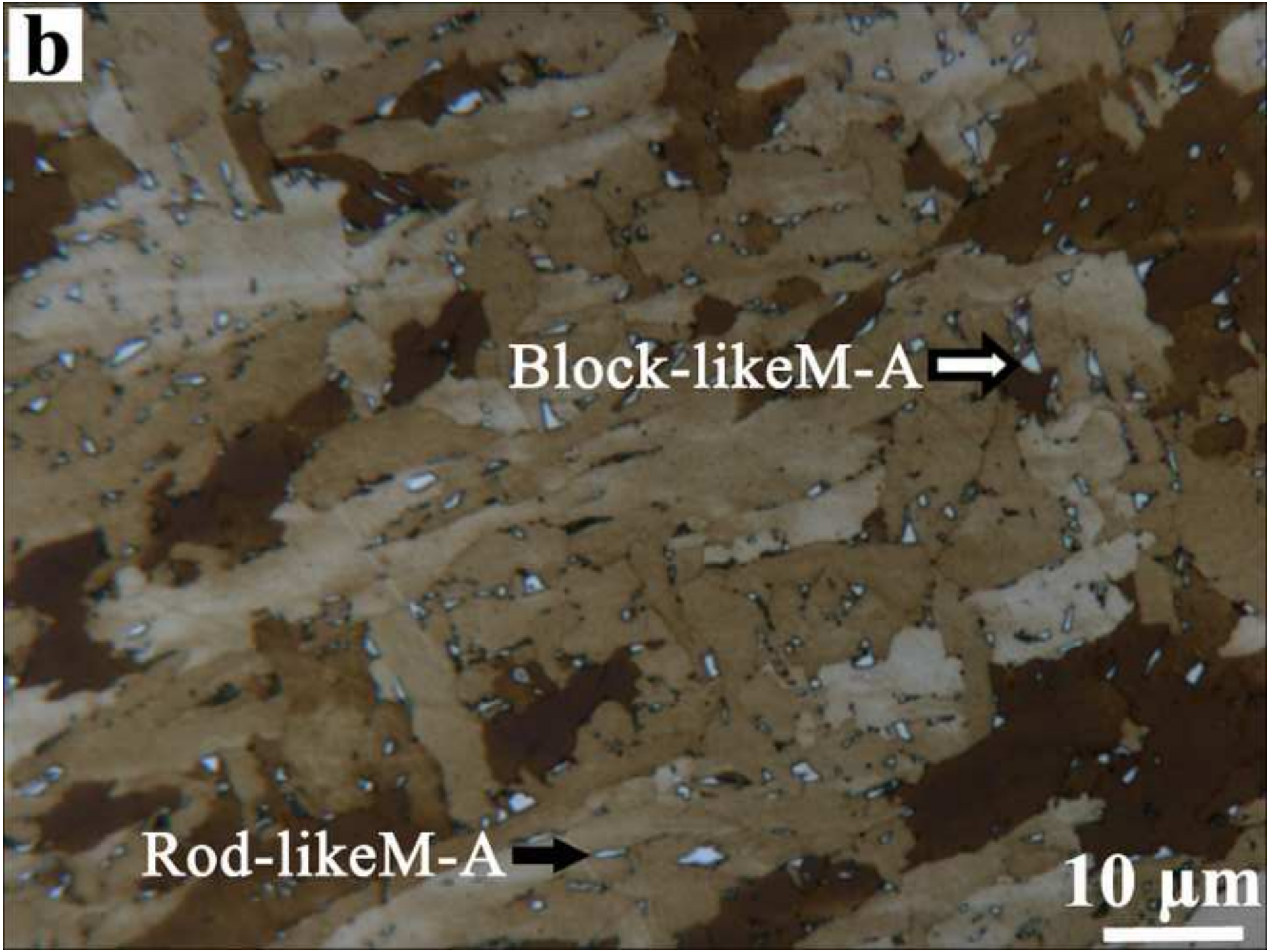

Fig.4c

Click here to download Colour figure (online version only) Fig.4c.tif

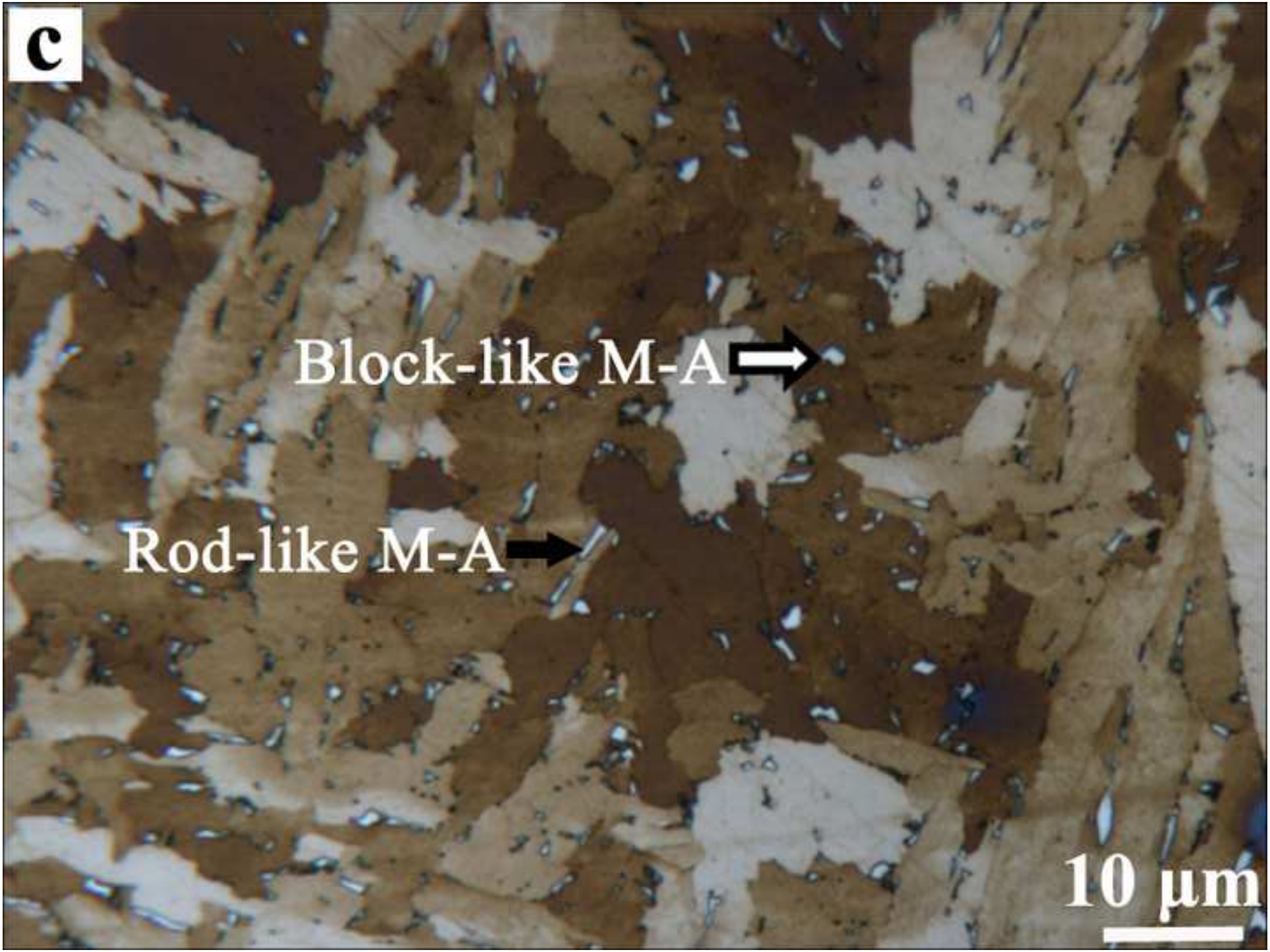

Fig.4d

Click here to download Non-colour figure Fig.4d.tif

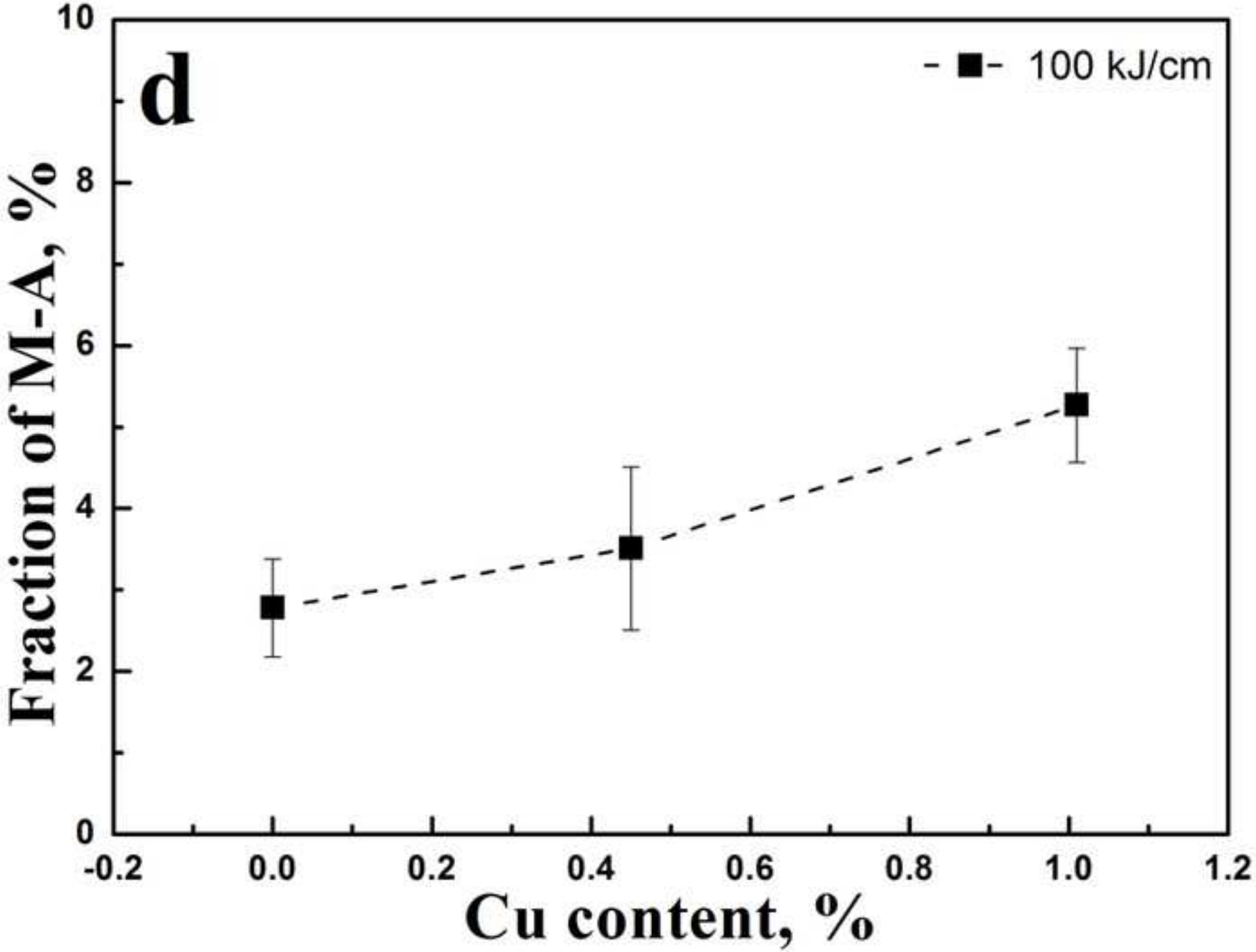

Fig.4e

Click here to download Non-colour figure Fig.4e.tif

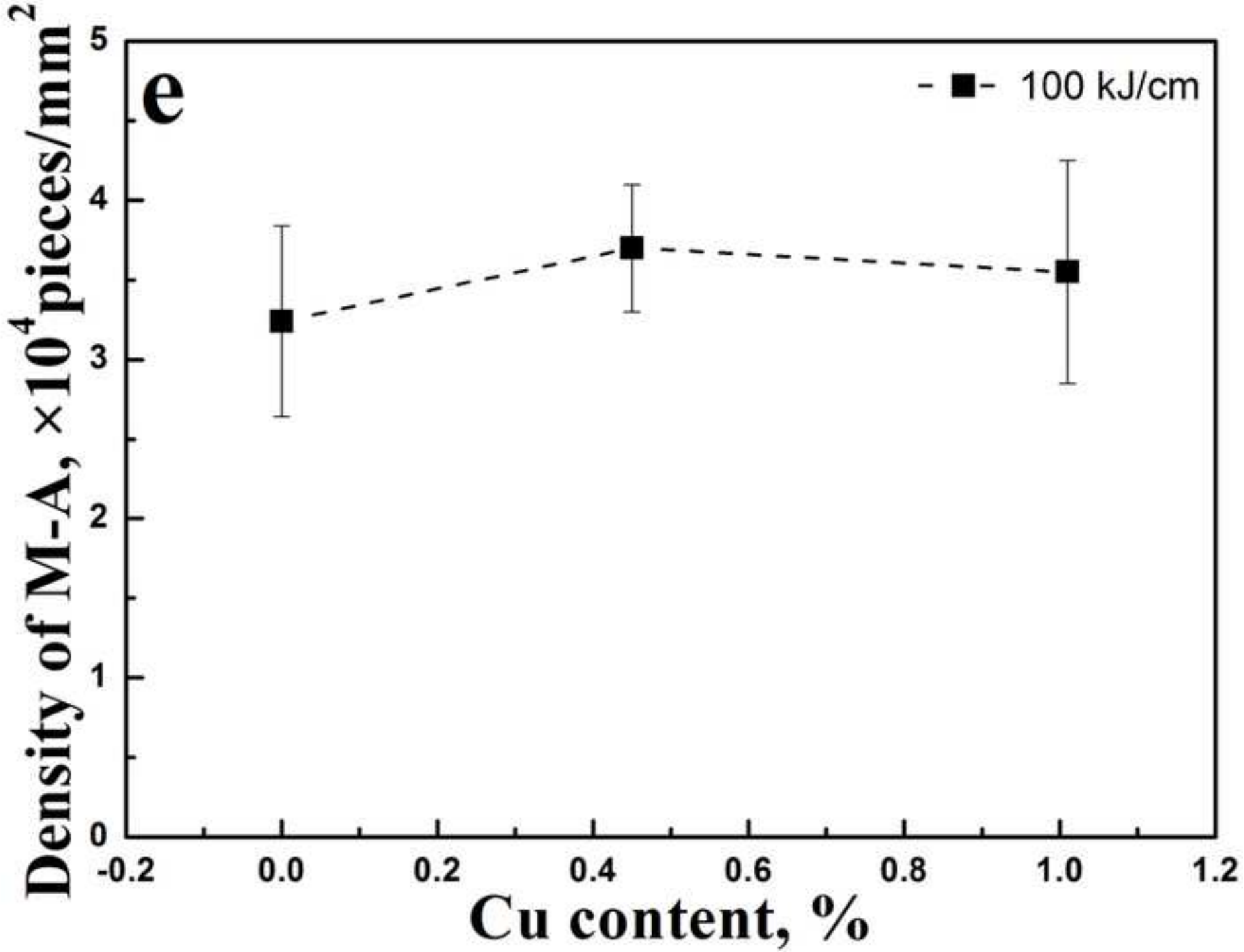

Fig.4f

Click here to download Non-colour figure Fig.4f.tif

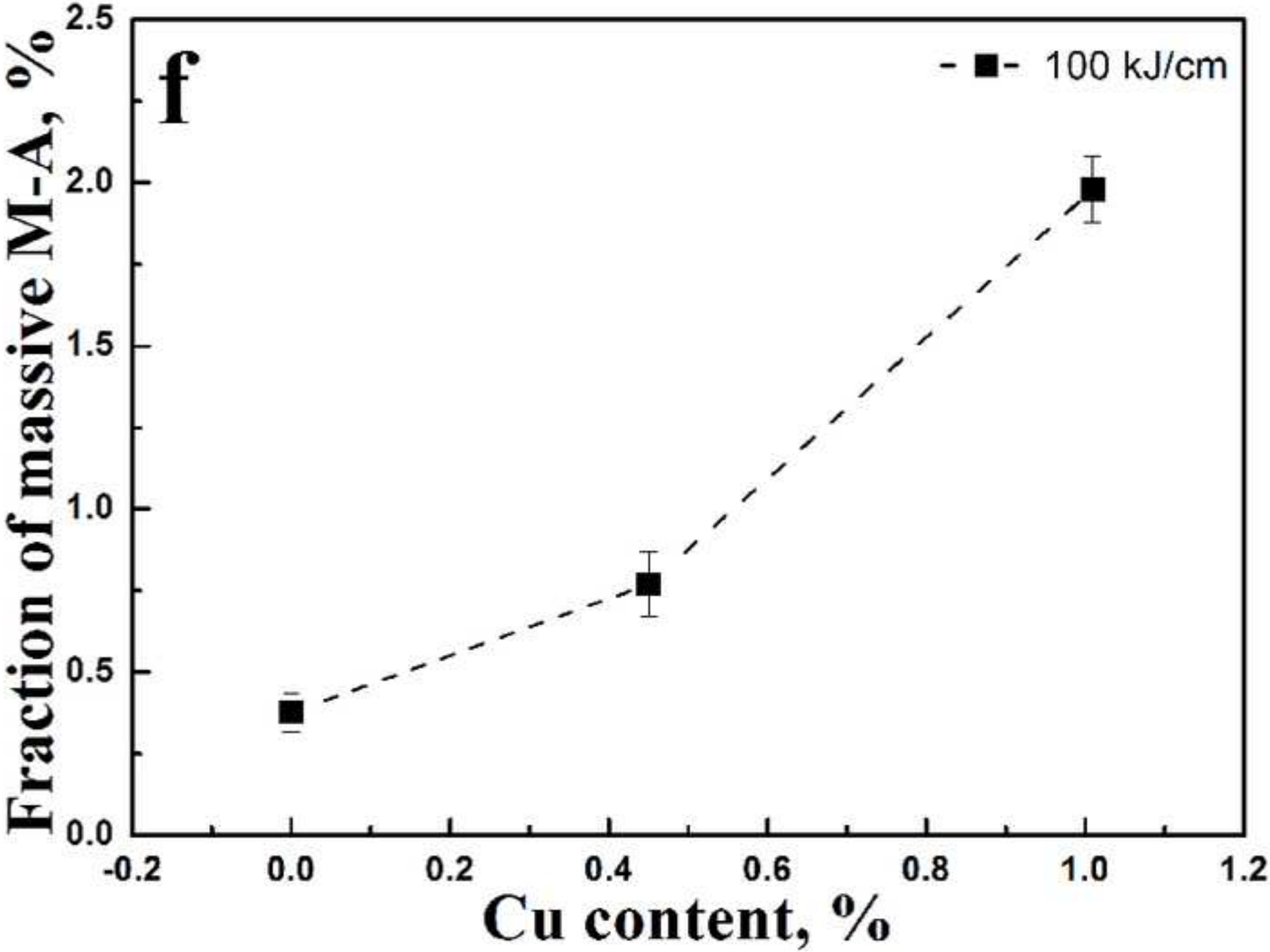

Fig.5a

Click here to download Colour figure (online version only) Fig.5a.tif

Fig.5b

Click here to download Colour figure (online version only) Fig.5b.tif

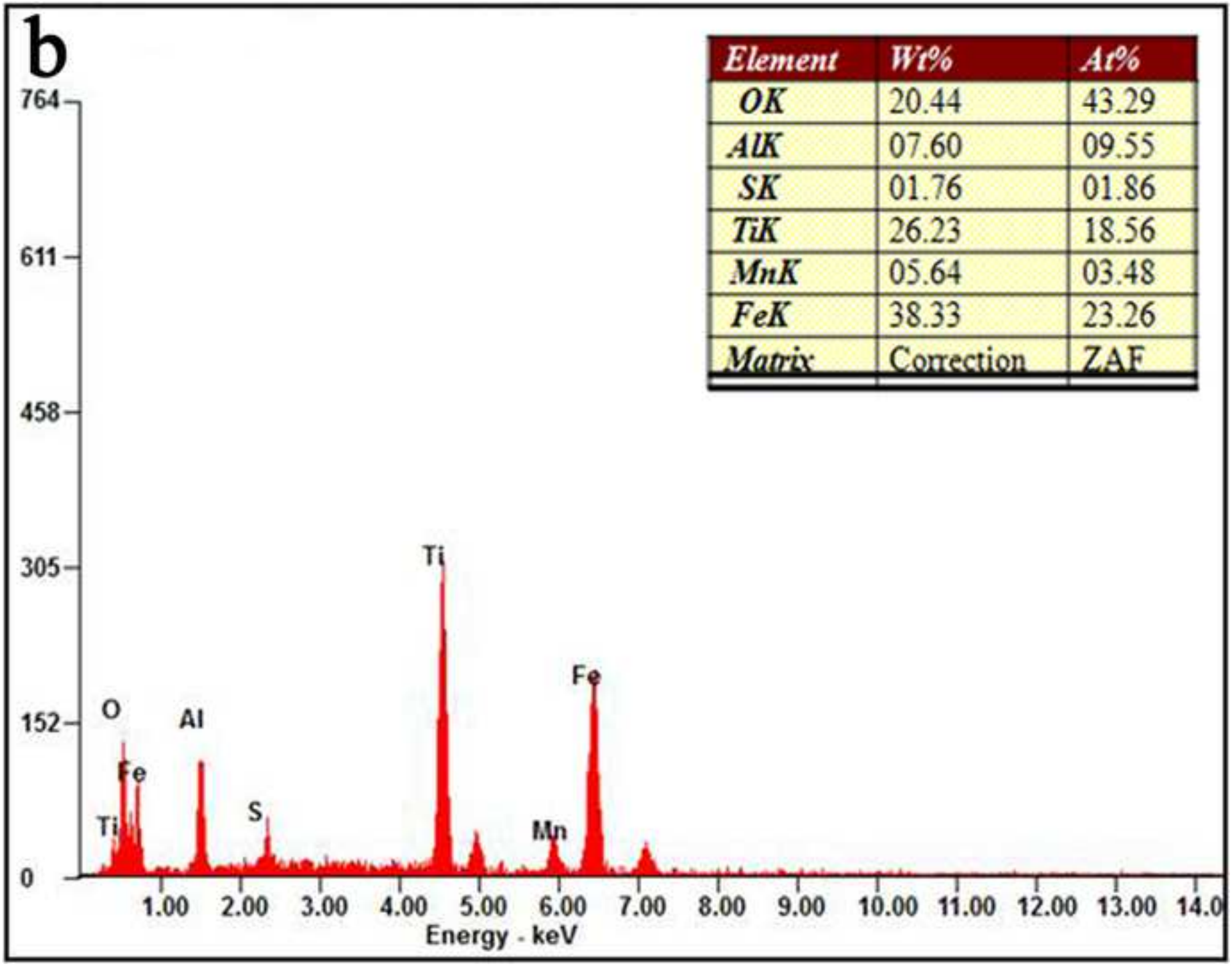

Element	Wt%	At%
OK	20.44	43.29
AlK	07.60	09.55
SK	01.76	01.86
TiK	26.23	18.56
MnK	05.64	03.48
FeK	38.33	23.26
Matrix	Correction	ZAF

Fig.5c

Click here to download Colour figure (online version only) Fig.5c.tif

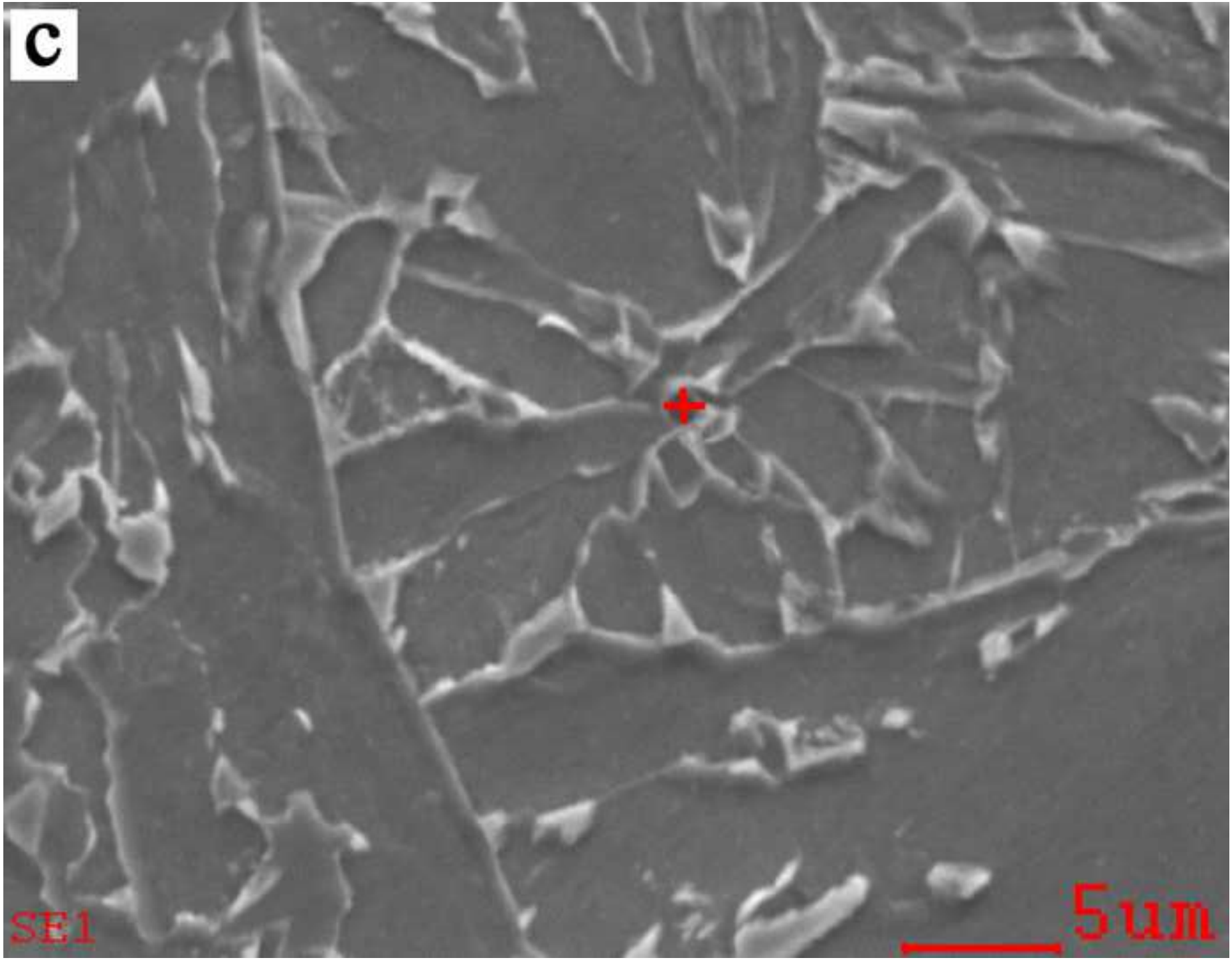

Fig.5d

Click here to download Colour figure (online version only) Fig.5d.tif

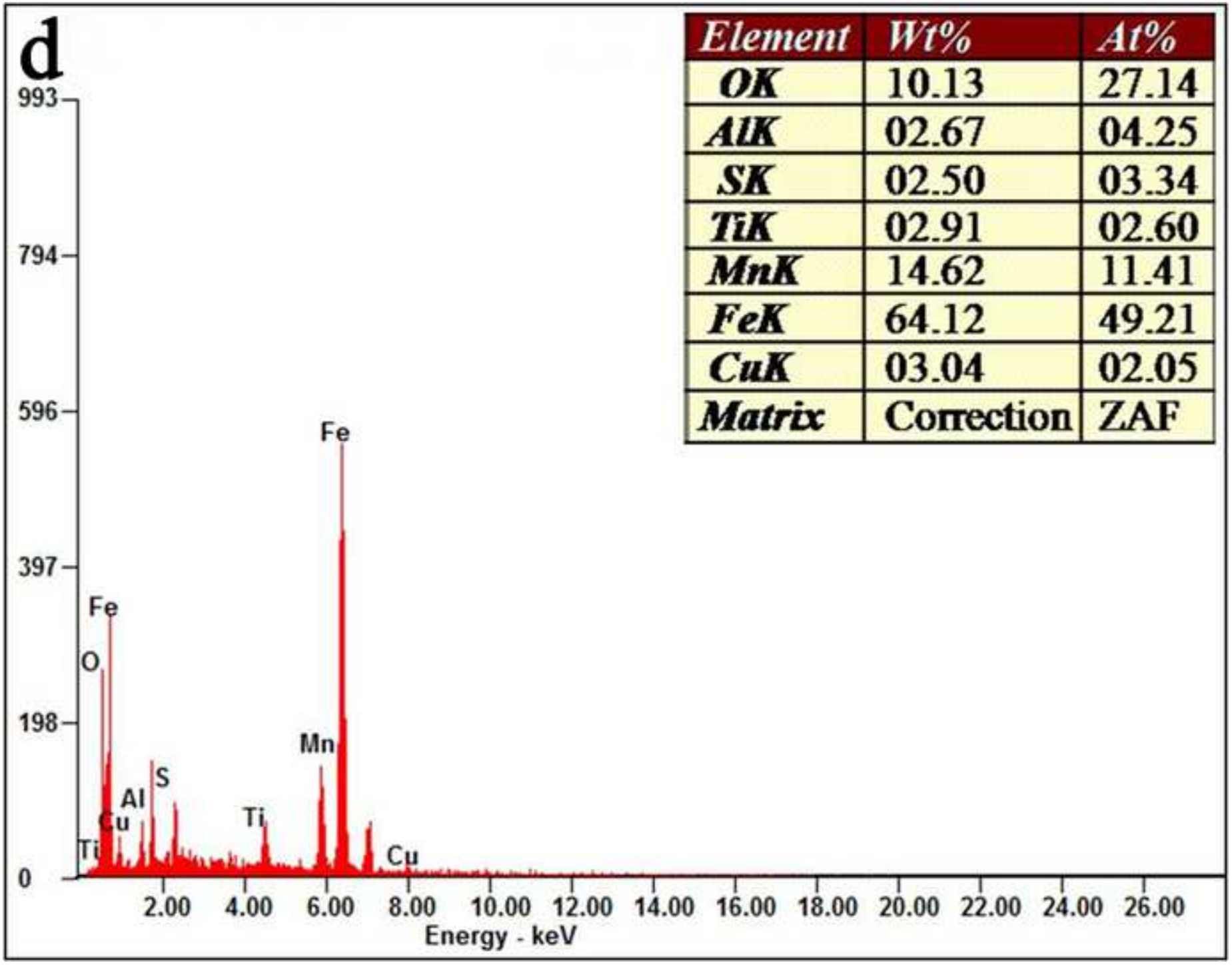

Element	Wt%	At%
OK	10.13	27.14
AlK	02.67	04.25
SK	02.50	03.34
TiK	02.91	02.60
MnK	14.62	11.41
FeK	64.12	49.21
CuK	03.04	02.05
Matrix	Correction	ZAF

Fig.5e

Click here to download Colour figure (online version only) Fig.5e.tif

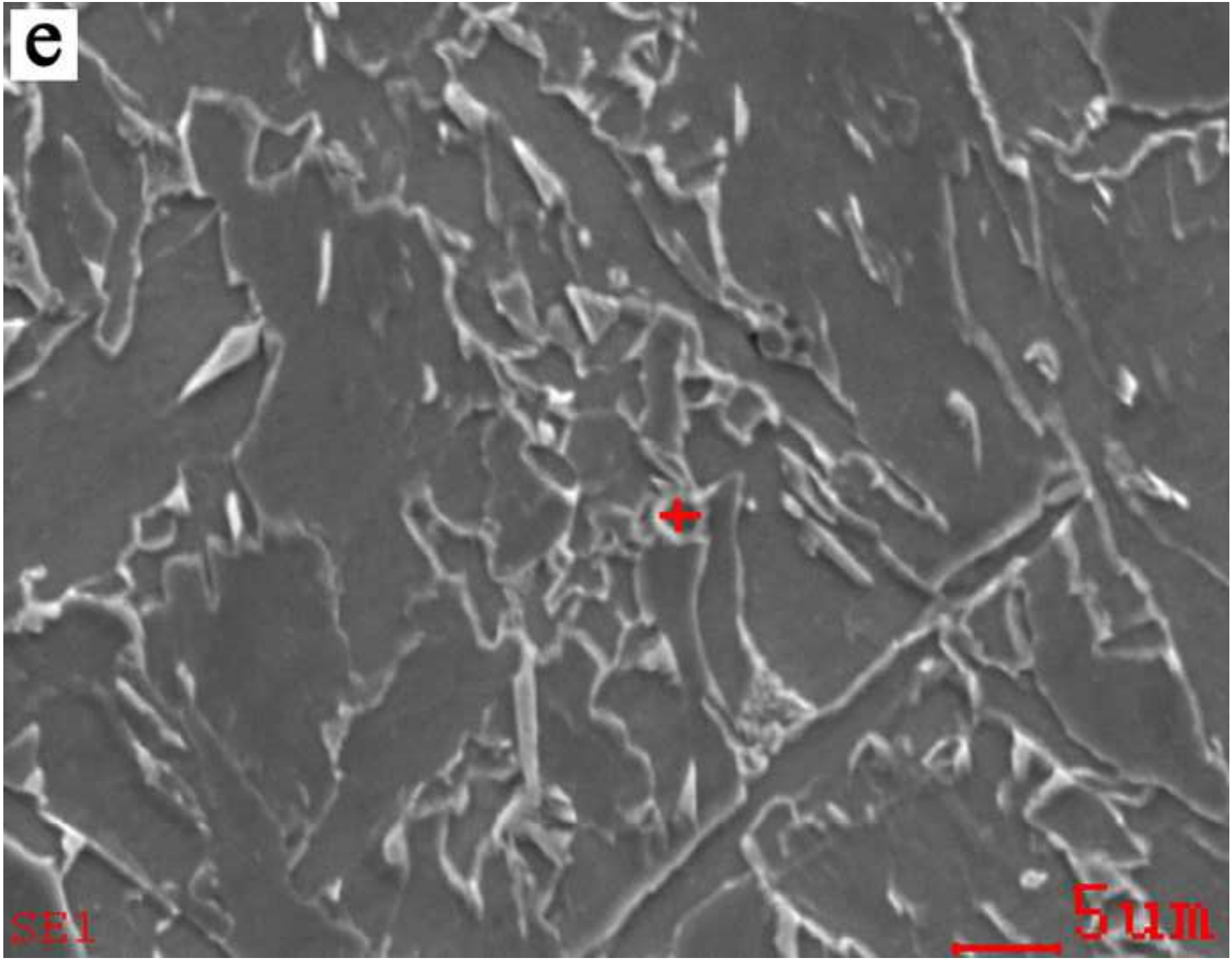

Fig.5f

Click here to download Colour figure (online version only) Fig.5f.tif

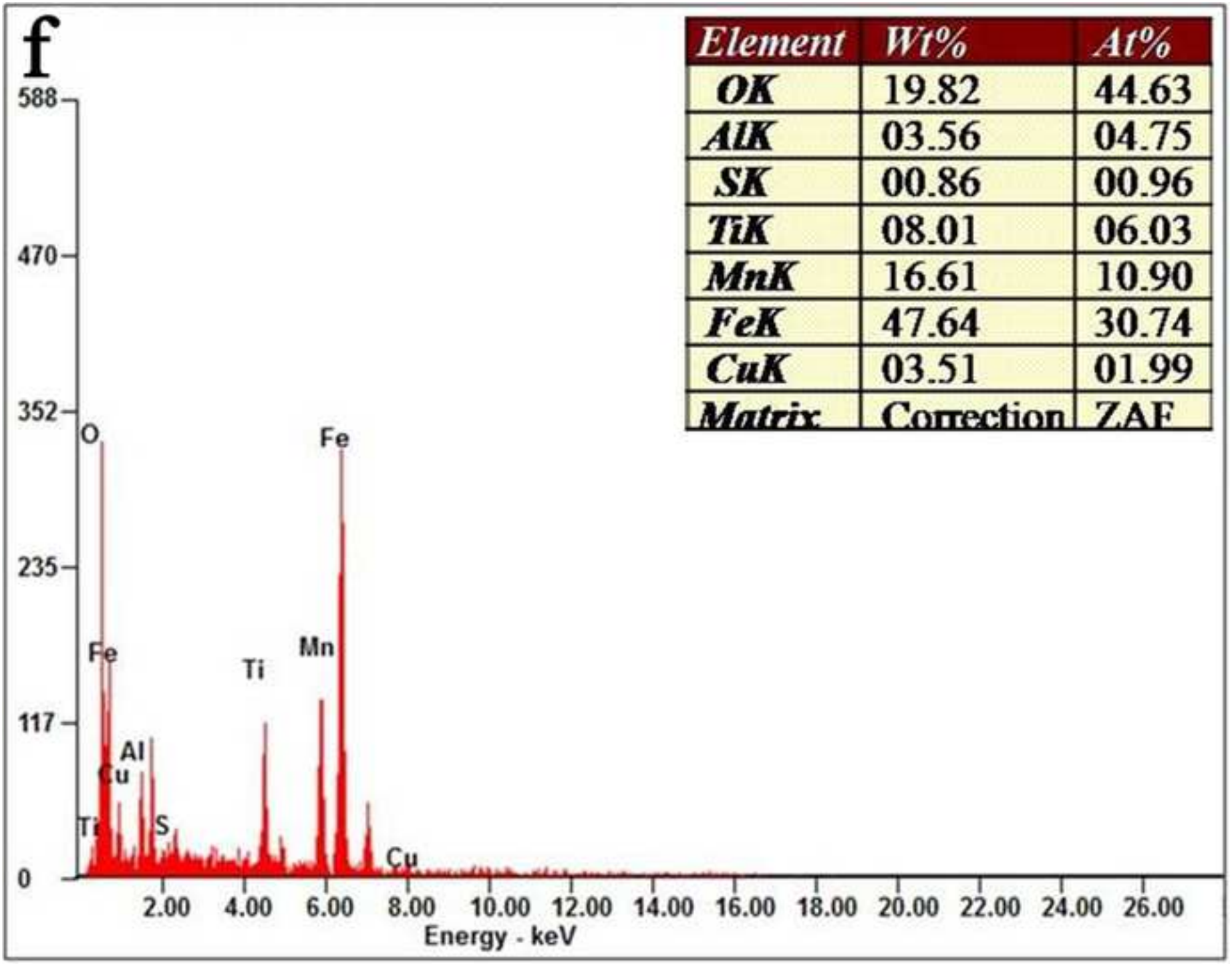

Element	Wt%	At%
OK	19.82	44.63
AlK	03.56	04.75
SK	00.86	00.96
TiK	08.01	06.03
MnK	16.61	10.90
FeK	47.64	30.74
CuK	03.51	01.99
Matrix	Correction	ZAF

Fig.6a

Click here to download Non-colour figure Fig.6a.tif

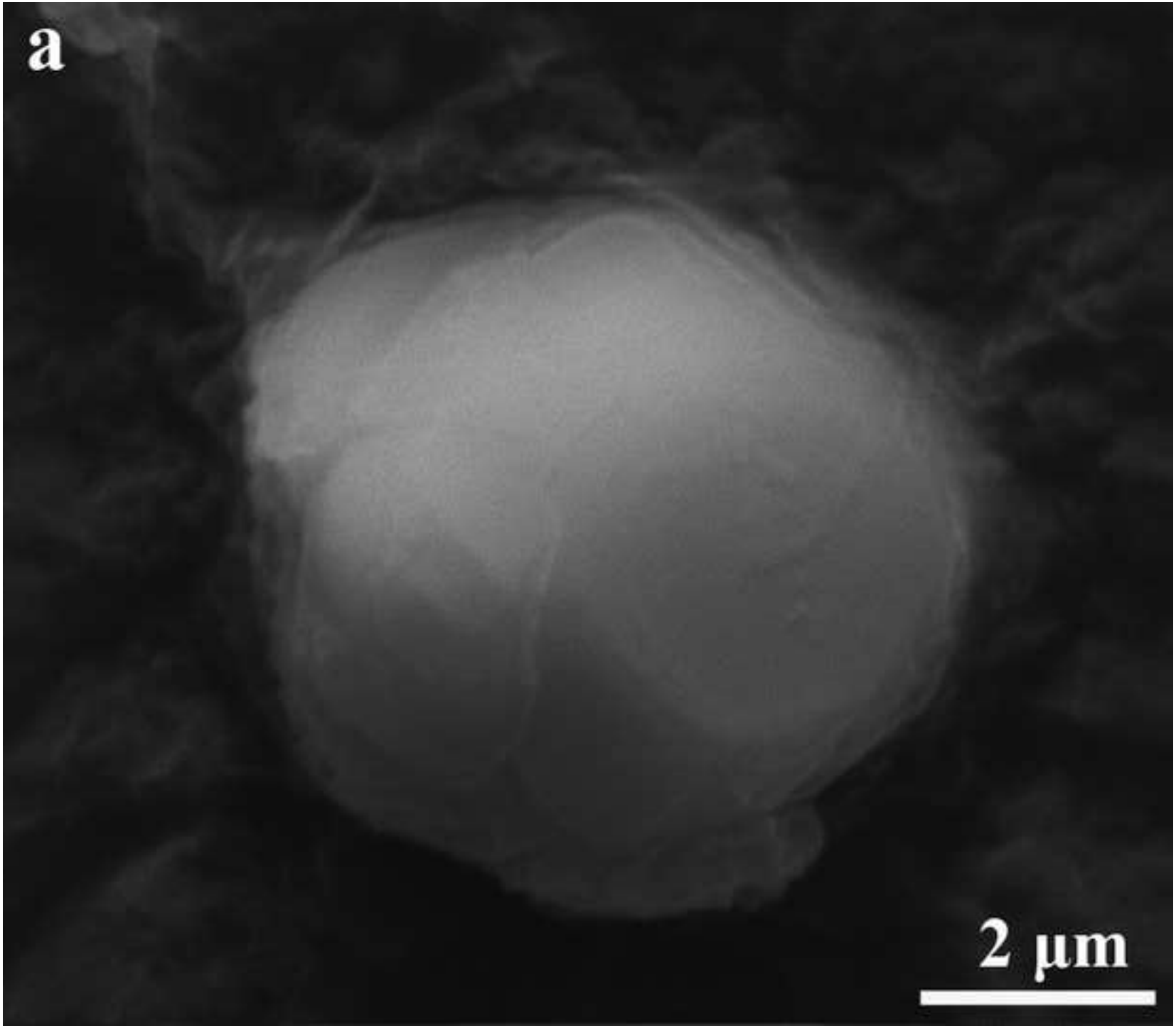

Fig.6b

Click here to download Colour figure (online version only) Fig.6b.tif

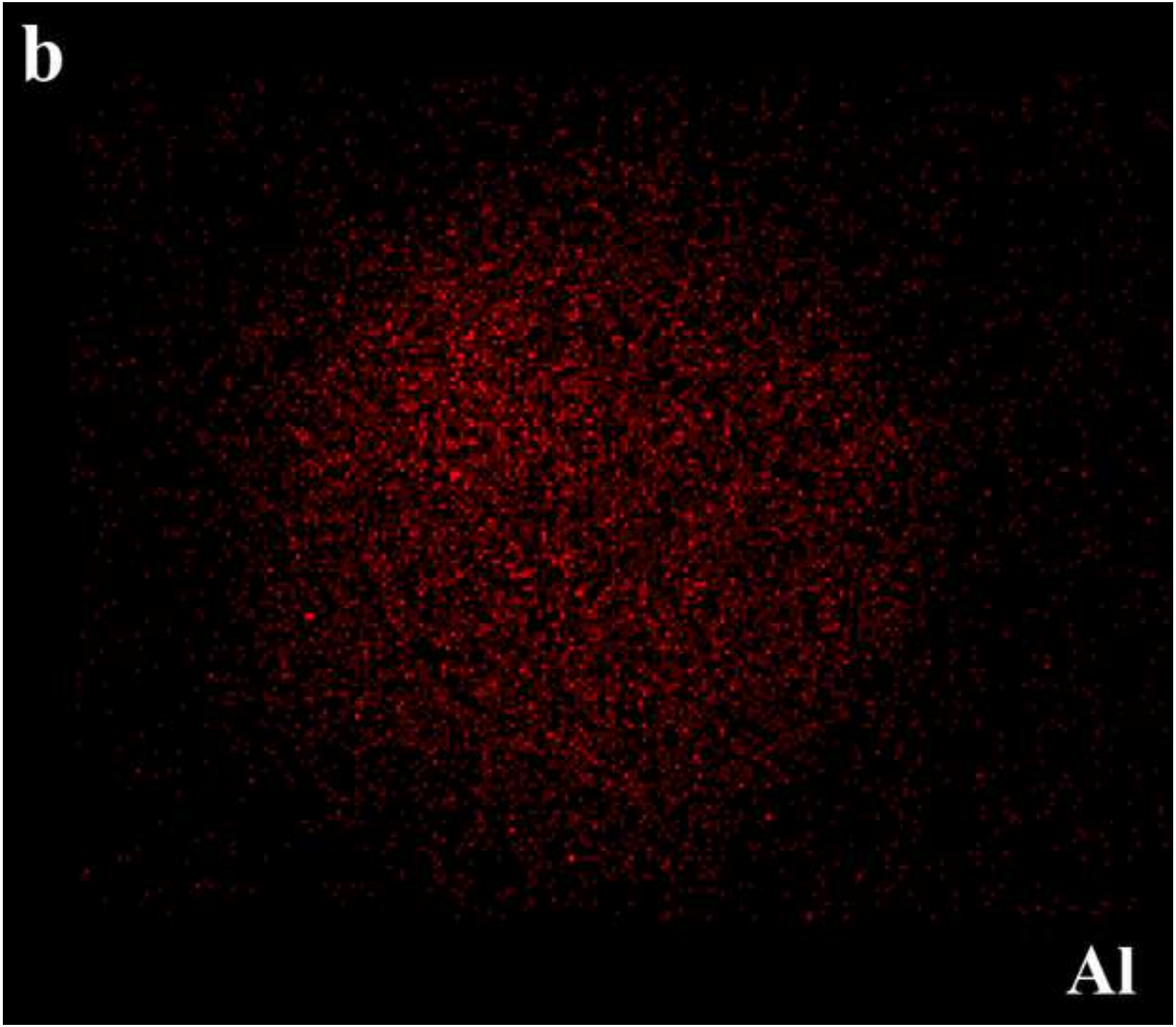

Fig.6c

Click here to download Colour figure (online version only) Fig.6c.tif

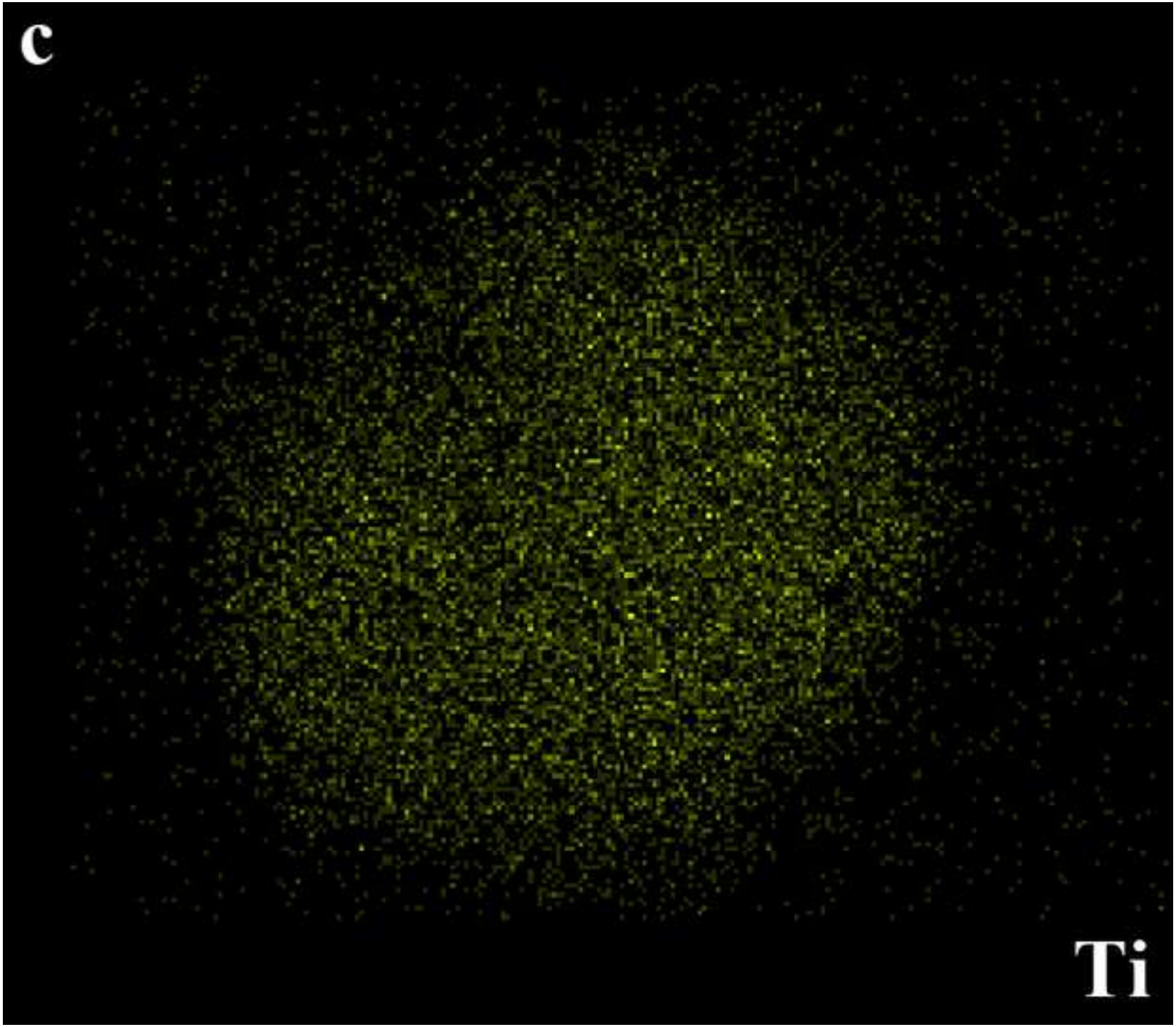

Fig.6d

Click here to download Colour figure (online version only) Fig.6d.tif

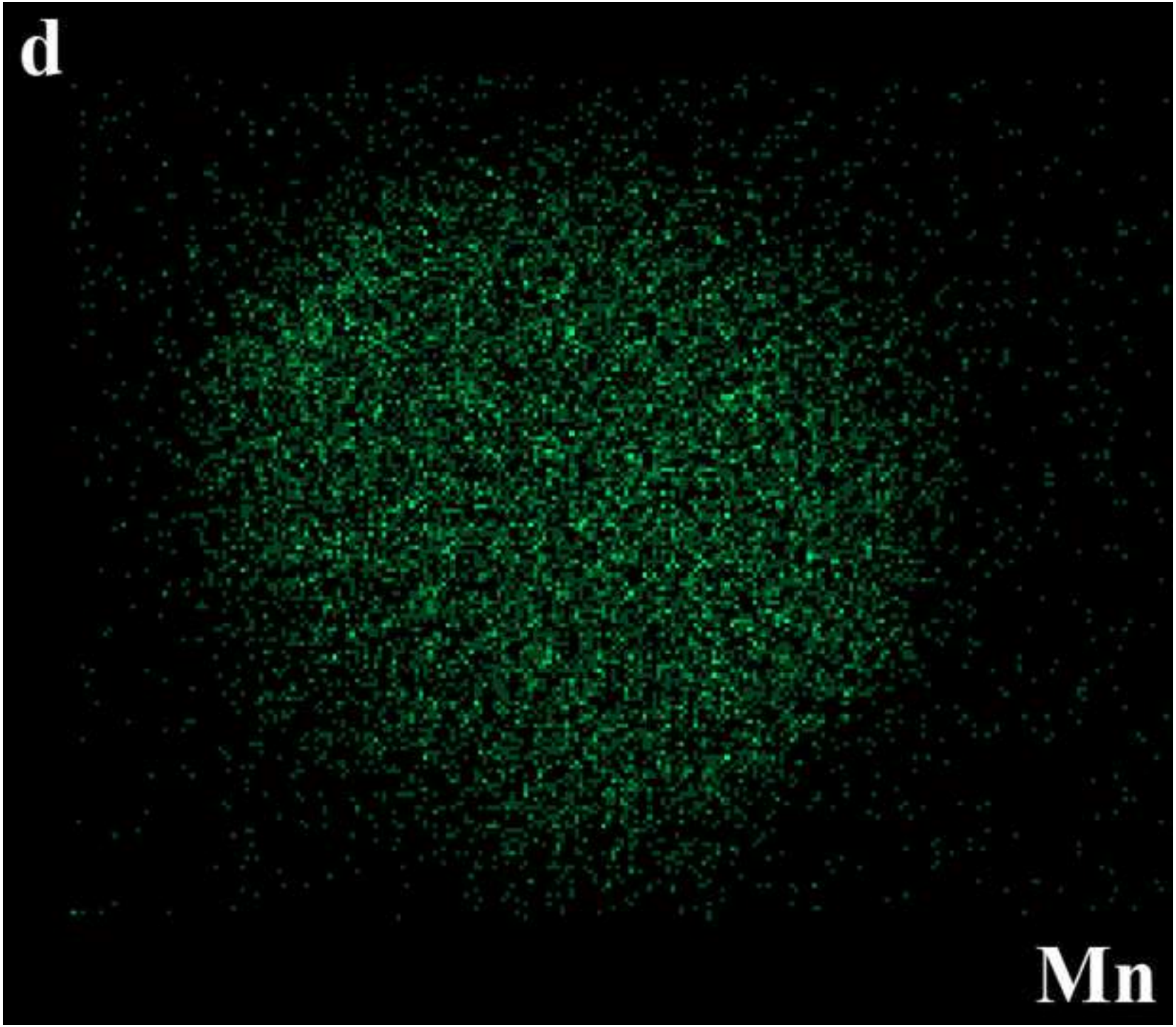

Fig.6e

Click here to download Colour figure (online version only) Fig.6e.tif

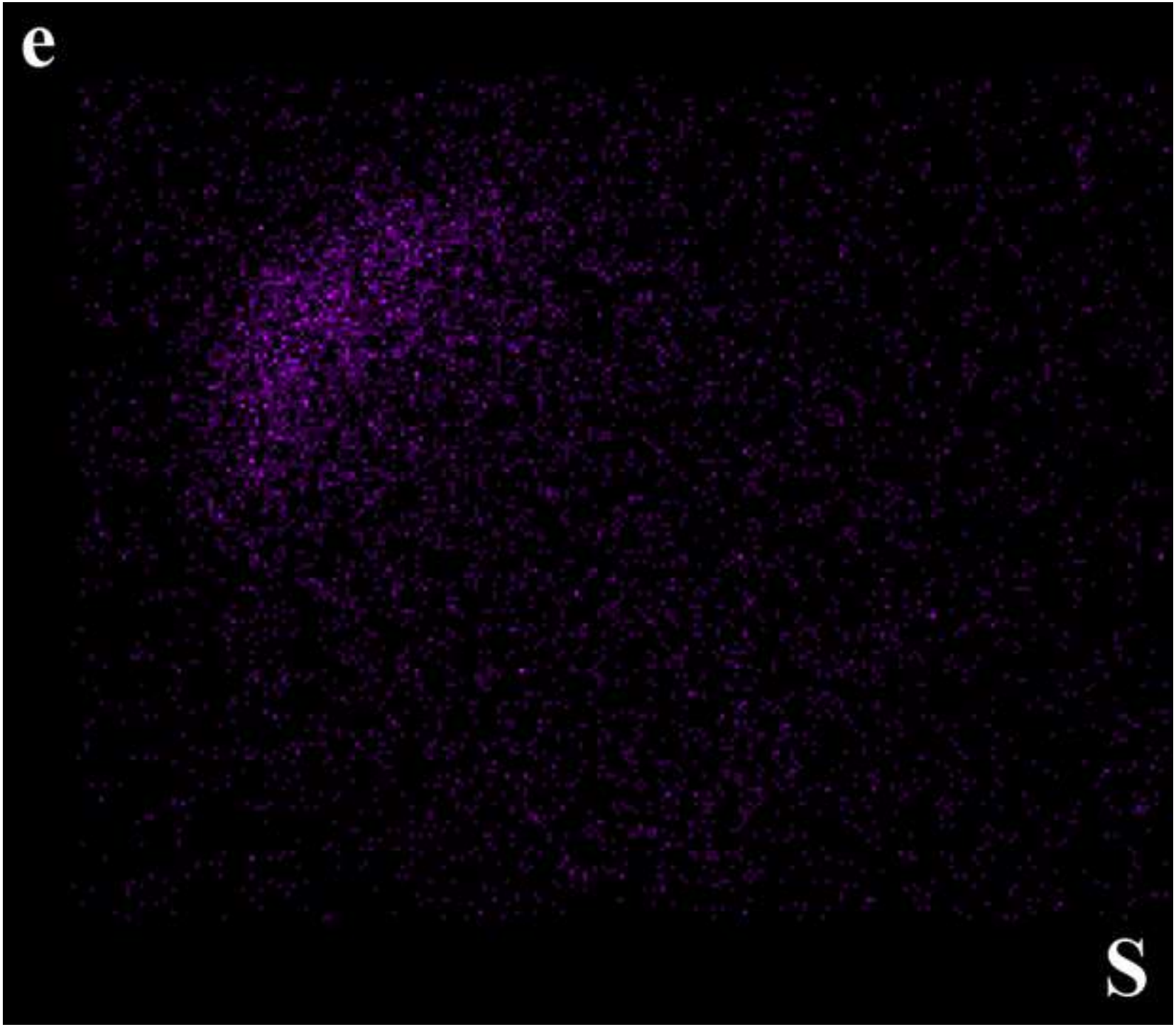

Fig.6f

Click here to download Colour figure (online version only) Fig.6f.tif

Fig.7a

Click here to download Non-colour figure Fig.7a.tif

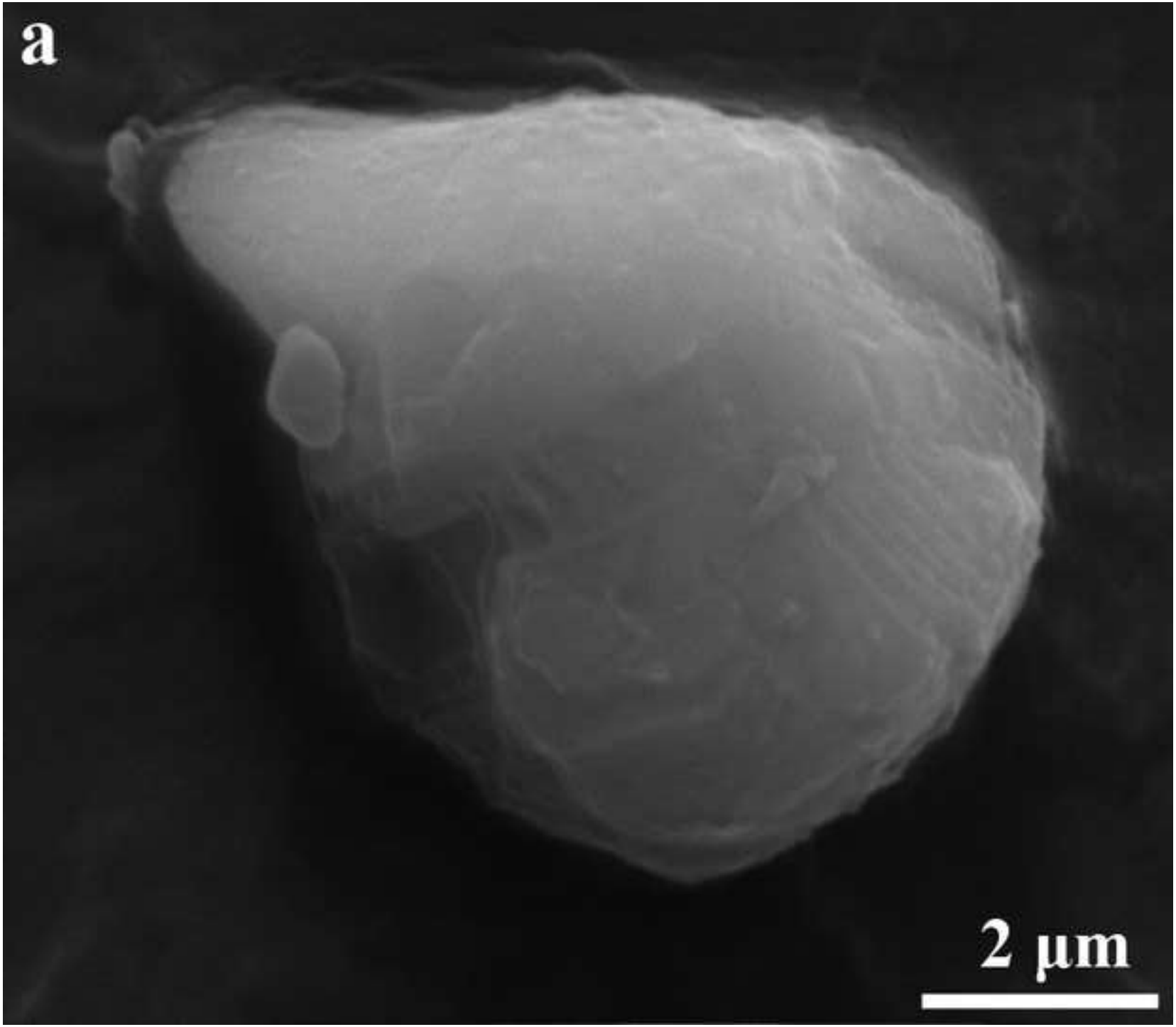

Fig.7b

Click here to download Colour figure (online version only) Fig.7b.tif

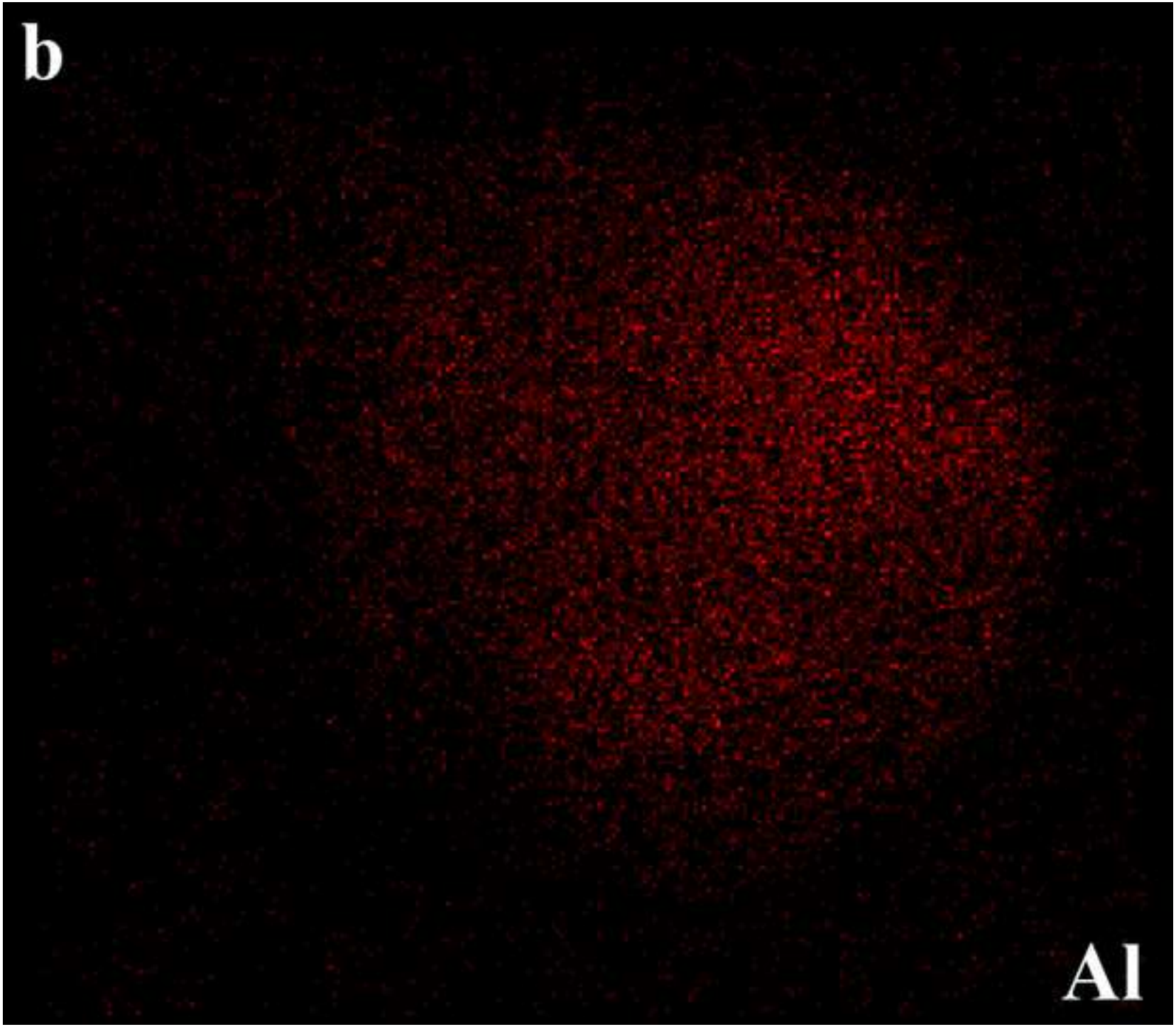

Fig.7b

Click here to download Colour figure (online version only) Fig.7b.tif

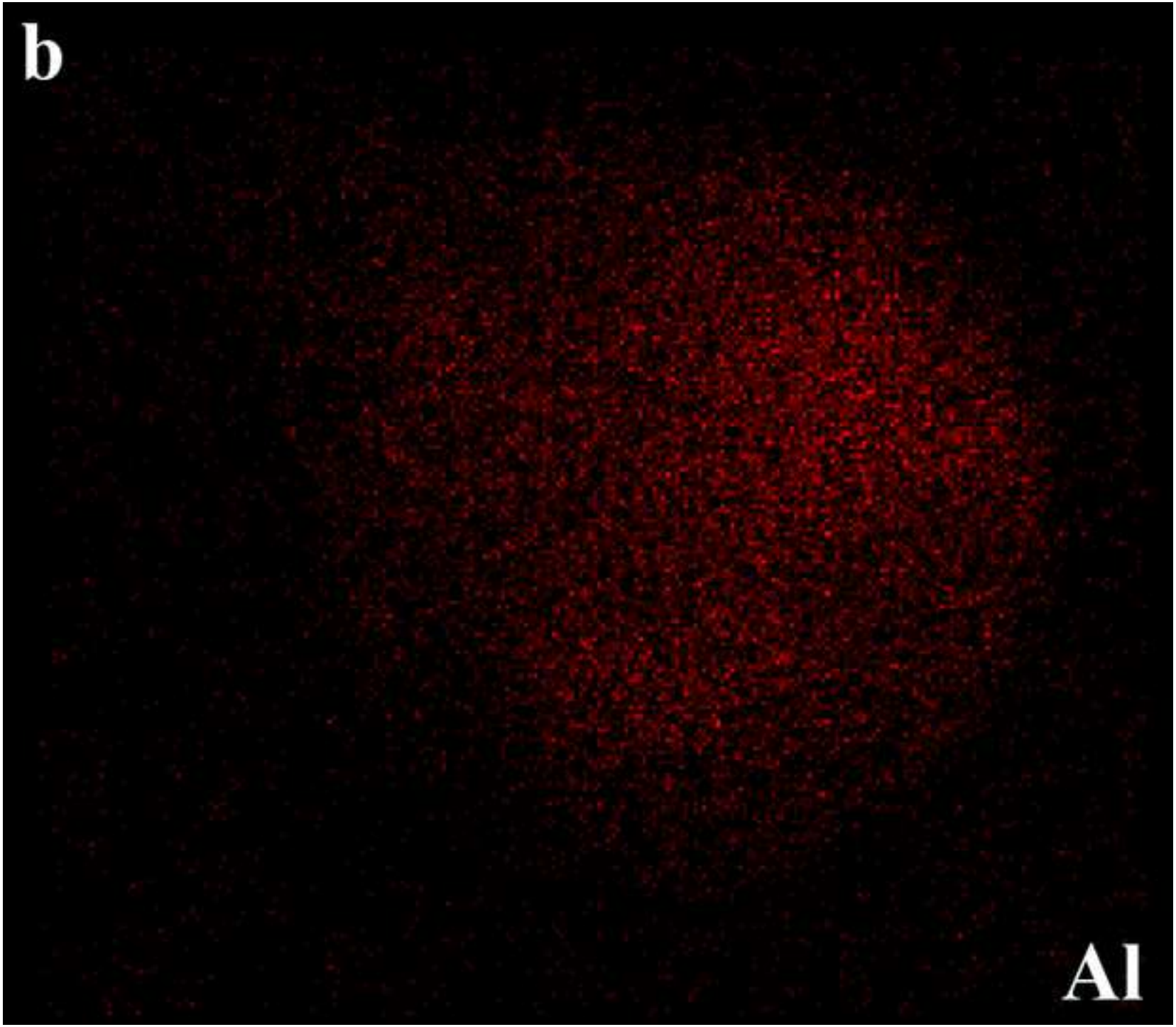

Fig.7c

Click here to download Colour figure (online version only) Fig.7c.tif

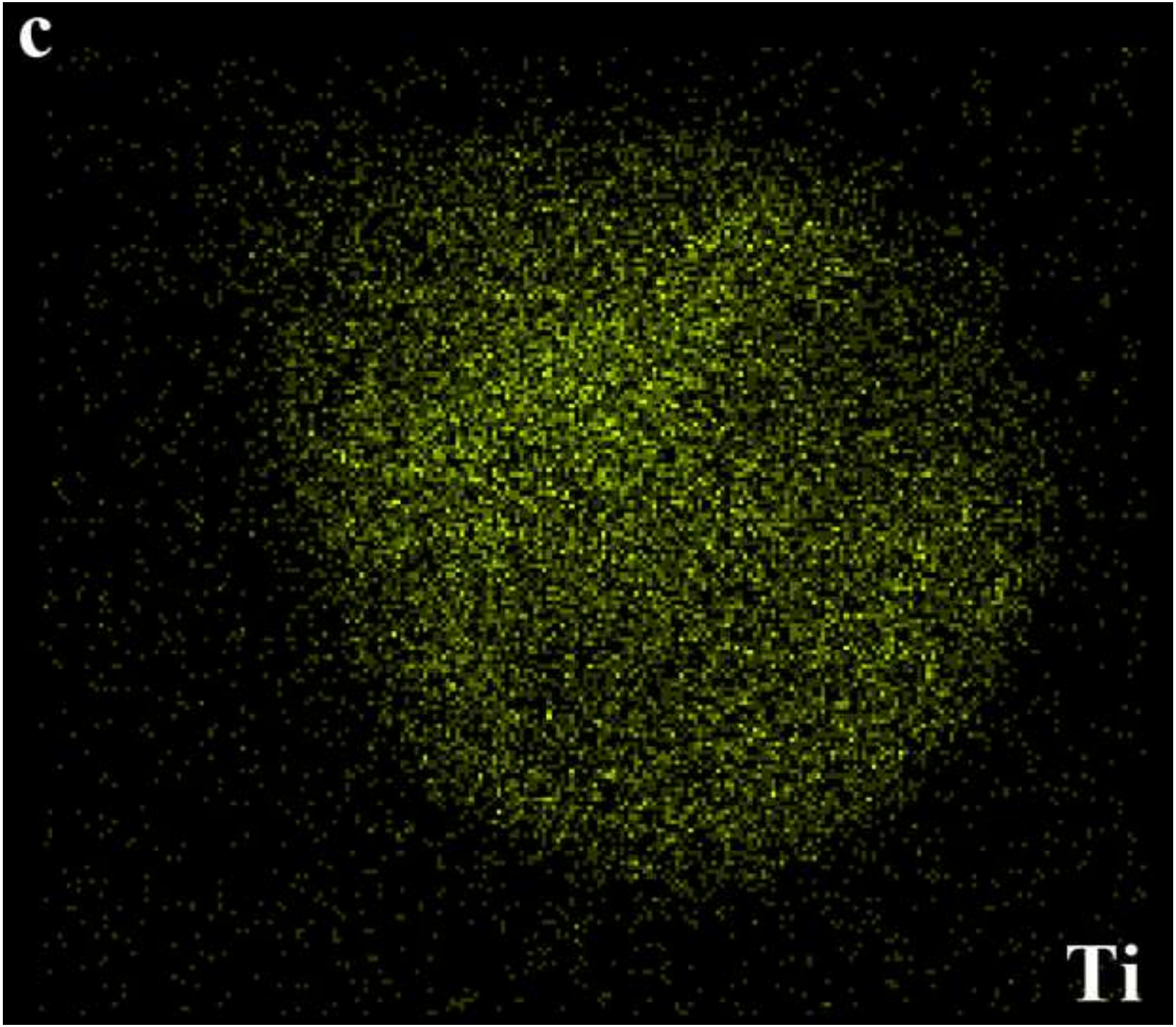

Fig.7d

Click here to download Colour figure (online version only) Fig.7d.tif

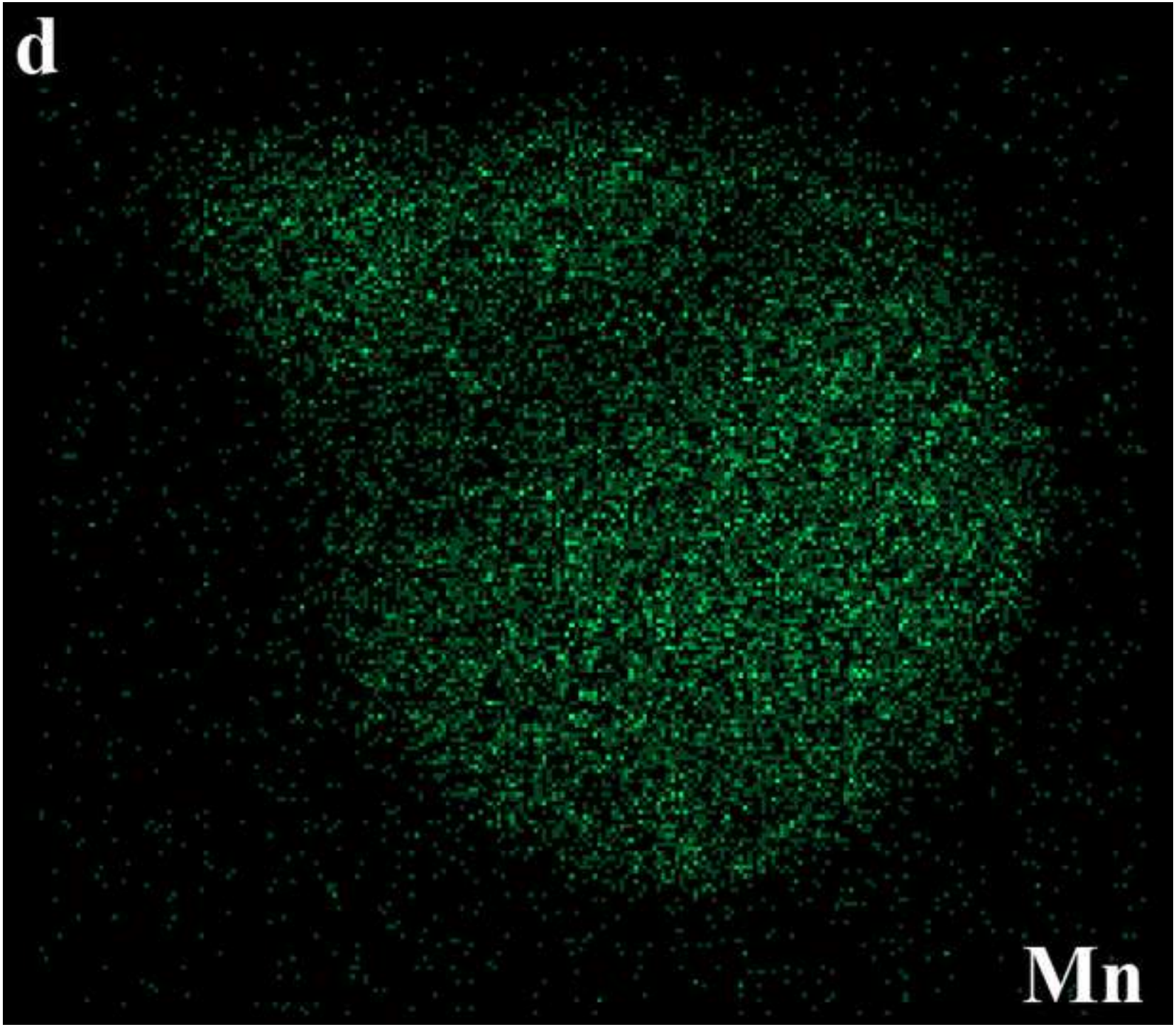

Fig.7e

Click here to download Colour figure (online version only) Fig.7e.tif

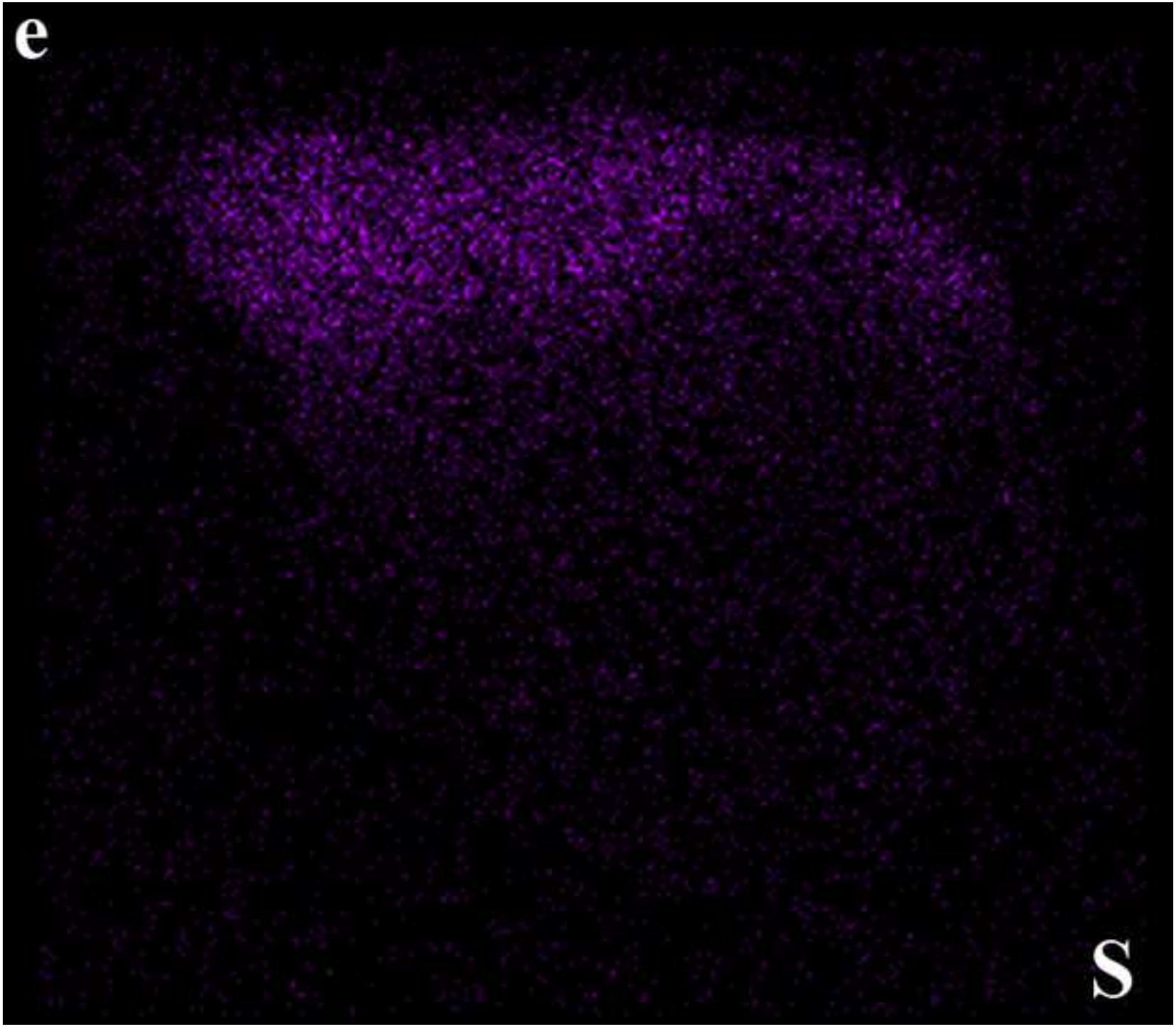

Fig.7f

Click here to download Colour figure (online version only) Fig.7f.tif

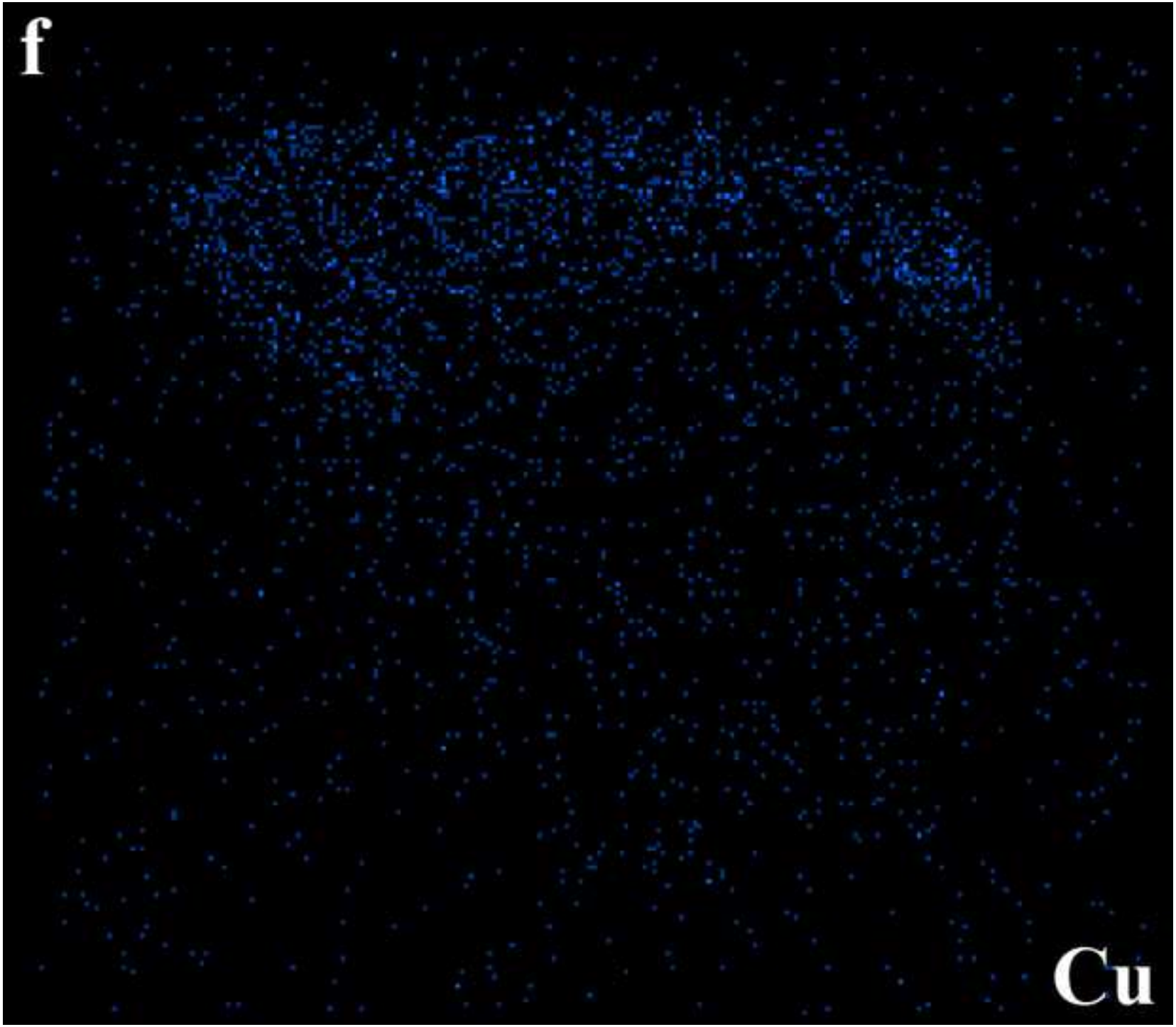

Fig.8a

Click here to download Non-colour figure Fig.8a.tif

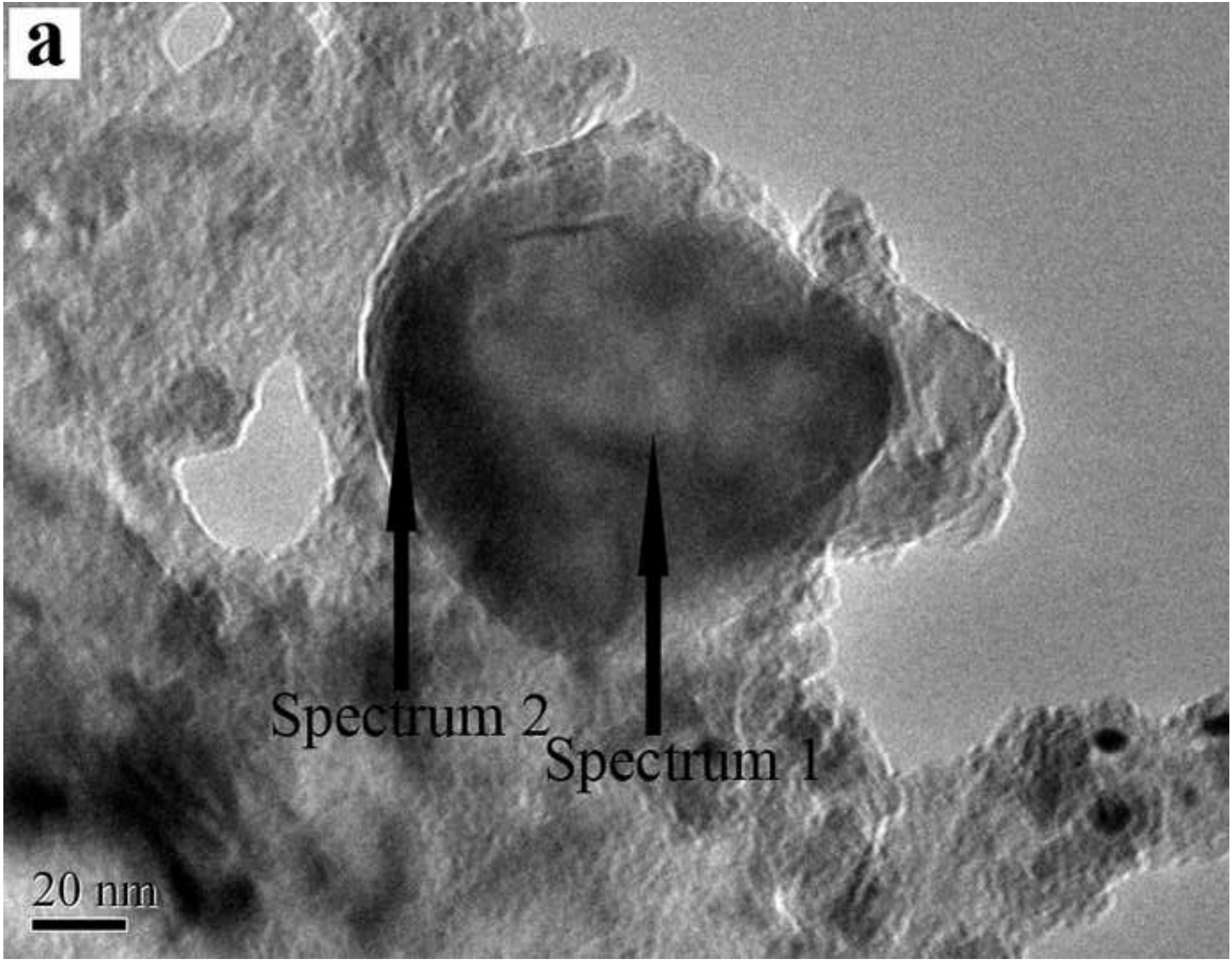

Fig.8b

Click here to download Non-colour figure Fig.8b.tif

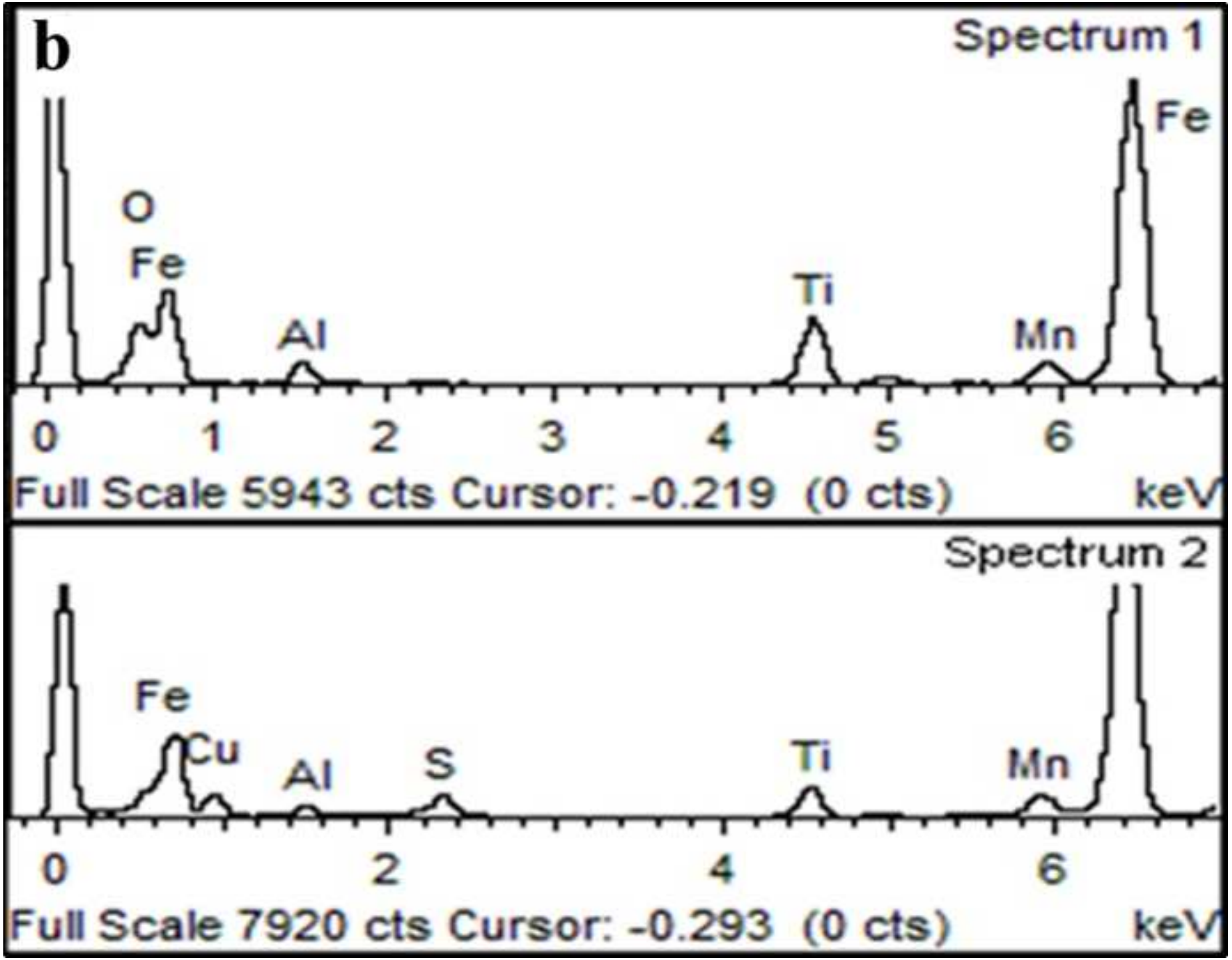

Fig.9a

Click here to download Non-colour figure Fig.9a.tif

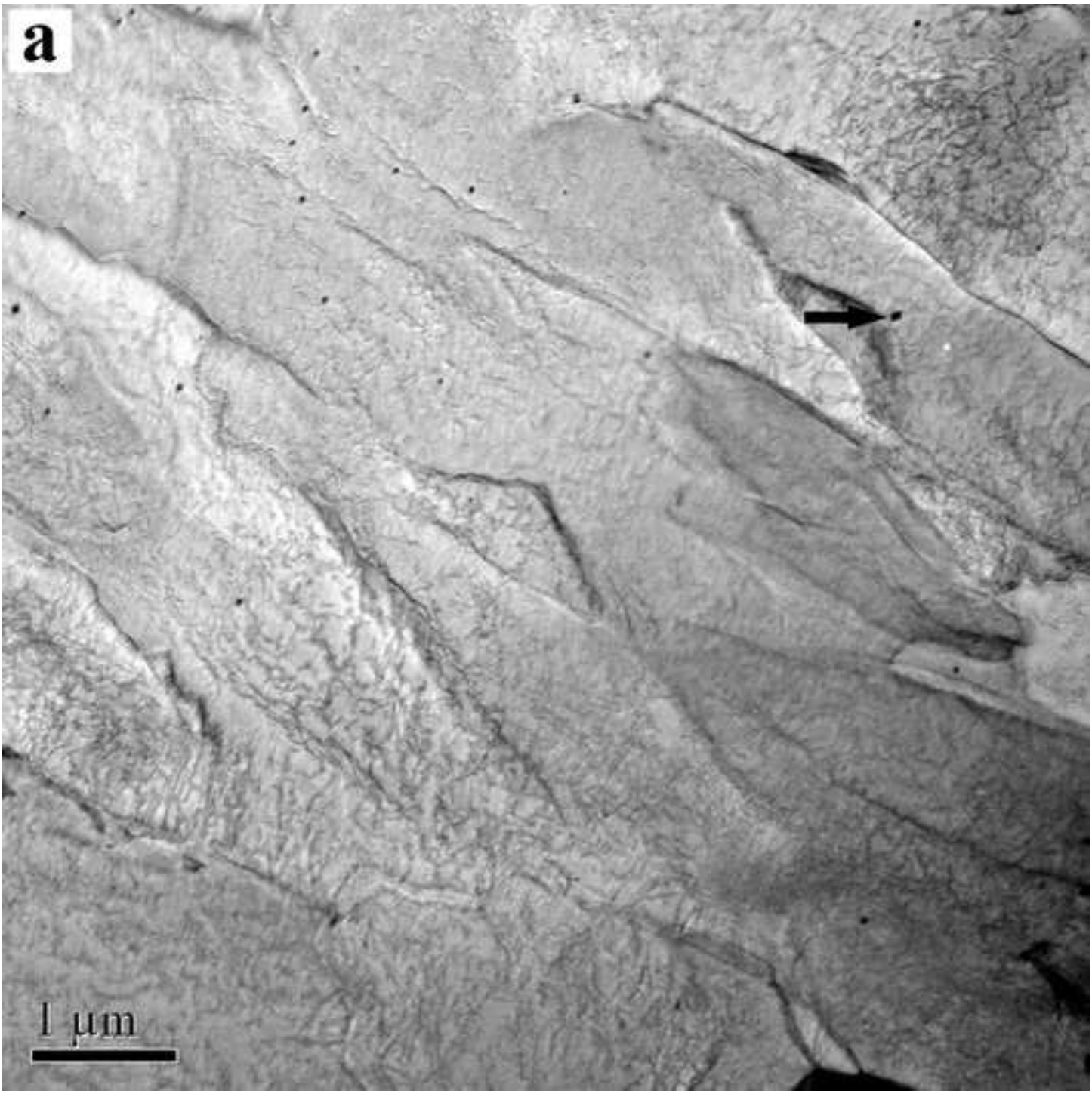

Fig.9b

Click here to download Non-colour figure Fig.9b.tif

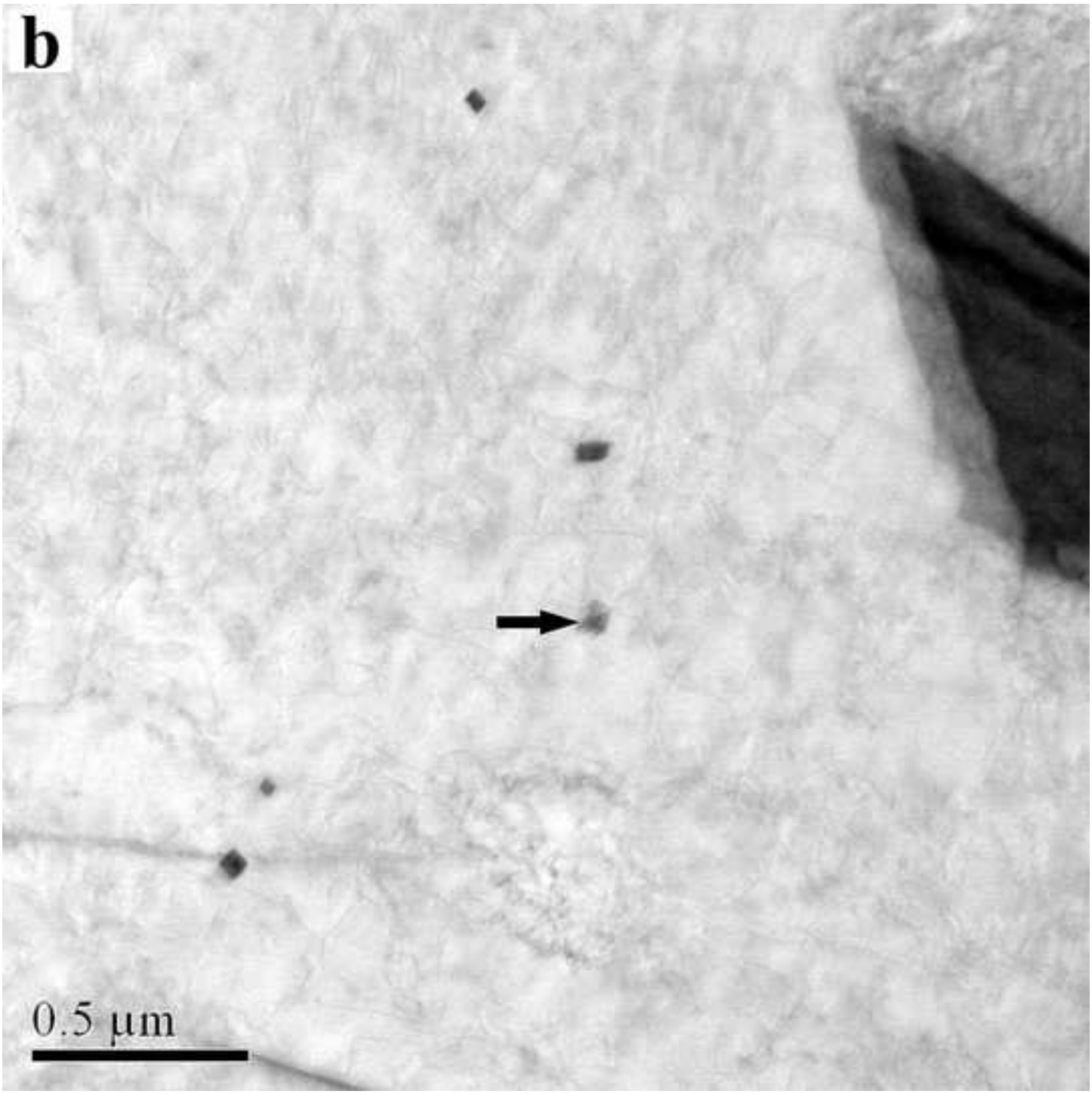

Fig.9c

Click here to download Non-colour figure Fig.9c.tif

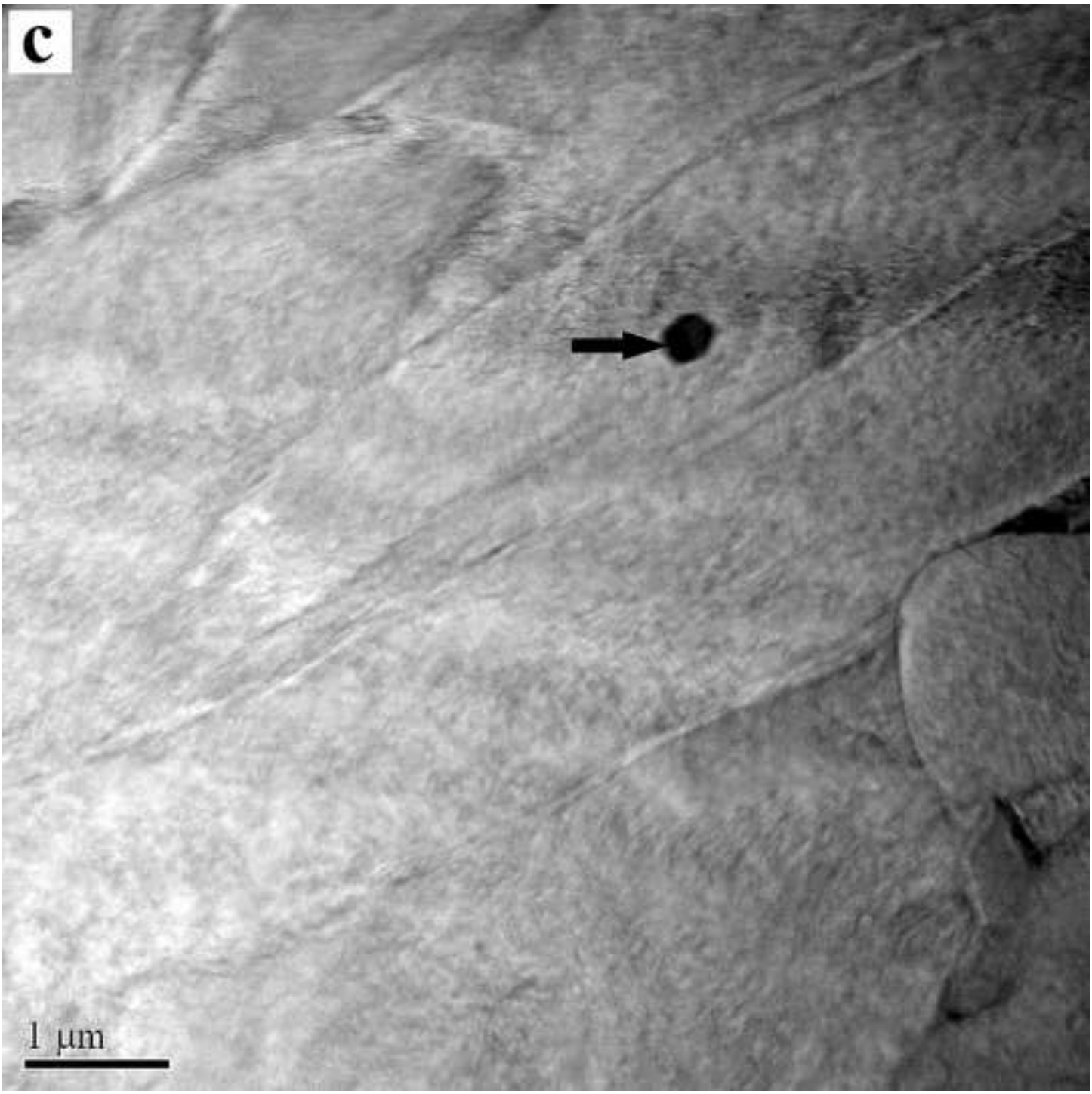

Fig.9d

Click here to download Non-colour figure Fig.9d.tif

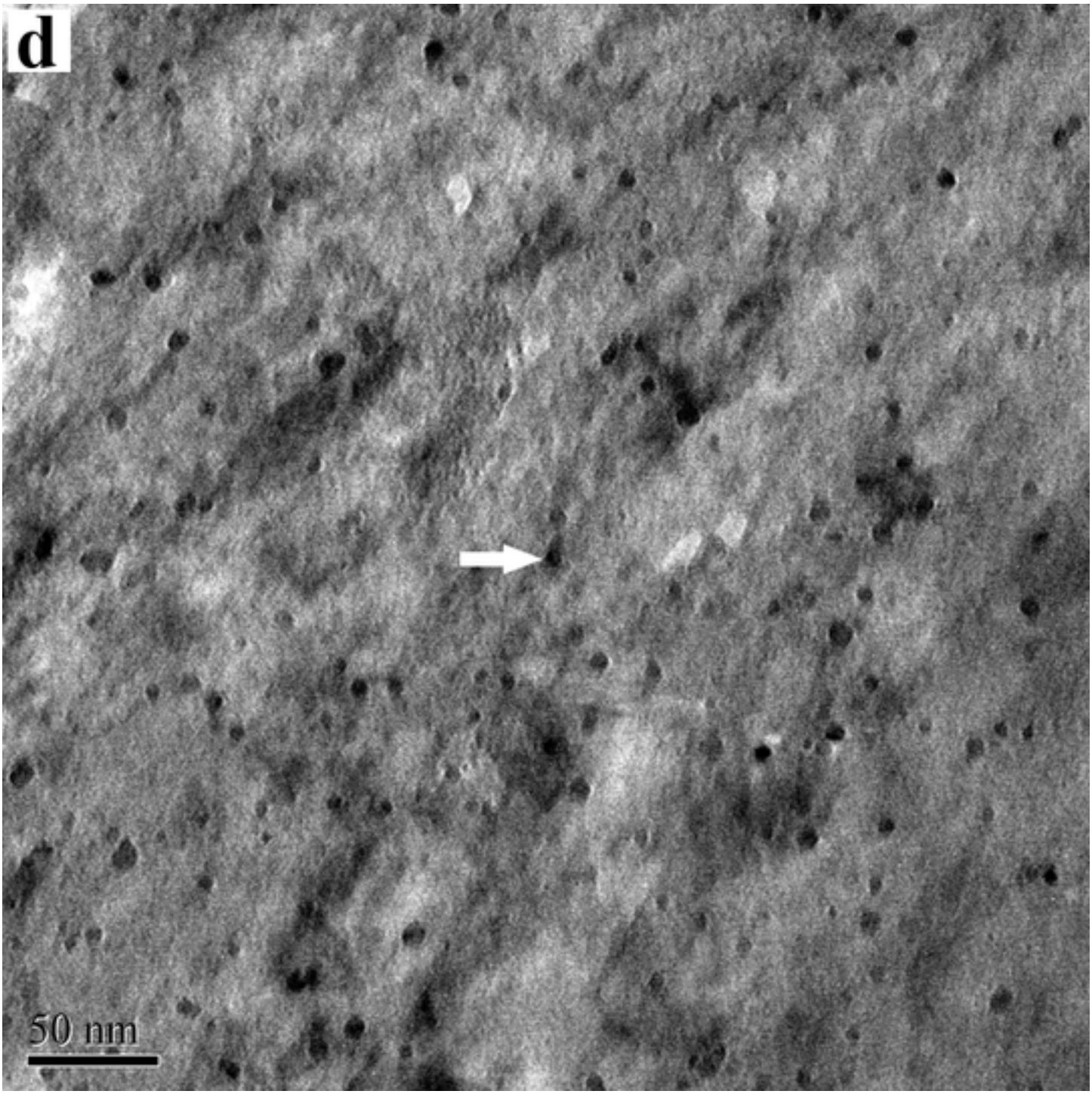

Fig.9e

Click here to download Non-colour figure Fig.9e.tif

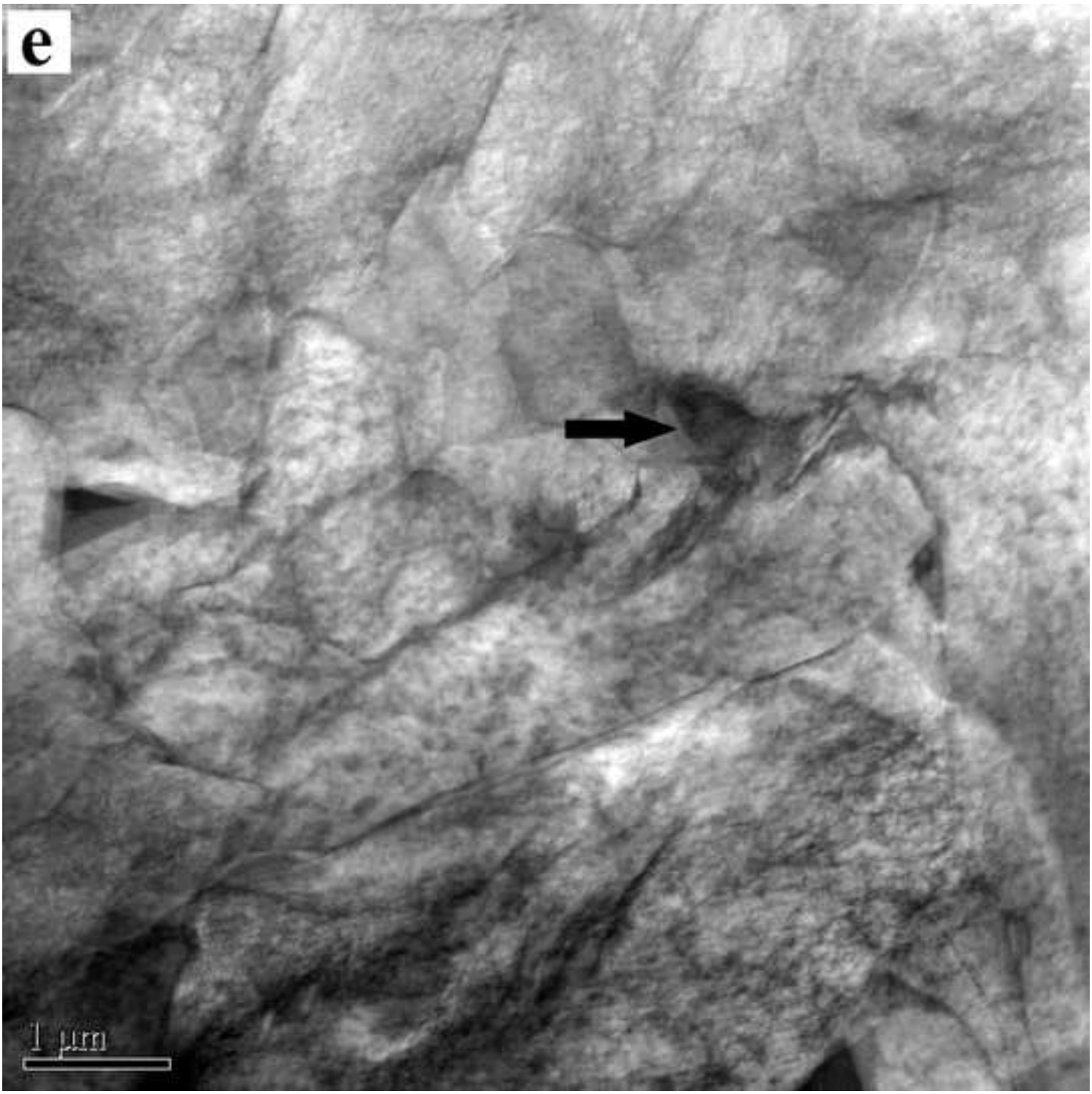

Fig.9f

Click here to download Non-colour figure Fig.9f.tif

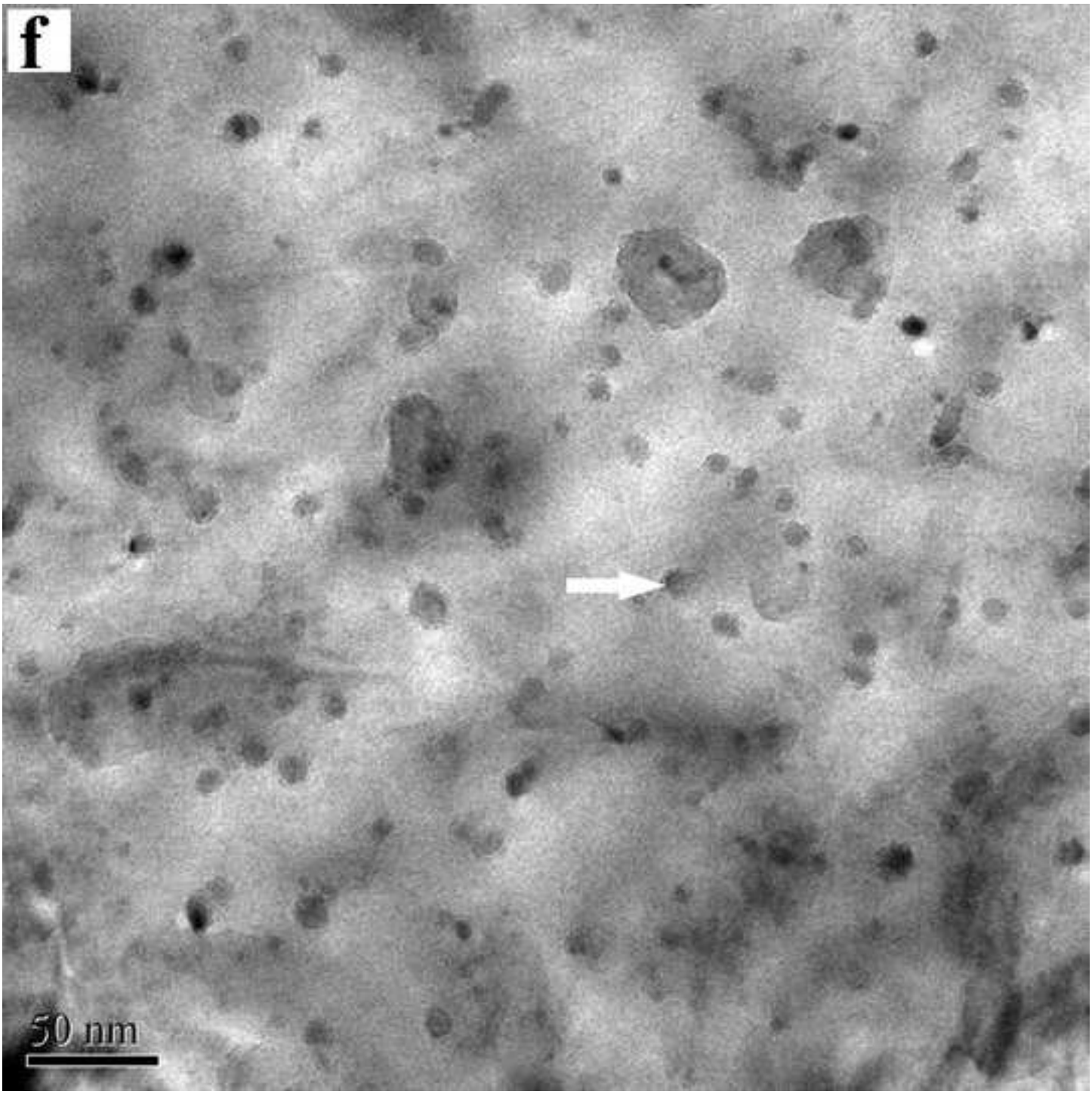

Fig.10a

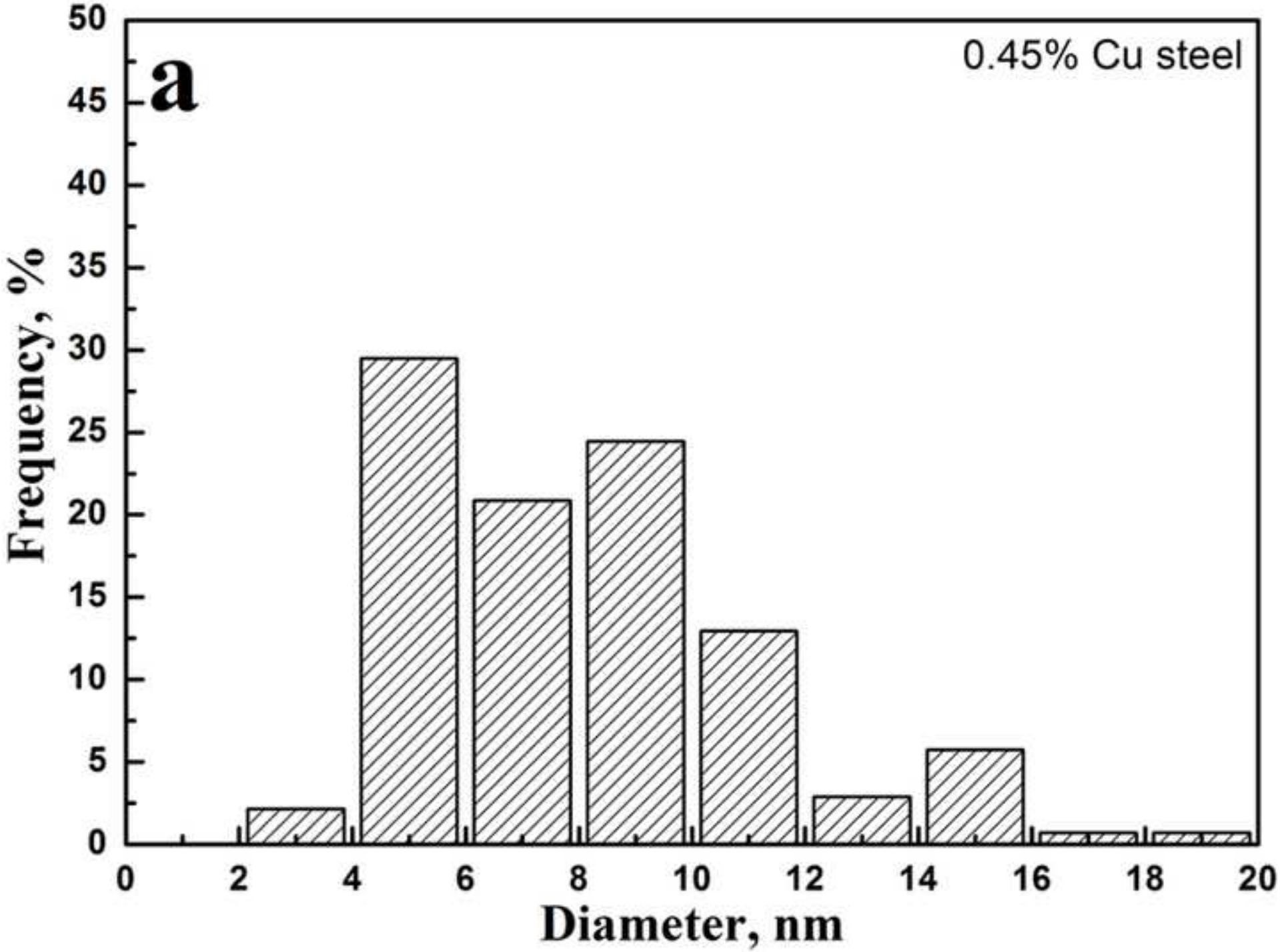

Fig.10b

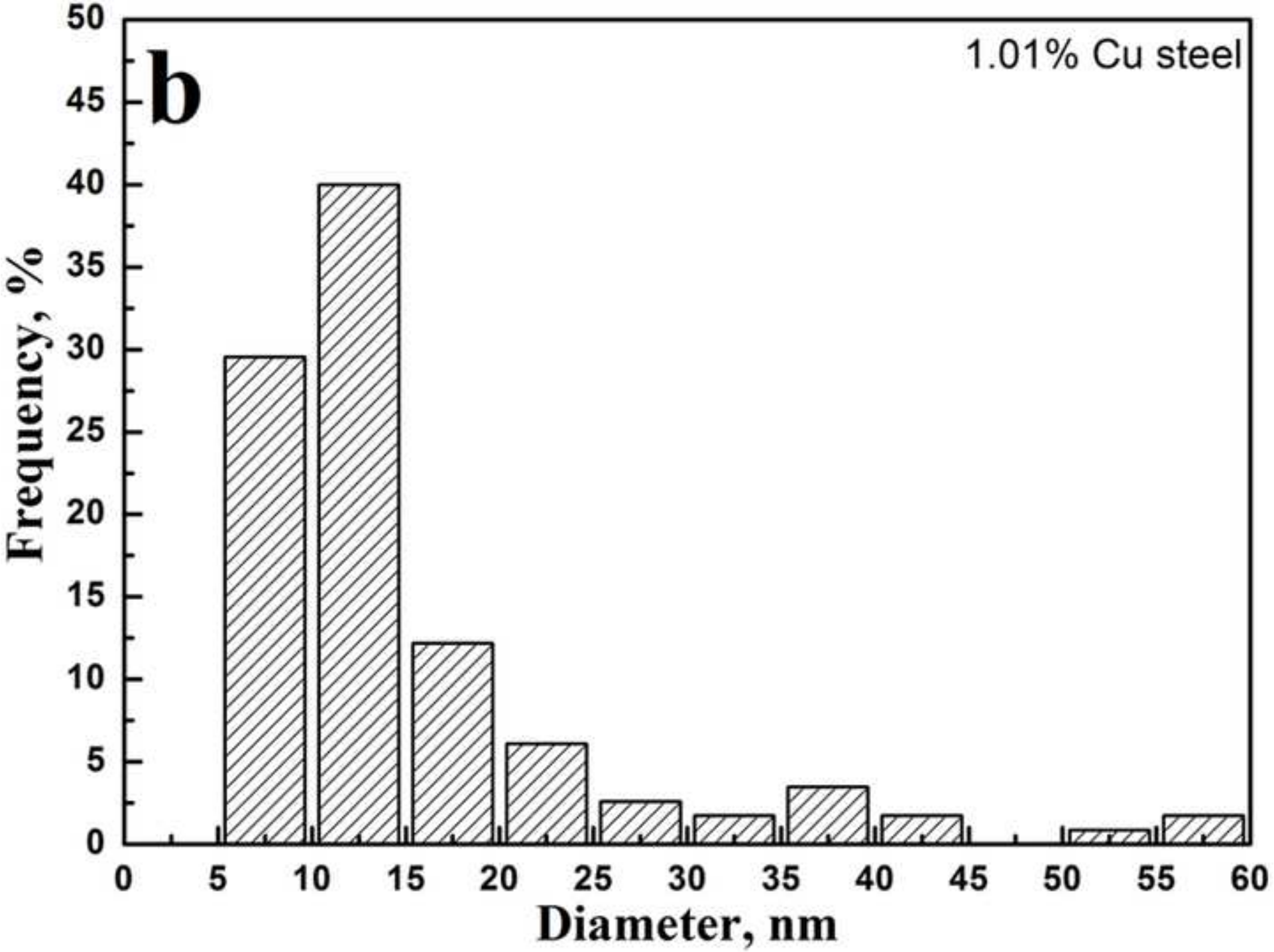

Fig.11a

Click here to download Colour figure (online version only)
Fig.11a.tif

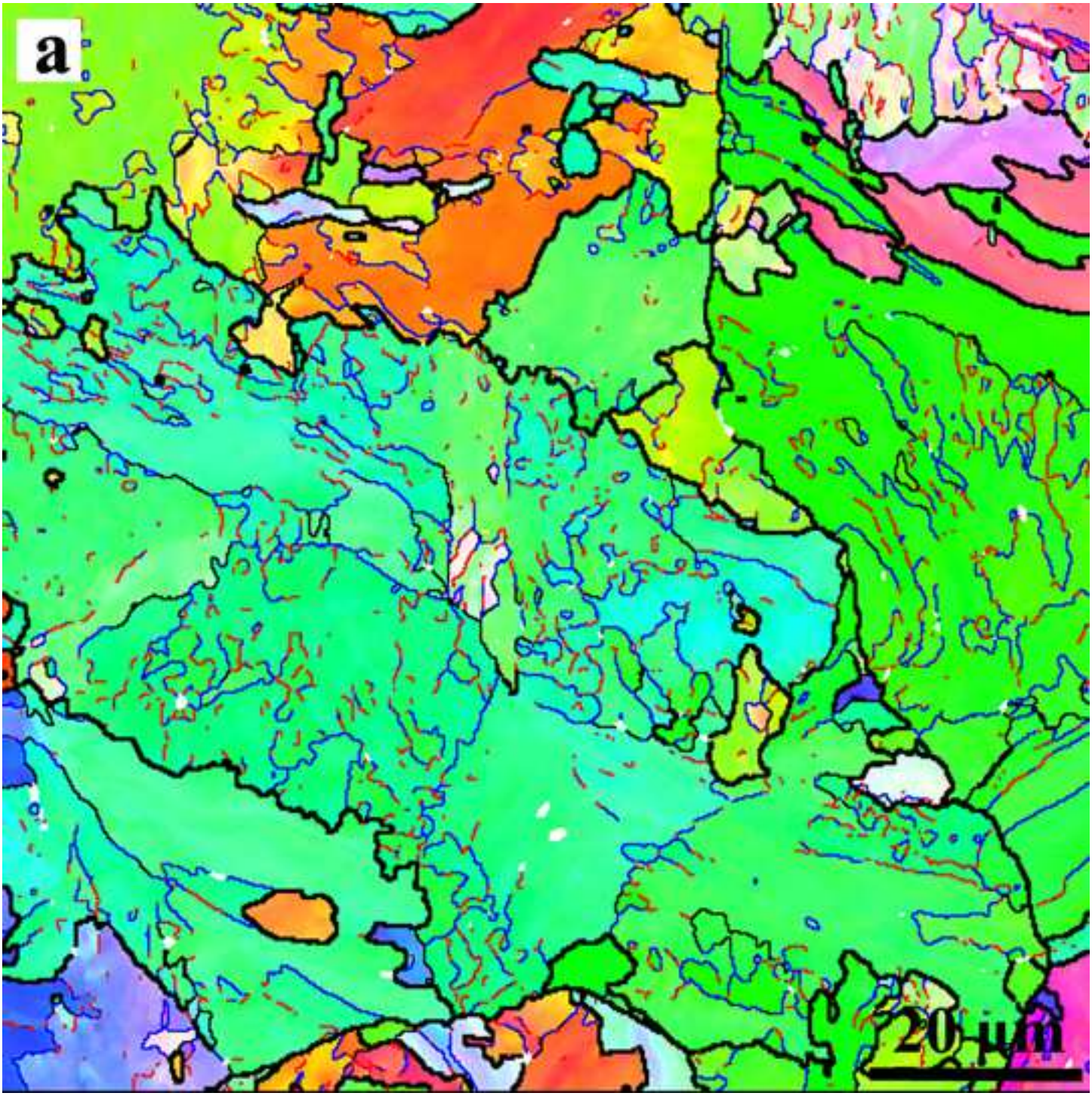

Fig.11b

Click here to download Colour figure (online version only)
Fig.11b.tif

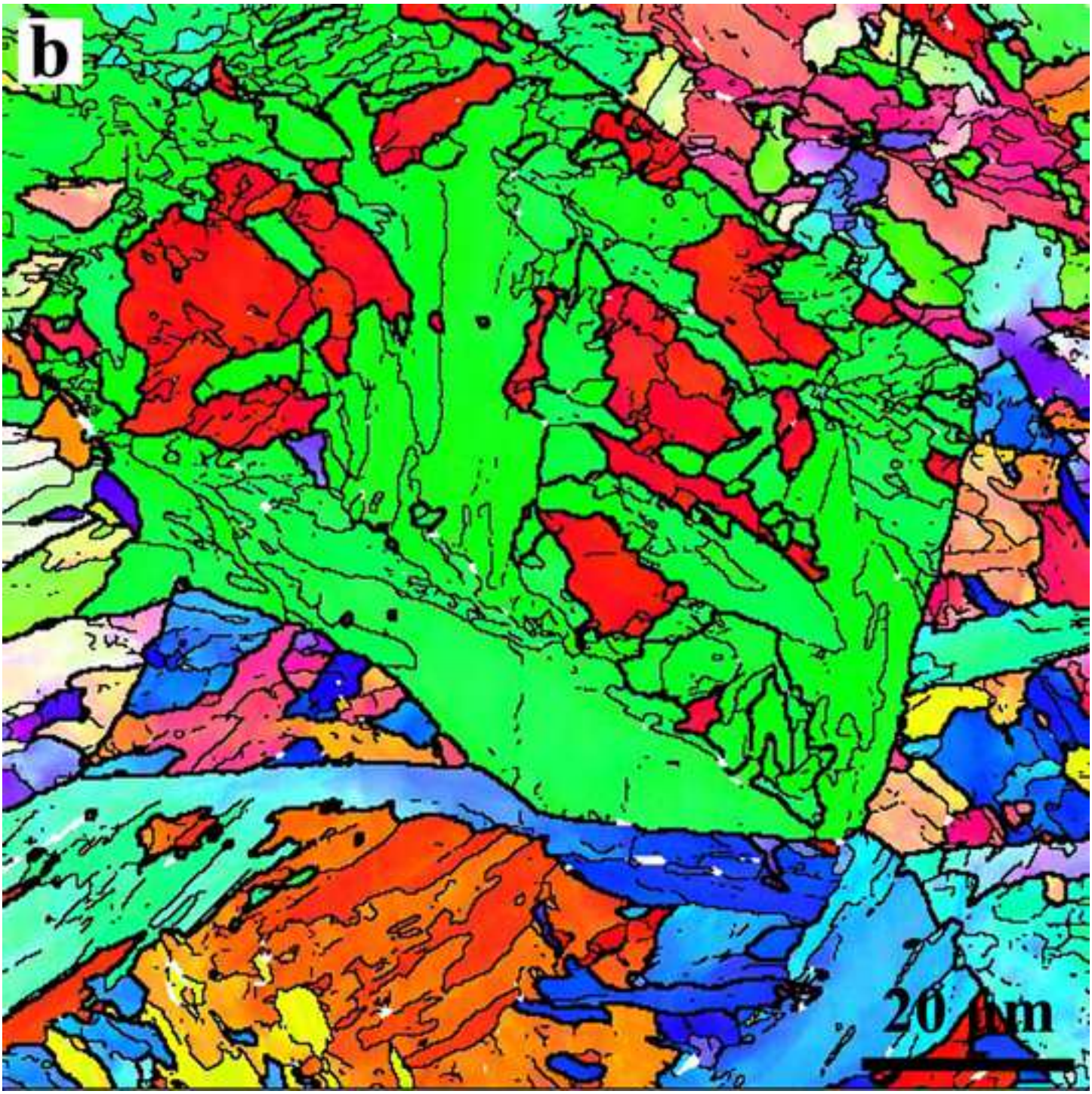

Fig.11c

Click here to download Colour figure (online version only) Fig.11c.tif

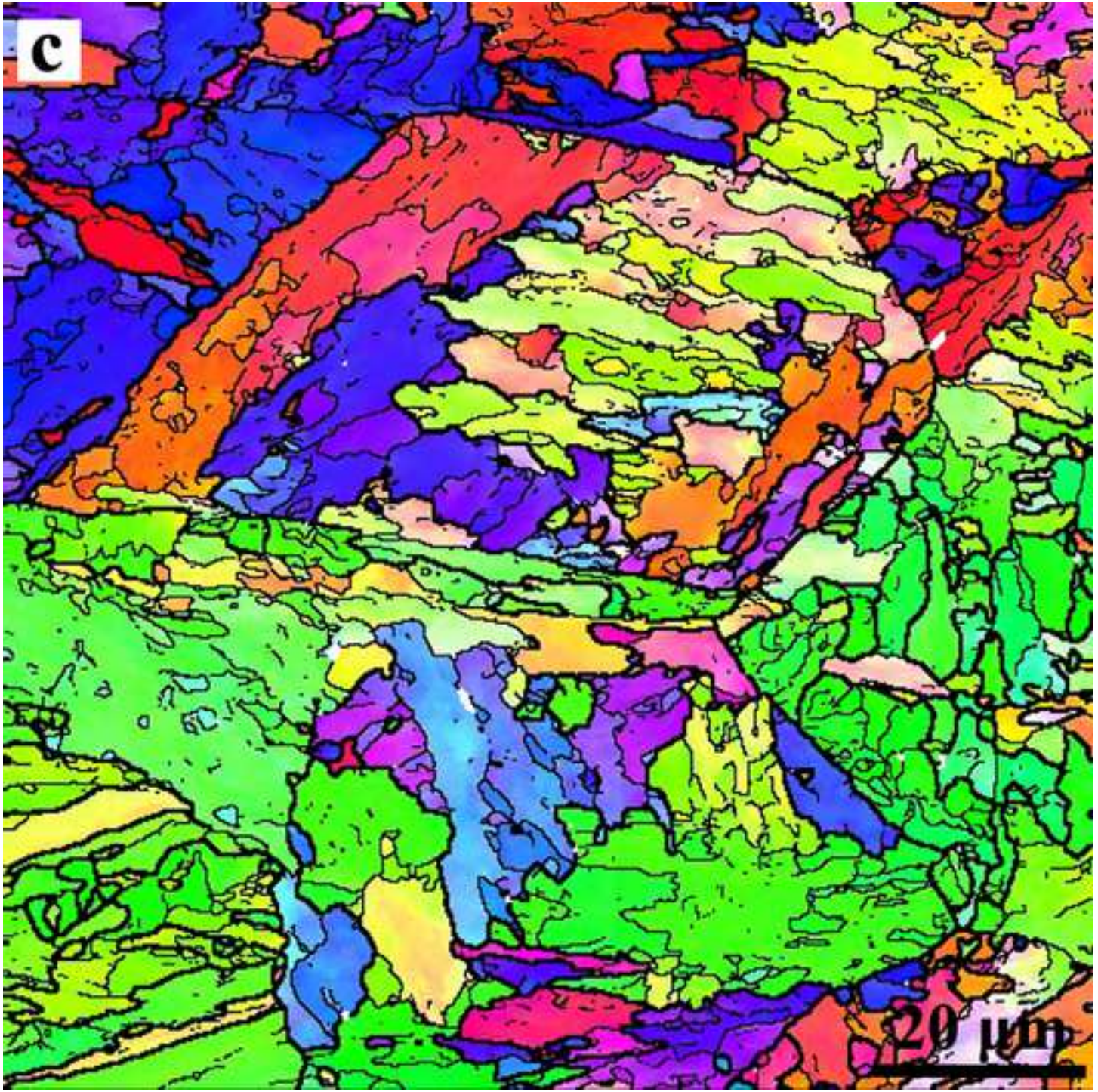

Fig.11d

Click here to download Colour figure (online version only) Fig.11d.tif

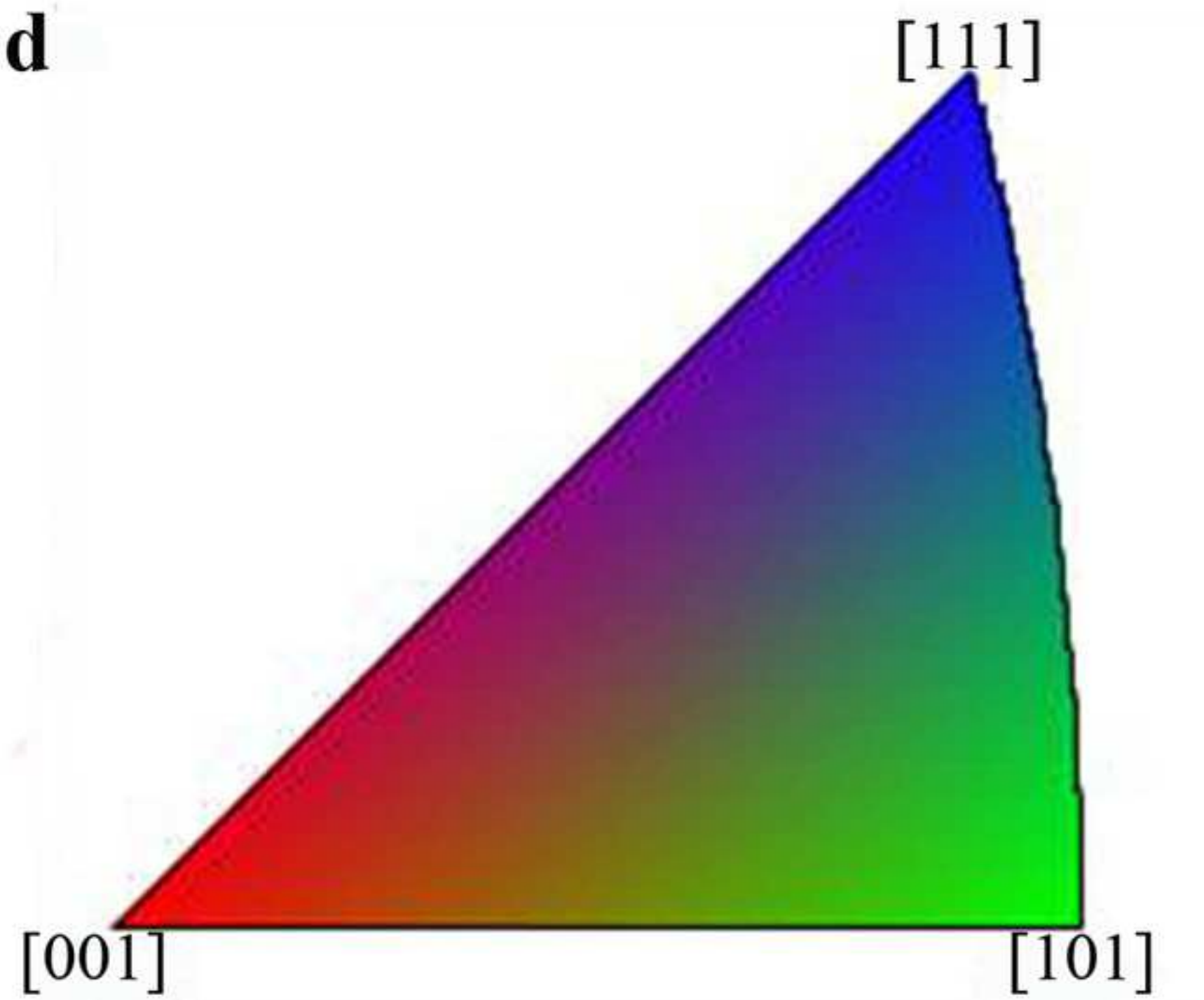

Fig.12a

Click here to download Colour figure (online version only) Fig.12a.tif

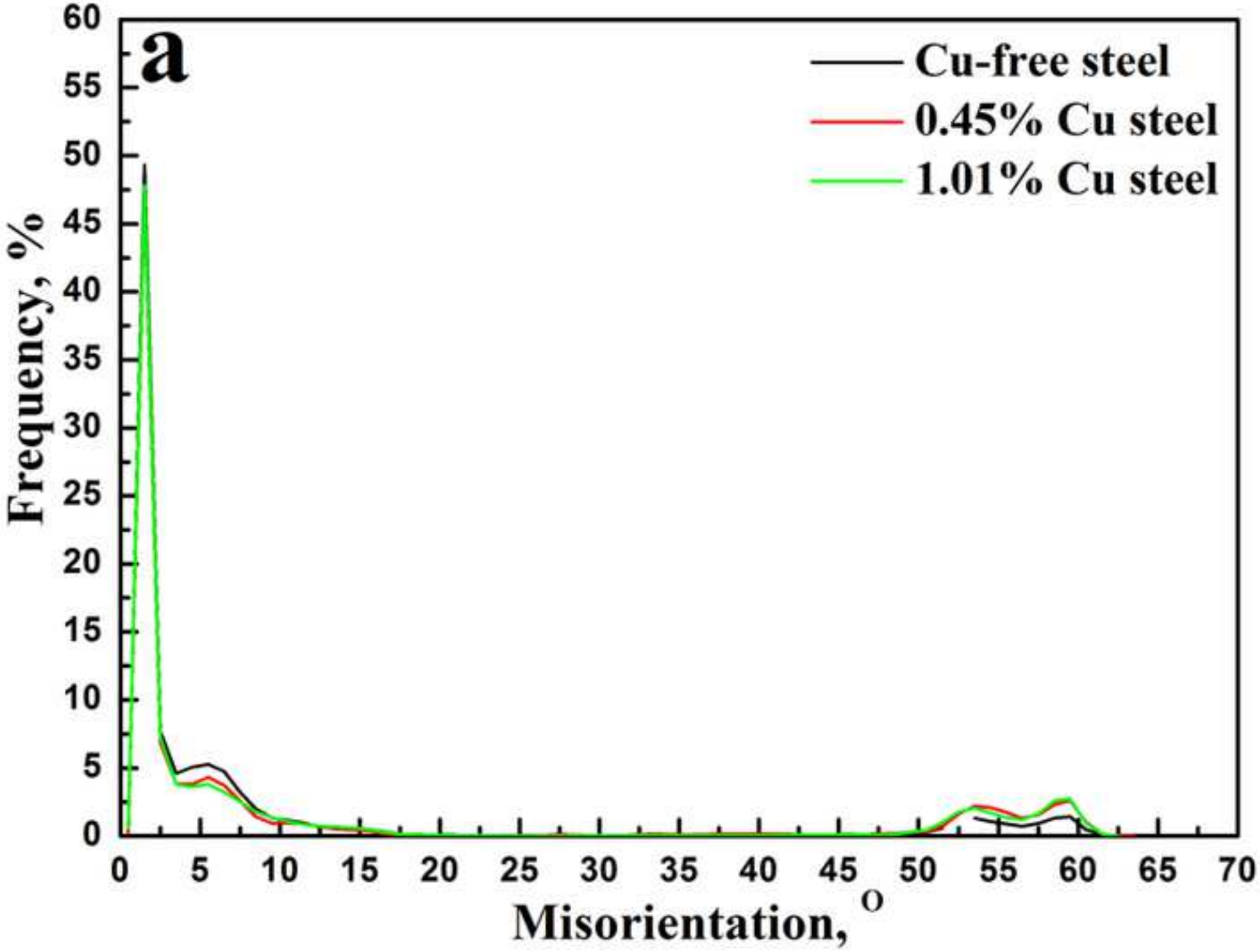

Fig.12b

Click here to download Colour figure (online version only) Fig.12b.tif

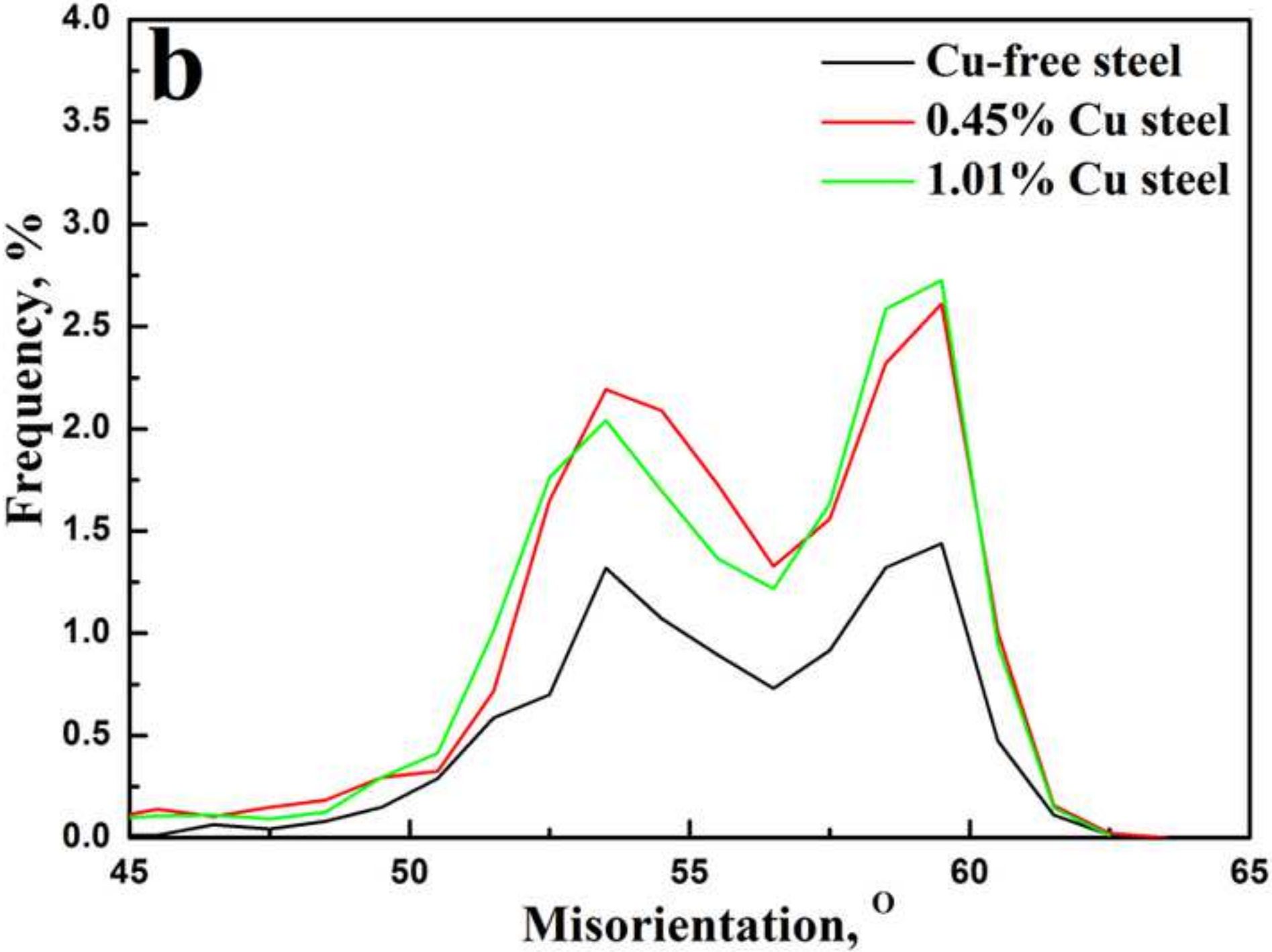

Fig.12c

Click here to download Colour figure (online version only) Fig.12c.tif

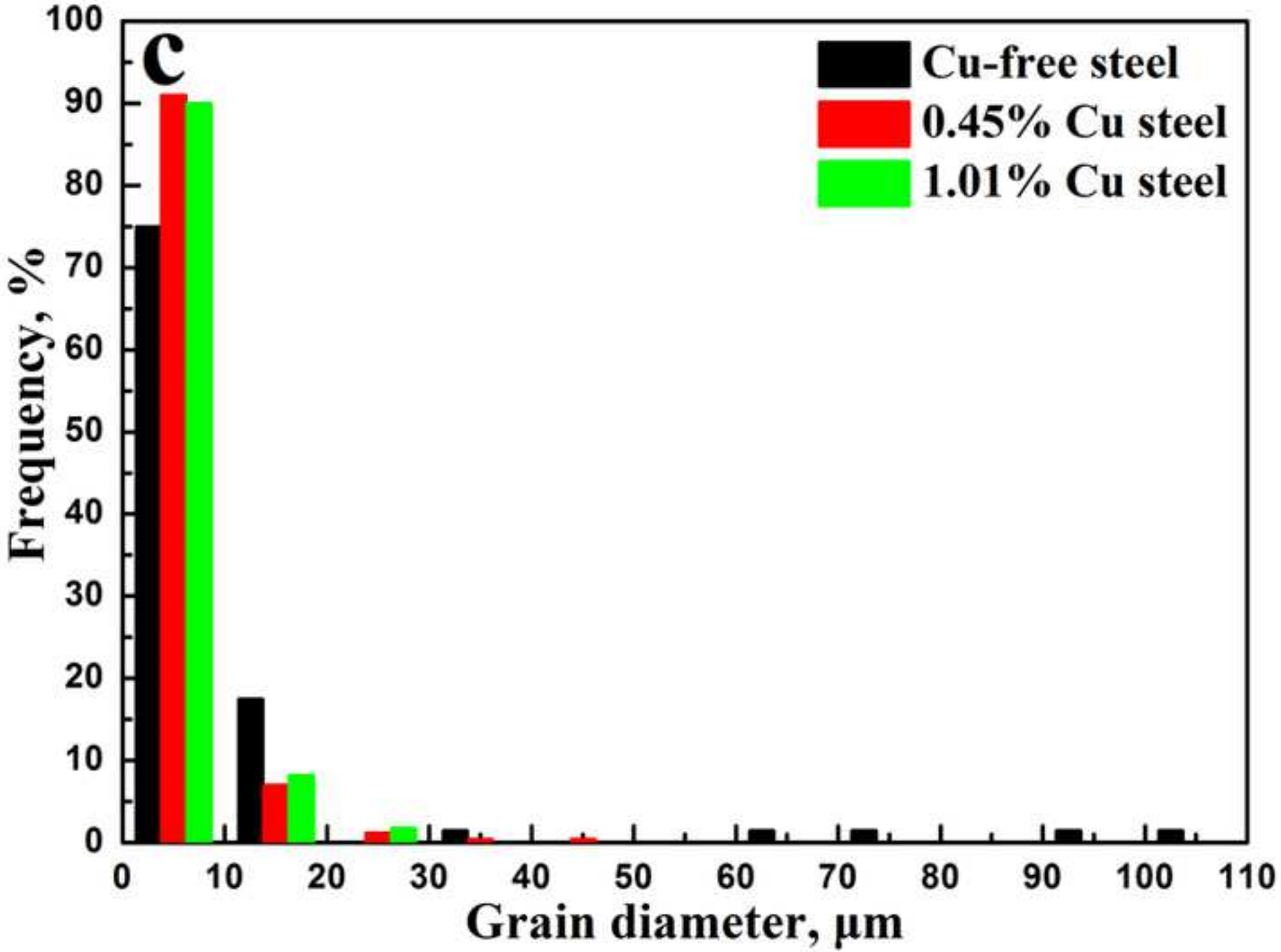

Fig.12d

Click here to download Non-colour figure Fig.12d.tif

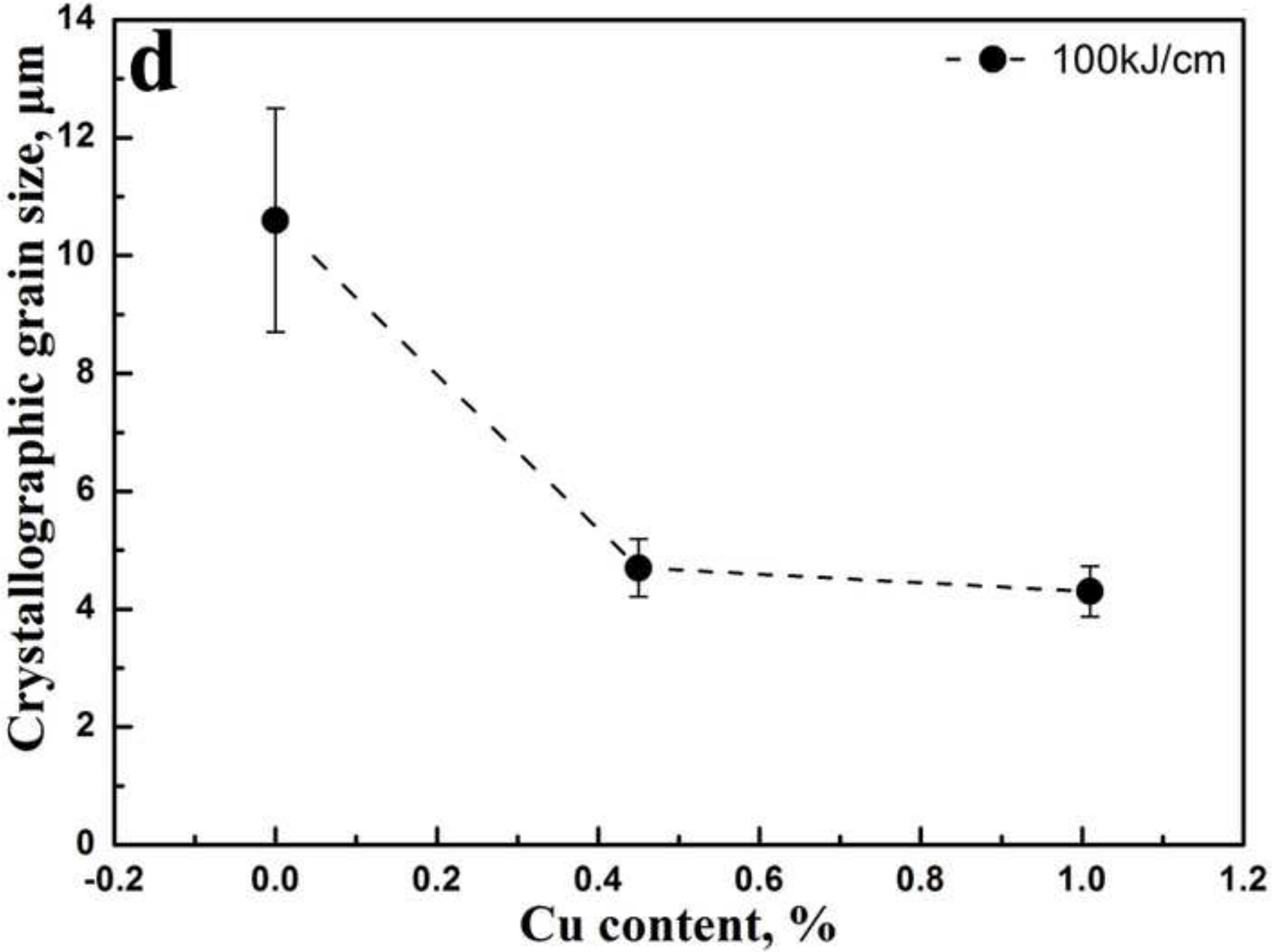

Fig.13

Click here to download Non-colour figure Fig.13.tif

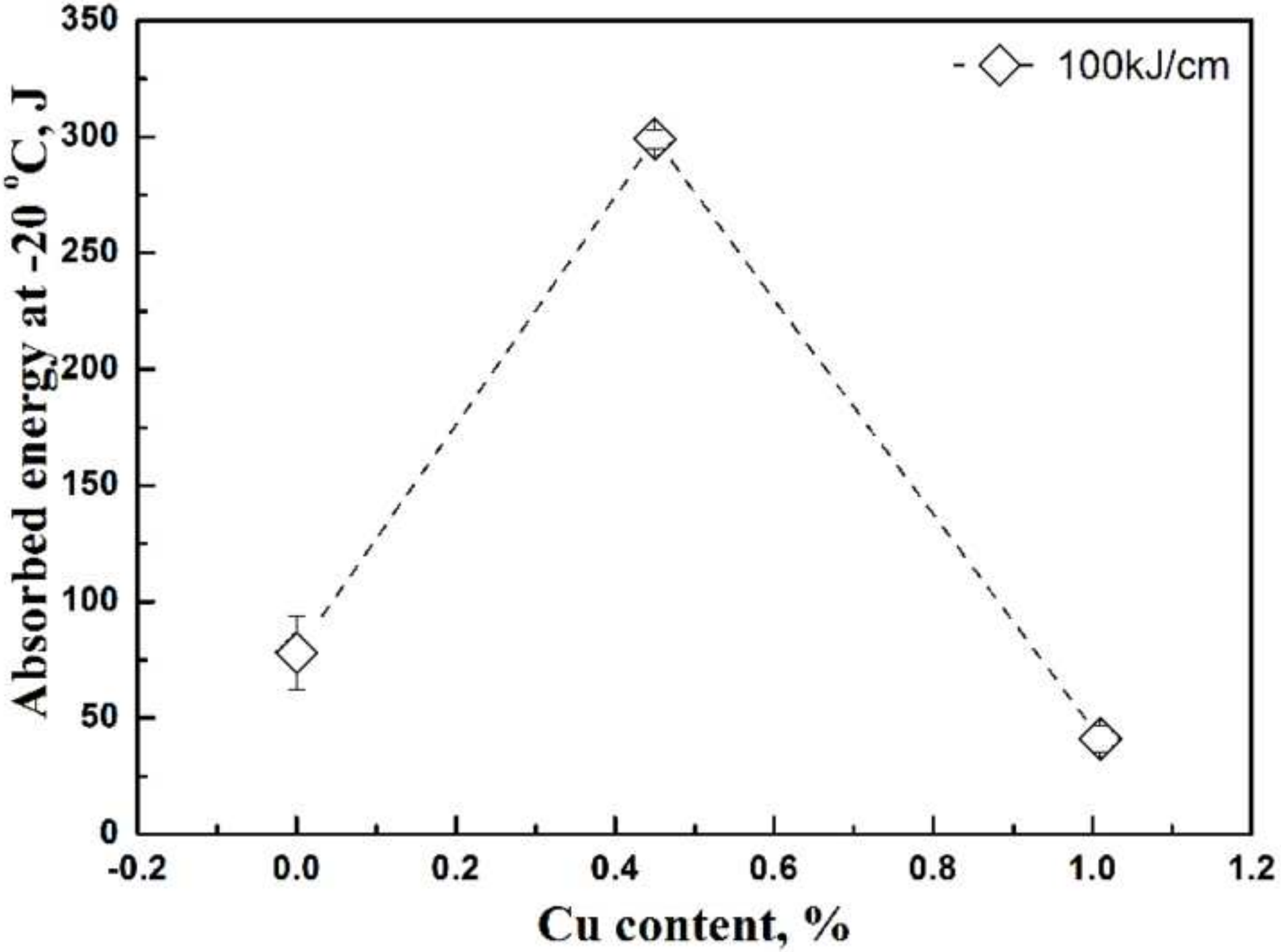

Fig.14a

Click here to download Non-colour figure Fig.14a.tif

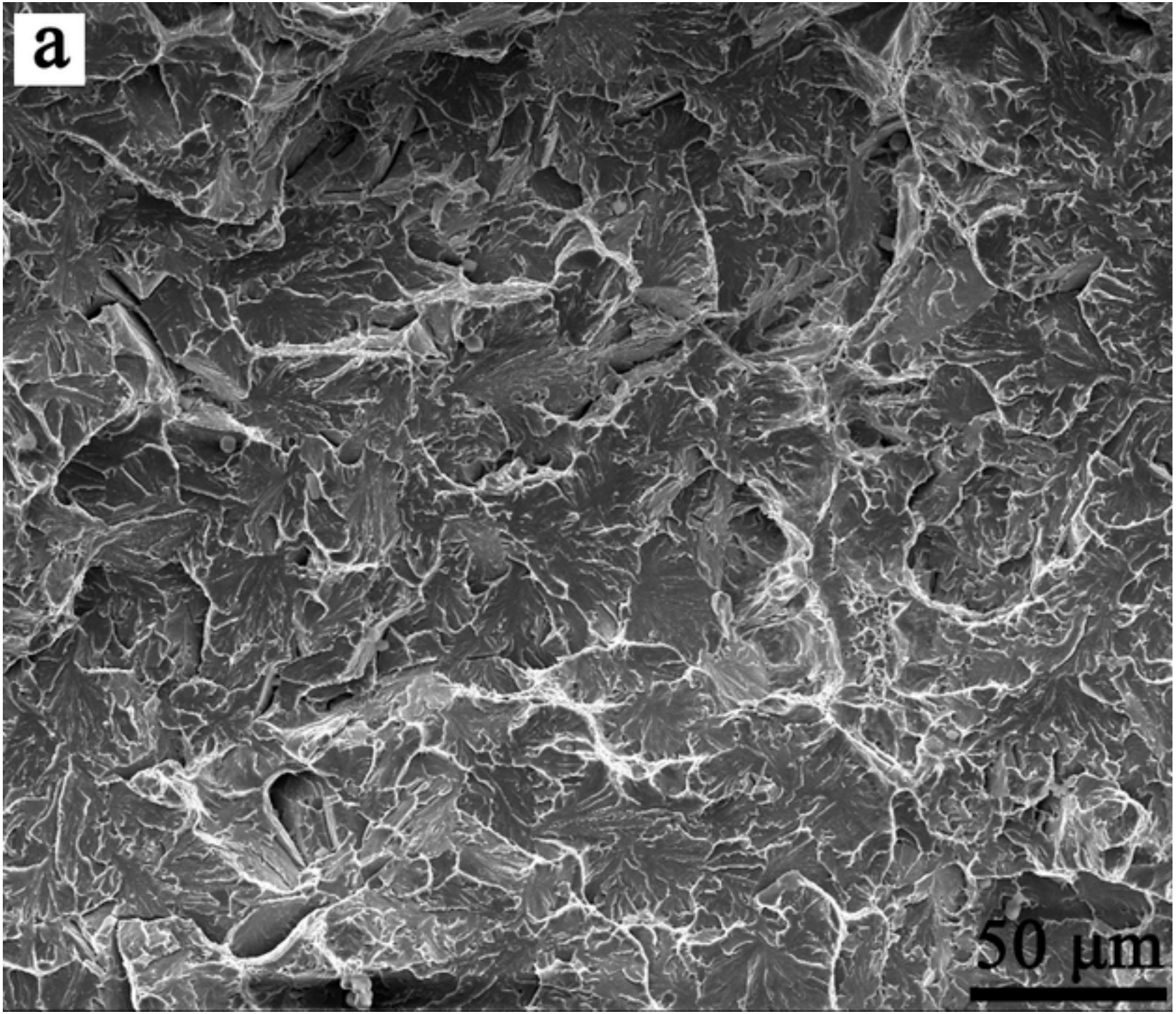

Fig.14b

Click here to download Non-colour figure Fig.14b.tif

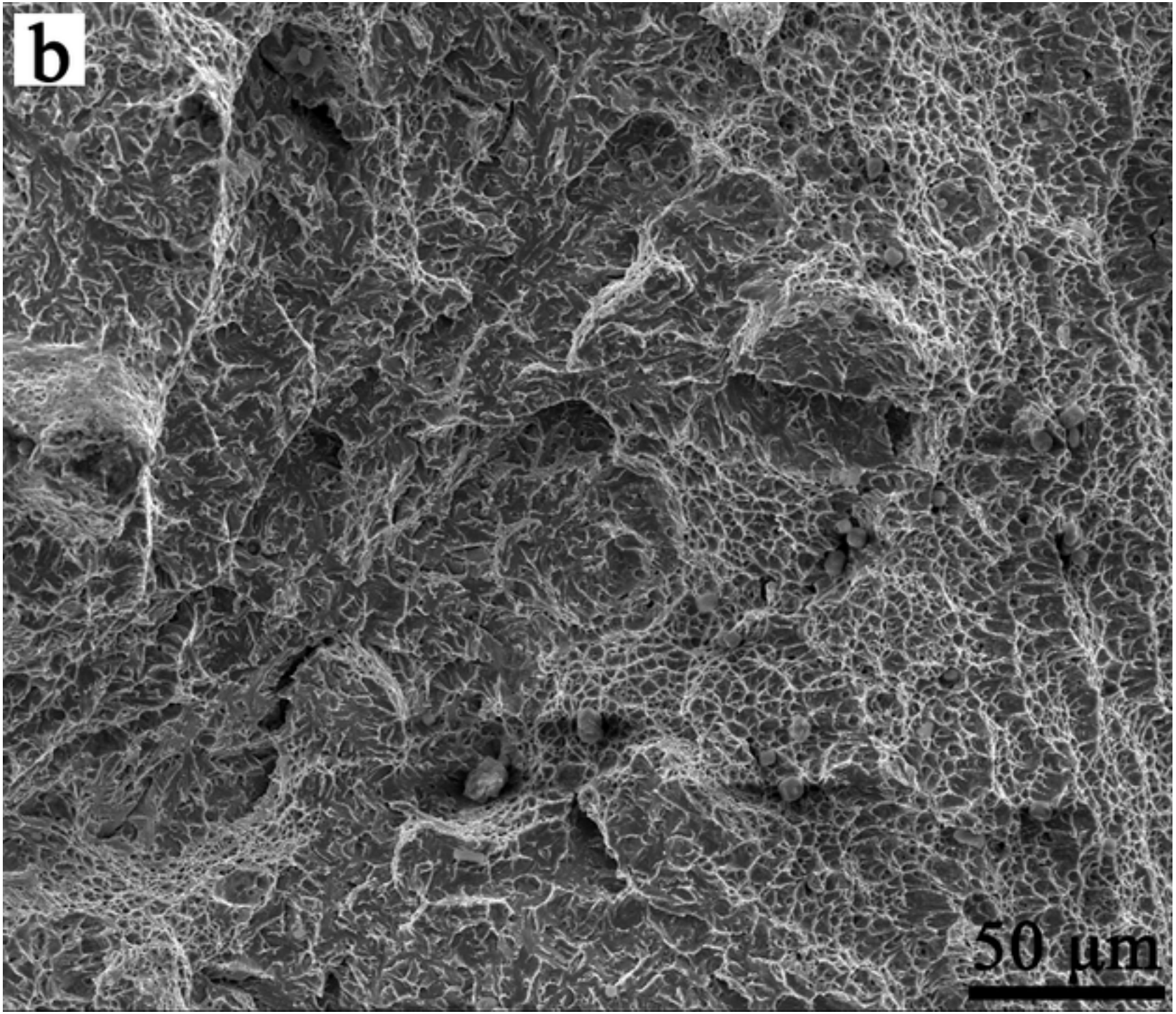

Fig.14c

Click here to download Non-colour figure Fig.14c.tif

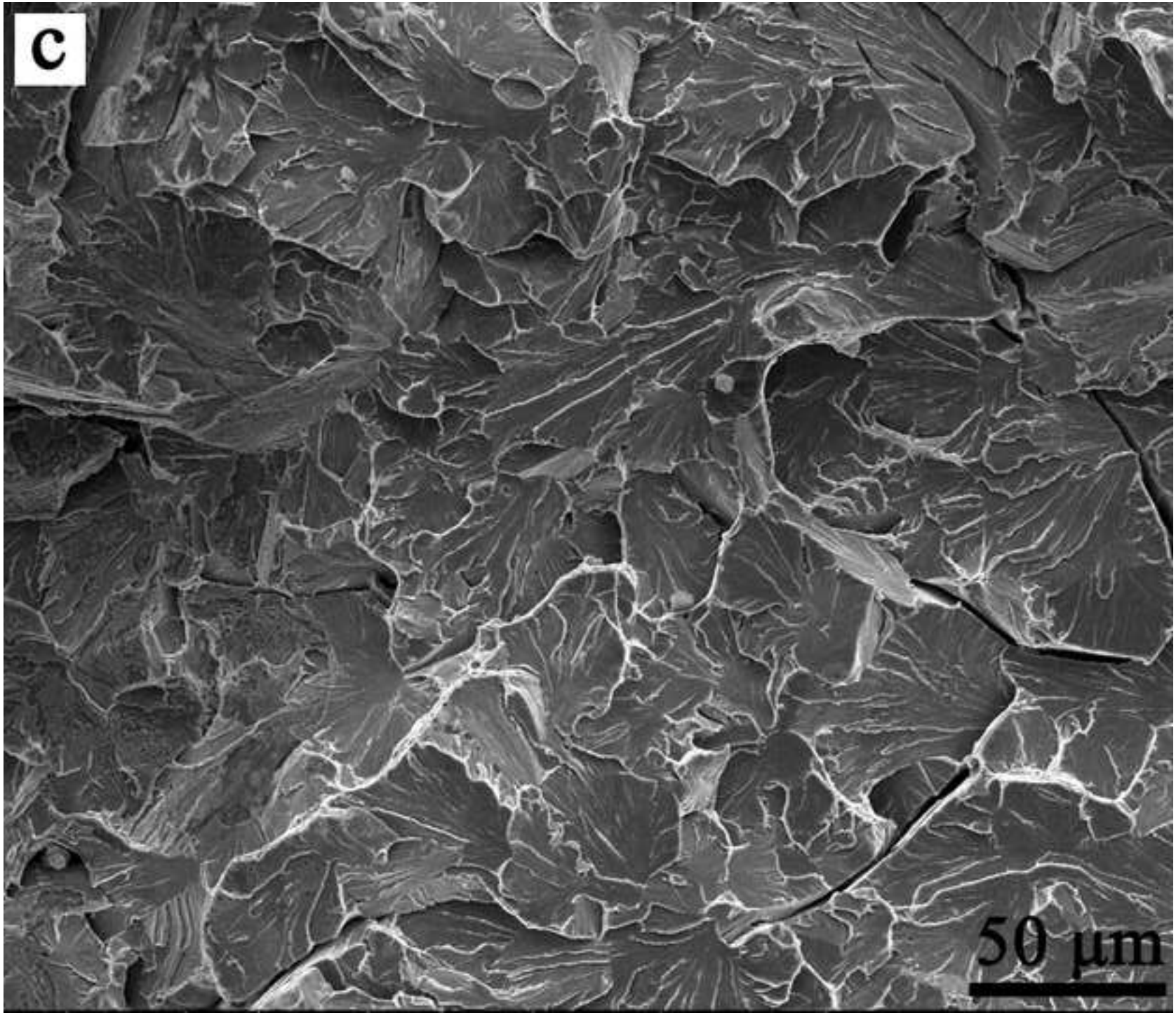

17 August 2016

The Editor of ***Materials Science and Technology***,

Paper No.: MST12200

Title: Effect of Cu addition on microstructure and impact toughness in the simulated coarse-grained heat-affected zone of high-strength low-alloy steels

Dear Editor and Reviewers:

Thank you very much for your useful comments and suggestions on our manuscript. We have modified the manuscript accordingly, and detailed corrections are marked with dark blue and listed below point by point:

Reviewer 1

(1) A kind of problem is that it deals with an old topic of creation of acicular ferrite in heat-affected zone of high strength steels. That theme was novel and popular in late 1990's. Also the role of Cu (ie., CuS) was investigated extensively already then: Madariaga I, Romero JL & Gutiérres I (1998) Upper acicular ferrite formation in medium-carbon microalloyed steel by isothermal transformation: Nucleation enhancement by CuS, Metallurgical and Materials Transactions A, 29A March:1003-1015. Díaz-Fuentes M, Madariaga I, Gutiérres I (1998) Acicular ferrite microstructure and mechanical properties in a low carbon wrought steel. Materials Science Forum 284-286: 245-252. Díaz-Fuentes M, Madariaga I & Gutiérres I (2000) Acicular ferrite microstructure formation in low and medium carbon steels. Proc. 39th Annual Conference of Metallurgists of CIM, Ottawa, Ontario, Canada, 20-23 August 2000. Eds. Yue S. & Essadiqi E: J. J. Jonas Symposium on Thermomechanical Processing of Steel, MET SOC: 489-500. There is also

a public extensive doctoral thesis with more than a hundred of references: Risto Laitinen, Improvement of weld HAZ toughness at low heat input by controlling the distribution of M-A constituents, Faculty of Technology, University of Oulu, P.O. Box 4000, FI-90014 University of Oulu, Finland, Acta Univ. Oul. C 234, 2006 Oulu, Finland. A very brand new paper on slightly different topic: X. Shi et al., Novel Cu-bearing high-strength pipeline steels with excellent resistance to hydrogen-induced cracking, Materials and Design, 92 (2016) 300-305.

The sentence "Cu is usually seen as an excellent aging hardening alloying element, and the adding of Cu content can effectively strengthen the weld metal [9-10]. However, the influence of Cu on microstructural transformation and impact toughness in CGHAZ of Cu-bearing HSLA steel is not well understood." has been changed to "Cu is usually seen as an excellent aging hardening alloying element, and the adding of Cu content can effectively strengthen the weld metal [9-10]. Many investigations have also been made on the influence of Cu content on microstructure evolution and mechanical properties of low carbon steels [11-14]. However, the influence of Cu on microstructural transformation and impact toughness in CGHAZ of Cu-bearing HSLA steel is relatively scarce, especially when subjected to high-heat input weld thermal cycles.".

(2) It is also known that a minimum austenite grain size for nucleation of acicular ferrite in the weld metals is 50-60 μm and 80-140 μm in the base plates and the HAZ, where the highest nucleation potential was achieved with austenite grain sizes of 180-190 μm. It is possible to achieve acicular ferritic microstructure in the weld HAZ in a wide heat input range. Hence, the results shown in the paper.

The sentences "Furthermore, it is also known that prior austenite grain size has an

important influence on acicular ferrite nucleation. The minimum austenite grain size for acicular ferrite nucleation is 50-60μm in the CGHAZ, where the highest nucleation potential was achieved with austenite grain sizes of 180-190 μm [13, 16, 28]. The larger austenite grain size in simulated CGHAZ of Cu-containing steels also has an important influence on formation of high intensity of acicular ferrite." has been added in the discussion.

(3) Concerning M-A constituents, nickel and copper have been stated to promote the formation of acicular ferrite due to a decrease in the austenite-ferrite transformation temperature. However, the amount of M-A constituents decreases by reducing nickel and copper in 500-600 MPa steel because of a decrease of hardenability and the content of upper bainite. Another observation shown in the paper.

On heating during welding thermal cycle, carbon atoms are uniformly distributed in austenite at high temperature. It will partition from ferrite to retained austenite during intermediate temperature transformation. Then the martensite forms in the high carbon retained austenite with further decrease in temperature and exist as M-A constituents. The addition of Cu has a notable influence on evolution of the M-A constituent during solid-state transformation. Because of decreasing temperature of A_{r3}, the carbon atoms have a lower diffusion rate in Cu-containing steel when the austenite starts to transform to bainitic ferrite. Therefore the retained austenite with lower carbon content in Cu-containing steel will be larger than that in Cu-free steel. This phenomenon induces increasing size and fraction of M-A constituents, especially for massive M-A constituents.

The sentence " In the present work, the A_{r3} temperature of the steels was calculated by JMatPro software. It reveals that the A_{r3} temperature decreases 13 °C when Cu content increased from 0.45% to 1.01%. In the present work, the volume fraction of M-A constituents increased gradually with increasing Cu content (Fig. 4)" has been changed to " In the present work, the A_{r3} temperature of the steels was calculated by JMatPro software. It reveals that the A_{r3} temperature decreases 9.8 °C and 22.8 °C when Cu content increased from 0 to 0.45% and 1.01%. the carbon atoms have a lower diffusion rate in Cu-containing steel when the austenite starts to transform to bainitic ferrite. Therefore the retained austenite with lower carbon content in Cu-containing steel will be larger than that in Cu-free steel. This phenomenon induces increasing size and fraction of M-A constituents, especially for massive M-A constituents (Fig. 4)".

(4) Why does austenite grain size increase with Cu-alloying (Fig. 4a) ?

The addition of Cu decreases the transformation temperature (A_{r3}) in low carbon steels, which means that ferritic transformation starting temperature decrease. In the present work, the A_{r3} temperature of the steels was calculated by JMatPro software. It reveals that the A_{r3} temperature decreases 22.8 °C when Cu content increased from 0 to 1.01%. Thus, the ferritic transformation started at lower temperature in Cu-containing steel. Because of decreasing temperature of A_{r3}, the austenite grain in simulated CGHAZ of Cu-containing steels has more time to coarsen at higher temperature. This phenomenon induces increasing size of austenite grain in simulated CGHAZ of Cu-containing steels.

(5) Ref. 9: Initials first, Ref. 16: a typo: Gutierrez, Refs 27, 28 dots; Ref. 29 initial.

The references have been changed.

(6) The second serious problem is that there are 59 figures altogether, which is a huge (impossible?) number. My humble suggestion is to reduce that number. Just examples can be given. For instance, the compositions of inclusions are well known so that elemental maps are not essential to show. Some of 15 figures have 6 sub-figures (Figs 2, 5, 6, 7, 8, 10 as examples). Fig. 1. The unit second s must be in lower case.

Figure 1 has been deleted.

(7) Another (more) interesting topic concerning the influence of Cu is if it can prevent local softening in the weld heat-affected zone in high-strength bainitic/martensitic steels. A practical problem with steels with high Cu alloying is that in order to prevent hot shortness (surface cracking) during hot rolling, an expensive Ni-alloying is required.

We agree with the reviewer's comments. In the present manuscript only the experimental results about impact toughness was presented. We will continue to further study the prevention of softening and surface cracking in these steels.

Reviewer 2

(1) Using only "Cu-containing steels" or "Cu-bearing steels" in the manuscript.

The word "Cu-bearing steels" has changed to "Cu-containing steels" in the revised manuscript.

(2) More details should be given about EBSD in Experimental procedures.

The sentence "The orientation relationship and crystallographic grain size of

microstructure was examined using electron backscattered diffraction (EBSD) by means of a Philips XL30W/TMP scanning electron microscope (SEM)" has been added in the revised manuscript.

(3) Inclusions including CuS/MnS were verified in the study, however, the sulfur content was not given in Table 1.

The sulfur content has been added in the revised manuscript.

(4) Explanation for how to define the "acicular ferrite" is needed. A acicular ferrite microstructure in the low-carbon microalloyed pipeline steels was defined as a highly sub-structure, nonequiaxial ferrite, formed during the continuous cooling process with a mix mode of diffusion and shear transformation in the temperature range slightly higher than the bainite. In this study, what's the difference between the two microstructures? Are they the same?

Many researchers thought the acicular ferrite should be replaced by the terms ‘intragranular bainite’ [Bhadeshia HKDH. Bainite in steels [M]. 2nd Ed. London: The Institute of Materials; 2001.] or ‘acicular bainite’ [Jae-Bok Seol, J.S. Kang, C.G. Park. Three-dimensional characterization of bainitic microstructures in low-carbon high-strength low-alloy steel studied by electron backscatter diffraction [J]. Materials Characterization, 2013, 79(3): 110-121.]. However, there were still some difference between the acicular ferrite and bainite. As examples in nucleation sites and growth behavior, the acicular ferrite was nucleated on nonmetallic inclusion or the broad face of the pre-formed acicular ferrite, and then radiate in many different directions from these point nucleation sites. The bainitic ferrite sheaves were nucleated on grain boundary and grew in the form of packets containing parallel plates with the same

crystallographic orientation in the previous work [Materials Characterization, 61 (2010) 726-731.]. In the present work, the ferritic microstructures nucleated on intragranular inclusions and grain boundaries on the specimen surface were described as acicular ferrite and bainite, respectively. A large amount of plates, which were not associated with inclusion or grain boundary on the specimen surface, would be distinguished by the growth behavior. The individual ferrite which had different growth direction with the neighbor ferrite was thought as acicular ferrite nucleated on the inclusion under the specimen surface. The ferrite, which grew at the same direction in sheaves and paralleled to each other, would be defined as bainite nucleated on the grain boundary under the specimen surface.

(5) If they are same, Cu addition to steels could promote the formation of low temperature bainite, not acicular ferrite. More expanation should be given.

Acicular ferrite and bainite are different, especially for nucleation site. Because of Cu addition, the inclusion was changed from complex inclusion with outer layer of MnS to MnS + CuS and thus high intensity of acicular ferrite is formed.

Because of the contribution to the stimulating discussion and the revision of the present manuscript, Dr. Irina Rodionova is added as a co-author.

The revised manuscript has been re-submitted to your journal. Thanks again.

Sincerely yours,

K.M. Wu